



Synthesis and characterisation of novel electronic materials.

MARSDEN, Sean D.

Available from the Sheffield Hallam University Research Archive (SHURA) at:

<http://shura.shu.ac.uk/20015/>

A Sheffield Hallam University thesis

This thesis is protected by copyright which belongs to the author.

The content must not be changed in any way or sold commercially in any format or medium without the formal permission of the author.

When referring to this work, full bibliographic details including the author, title, awarding institution and date of the thesis must be given.

Please visit <http://shura.shu.ac.uk/20015/> and <http://shura.shu.ac.uk/information.html> for further details about copyright and re-use permissions.

POLYTECHNIC LIBRARY
FOND STREET
SHEFFIELD S1 1WB

100263111 4

TELEPEN



Sheffield City Polytechnic Library

REFERENCE ONLY

ProQuest Number: 10697322

All rights reserved

INFORMATION TO ALL USERS

The quality of this reproduction is dependent upon the quality of the copy submitted.

In the unlikely event that the author did not send a complete manuscript and there are missing pages, these will be noted. Also, if material had to be removed, a note will indicate the deletion.



ProQuest 10697322

Published by ProQuest LLC (2017). Copyright of the Dissertation is held by the Author.

All rights reserved.

This work is protected against unauthorized copying under Title 17, United States Code
Microform Edition © ProQuest LLC.

ProQuest LLC.
789 East Eisenhower Parkway
P.O. Box 1346
Ann Arbor, MI 48106 – 1346

Synthesis and Characterisation of Novel Electronic Materials

by

SEAN D. MARSDEN BSc.

A thesis submitted to the Council of National Academic Awards
in partial fulfilment of the requirements for the degree of
Doctor of Philosophy

Sponsoring Establishment : Department of Chemistry
Sheffield City Polytechnic

Collaborating Establishment : I.C.I. Electronics Group,
Runcorn

April 1990

S. D. MARSDEN

ABSTRACT

The synthesis, electrical and magnetic properties of a series of TCNQ salts including congeners of the model ternary complex (pentamethyl dipyrromethene (3',4')Br)₂ (TCNQ) and a second series of salts based upon the bipyridinium cations are reported. The effect of solvent inclusion on the properties of ternary salts are also presented. Finally the synthesis and properties of Langmuir-Blodgett films of amphiphilic dipyrromethene, bipyridinium and picolinium salts are discussed.

The stoichiometry of a bipyridinium TCNQ salt takes the value of 1:5, where the cation length determines the stoichiometry. The salt is a small band gap semiconductor. The temperature dependence of the magnetic susceptibility varies according to the Curie-Weiss law:

$$\chi = c/(T+\theta)$$

The other bipyridinium forms a 1:1 charge transfer complex with p-phenylene diamine. The synthesis of the polyviologen produces a highly insoluble low molecular mass polymer.

The majority of the dipyrromethene TCNQ complexes are all diamagnetic insulators. However, the magnetic susceptibility of two of the salts were temperature independent and was characterised as Van Vleck paramagnetism. The room temperature conductivity of the penta methyl was 10^{-4} Scm^{-1} whereas the hexamethyl was insulating. This was proposed to be due to differing stacking characteristics.

The properties of the ternary salts were proved to be intrinsic and not solvent induced.

The failure of the amphiphilic dipyrromethene to complex with TCNQ was proposed to be due to steric hindrance which encumbers the close approach of the TCNQ. The Langmuir film of the dipyrromethene was shown to undergo re-orientation on the subphase. The L-B film of a picolinium TCNQ charge transfer salt was shown not to undergo a molecular re-orientation due to the increase in the area of the hydrophobic aliphatic chains.

Acknowledgements

I would like to thank Dr. A. T. Hewson and Dr. G. J. Ashwell for many stimulating discussions relating to this work, their constructive supervision and patience. I am grateful to the National Advisory Board for their support. I am also indebted to my parents and my wife for their encouragement. I wish to express my gratitude to Catherine Appleton for all her hard work in typing this thesis. Finally, I acknowledge my colleagues Sean Cockett, Ian Walker, Richard Broughton and all the technicians at Sheffield City Polytechnic particularly Joan and Lesley for all their help.

Contents

Page No.

Chapter 1 Introduction

1.0	Introduction	1
1.1	Historical Progress	1
1.2	Magnetic Susceptibilities	11
1.2.1	Introduction	11
1.2.2	Basic Theory of Magnetism	14
1.3	Electrical Conductivity	24
1.3.1	Design of Organic Metals	24
1.3.2	One Dimensional Effects	29
1.3.3	The Temperature Dependence of Conductivity	34
1.4	References	38

Chapter 2 Bipyridinium Complexes

2.0	Introduction	45
2.1	Aim	55
2.2	Synthesis	58
2.3	Optical Studies	68
2.4	Electrical and Magnetic Properties	71
2.5	Experimental	77
2.5.1	General Information	77
2.5.2	Experimental Methods	77
2.6	References	84

Chapter 3 Ternary Complexes

3.0	Introduction	88
3.1	Solvent Inclusion in the Sulphonium Ternary Salts ..	90
3.1.1	Introduction	90
3.1.2	Synthesis	91
3.1.3	Differential Scanning Calorimetry Studies	91
3.1.4	Magnetic Studies	93
3.2	Dipyrrylmethene Ternary Complexes	99
3.2.1	Introduction	99
3.2.1.1	Properties and Reactions	102
3.2.2	Synthesis	103
3.2.2.1	Preparation of 3,4,5,3',4',5'-hexamethyl dipyrrylmethene hydrobromide	103
3.2.2.2	Hydrolysis of 2-ethoxycarbonyl-3,4,5-trimethyl pyrrole	104
3.2.2.3	Penta and Tetramethyl Dipyrrylmethenes	107
3.2.2.4	Preparation of the charge transfer complexes of TCNQ with Dipyrrylmethene	110
3.2.3	Stoichiometry.. .. .	112
3.2.4	Electrical Conductivity and Magnetic Susceptibility Measurements.. .. .	116
3.2.5	Infra-Red Studies	117
3.3	Experimental	124
3.3.1	General Information	124
3.3.2	Experimental Methods	124
3.4	References	137

Chapter 4 Langmuir-Blodgett Films

4.0	Introduction	141
4.0.1	Historical Review	141
4.0.2	Molecular Assembly Technique	142
4.0.3	Deposition Techniques	145
4.0.4	Film Forming Materials	148
4.0.5	Conducting Films	154
4.1	Aim	160
4.2	Synthesis of Amphiphilic Donors	162
4.2.1	Preparation of 3,5,3',5'-tetramethyl-4,4'-dioctadecyl- dipyrrylmethene hydrobromide	162
4.2.2	Synthesis of the Semi-amphiphilic donor N-dicyanomethylide -N'-octadecyl bipyridinium halide	169
4.2.3	Synthesis of the surface active donor N-methyl-4- dioctadecyl picolinium	171
4.3	Results and Discussion	172
4.3.1	Langmuir-Blodgett Film of 4,4-dioctadecane-3,5,3',5'- tetramethyl dipyrrylmethene hydrobromide	172
4.3.1.1	Formation of the Langmuir Film	173
4.3.1.2	Transfer of monolayers onto the substrate	178
4.3.1.3	Electronic Absorption Spectrum	180
4.3.2	Langmuir Film of N-methyl-4-dioctadecyl Picolinium-TCNQ charge transfer salt	181
4.3.2.1	Formation of the Langmuir Film	181
4.3.2.2	Pressure Area isotherm	183

4.4	Experimental	184
4.4.1	The Langmuir Trough	184
4.4.2	Experimental Procedure of a L-B Film	186
4.4.2	General Information	186
4.4.3	Experimental Methods	187
4.5	References	196
	<u>Appendix</u>	201

1.0 INTRODUCTION

1.1 Historical Progress

In the past few years, the field of quasi-one-dimensional (1-D) organic metals has emerged as being a lively area of research¹⁻⁴. However, relatively few salts synthesised have shown conductivity characteristics of metals, the ones that have include two bipyridinium tetracyano-p-quinodimethane (TCNQ) salts⁵⁻⁷, TTF[Ni(dmit)₂]₂⁸ and BEDT-TTF₂I₃⁹. The majority show conductivity maxima and transitions to insulating states.

Interest in organic materials as being potentially highly conductive began in the 1950's. The first 'organic metal', reported in 1954 was a perylene-bromine complex (perylene-Br_x) which had an electrical conductivity of 1 Scm⁻¹ 10. However, in 1960, Acker and co-workers at Dupont reported the synthesis of the powerful electron acceptor 7,7,8,8-tetracyano-p-quinodimethane (TCNQ) (Figure 1.1.1) and the conductive properties of its simple and mixed valence salts with a variety of cations¹¹.

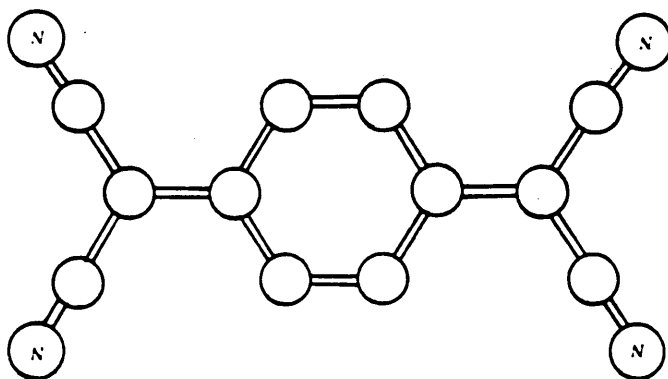
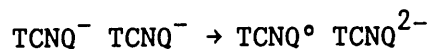


Figure 1.1.1 The acceptor TCNQ.

The simple salts are $M^+(TCNQ)^-$, where M^+ is the cation, and in general these salts are of low conductivity. Examples include alkali metal salts such as $Na^+ TCNQ^-$ which has a room temperature conductivity of $10^{-6} Scm^{-1}$. The conduction requires an electron to be excited from one ionic site to another,



and the low conductivities arise from the need to place two conduction electrons on the same TCNQ molecule.

The mixed valence salts are of the form $M^+(TCNQ)_n^-$, where $n > 1$. An example of this type includes Quinolinium TCNQ ($Qn(TCNQ)_2$) which with a room temperature conductivity of $100 Scm^{-1}$ was the best organic conductor known at that time.

The difference in the conductivities by several orders of magnitude was found to be dependent upon the stoichiometry and the stacking characteristics of the complex.

For high conductivity it is necessary for the molecules to form segregated, for example, -DDDDD- and/or -AAAAA- stacks with a favourable overlap and a short uniform spacing along the stacks. A convenient classification for the stacking characteristics was introduced by Dahm et al¹². The example above is termed 'homosoric', those in which different molecules stack alternately 'heterosoric' and the non-stacked types 'non-soric'. The high conductive metallic form of N-methylphenazinium-TCNQ, NMP_2-TCNQ_3 ¹³ can in part be attributed to its homosoric stacking characteristics, whereas

the semi-conductive form consists of isolated TCNQ triads, which was later described by Ashwell¹⁴ as 'pseudosoric'.

Together with the structural criteria given above Torrance¹⁵, established that another major contribution for high conductivity was the partial transfer of electrons from donor to acceptor.

The suggestion of superconductivity in organic conductors proposed by Little in 1964¹⁶, caused many chemists, physicists and theoreticians to enter the field of organic metals.

However, the next major advance occurred almost a decade after TCNQ had been discovered with the synthesis of the organic donor tetrathiafulvalene (TTF)¹⁷ (Figure 1.1.2) in 1970.

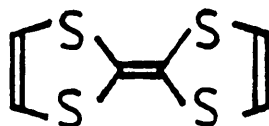


Figure 1.1.2: The donor molecule TTF

This led two years later to the discovery that the chloride salt had a room temperature conductivity of 0.2 Scm^{-1} ¹⁸. In 1973, the 1:1 complex of TTF and TCNQ was formed¹⁹. The degree of charge transfer from donor to acceptor was found to be $0.59e$ ²⁰. The TTF-TCNQ salt was found to be metallic at room temperature with σ 500 Scm^{-1} measured along the direction of the stacking. The conductivity rises dramatically below room temperature to 10^4 Scm^{-1} at 58K, where it undergoes a transition to an insulating state. Since the initial reports on TTF-TCNQ, synthetic chemists have given much attention to new donors containing the 1,3-dithiole ring system of TTF. The preparation of analogues where all the hydrogens were substituted by alkyl groups (such as tetramethyl^{tetra}thiafulvalene TMTTF²¹) was attempted first, closely followed by synthesis to extend the π -orbital system, for example, dibenzotetrathiafulvalene²². Research was not only confined to tetrathiafulvenic derivatives but also tetraselenated^{23,24} and tetratellurated²⁵⁻²⁶ derivatives (for recent reviews on routes to TTF derivatives see M.R. Bryce²⁷ and A. Krief²⁸).

Research is still active in the field with the recently published work of Sugimoto²⁹. Table 1.1.1 provides a summary of the electrical conductivity data on the TCNQ salts of TTF and its derivatives.

Salt	$\sigma RT(\text{Scm}^{-1})$	σ_{max}	T_{max}	$T_{\text{M-I}}$	References
TTF-TCNQ	200-600	$>10^4$	58	58	19, 30, 31
TSF-TCNQ	800	$>10^4$	40	40	23, 32, 33
TMTSF-TCNQ	1000	7000	65	57	34
TMTTF-TCNQ	500	2×10^3	80	50	35
HMTSF-TCNQ	1500	7×10^3	45-75	-	24
TMTTF-DMTCNQ	120	360	80	51	34
TMTSF-DMTCNQ	500	5000	47	42	34

$T_{\text{M-I}}$ is the metal insulator transition temperature.

Table 1.1.1 A summary of the properties of TTF and its derivative complexes

The highly conductive C-T complexes have in common segregated donor and acceptor columns with a short interplanar spacing and incomplete charge transfer. The majority are metallic, but the TSeF complexes with TCNQ show favourable changes in the metallic properties, i.e. stabilisation of the metallic state to lower temperatures, which appears to be due to the presence of the selenium d orbitals.

In comparison to the success of synthesising donor derivatives, far less work has been published on the preparation of new acceptors. Although a new route for TCNQ has been developed³⁶ and significant advances with TCNQ derivatives have been made, early hopes that they would afford conducting complexes have not been realized.

Another major advance in organic metal research came with the observation of the abrupt disappearance of the metal-semiconductor transition at 42K under pressure of the complex tetramethyl tetraselenafulvalene (TMTSF) and 2,5-dimethyl-TCNQ³⁷ and the realization that this transition was associated with the TMTSF stacks. This coupled with the extremely high electrical conductivity with decreasing temperature led Bechgaard et al³⁸ to study a new series of highly conductive salts of TMTSF containing only simple anions of the general formula $(\text{TMTSF})_2\text{X}$, where X is, for example, PF_6^- , AsF_6^- , SbF_6^- , BF_4^- and NO_3^- . A summary of the properties of the TMTSF salts is given in table 1.1.2.

Salt	$T_{M-I}(k)$	$T_c(k)$	Pressure (k bar)	References
$(TMTSF)_2PF_6$	15	0.9	12	38, 39
$(TMTSF)_2AsF_6$	15	1.1	12	38, 40
$(TMTSF)_2ClO_4$	-	1.2	10^{-3}	41
$(TMTSF)_2NO_3$	12	-	-	38
$(TMTSF)_2BF_4$	39	-	-	38
$(TMTSF)_2TaF_6$	-	1.35	<11	42
$(TMTSF)_2SbF_6$	17	0.38	10.5	38, 42

T_{M-I} is the metal-insulator transition temperature.

Table 1.1.2 A summary of the properties of the TMTSF Salts

The materials were found to have high conductivities and low temperature metal insulation transitions³⁸⁻⁴². The series is isostructural and consists of nearly uniform stacks of TMTSF molecules ordered in sheets separated by anion X^- sheets. Application of hydrostatic pressure to $(TMTSF)_2 PF_6$ led to the first observation of a bulk superconducting state in an organic conductor, at a temperature of approximately $0.9K$ ⁴⁰. This was confirmed by observation of a partial Meissner effect⁴³. This was followed by the discovery that the perchlorate salt was found to superconduct at ambient pressure and at a temperature of $1.2K$ ⁴¹.

The isostructural nature and observation that the Se-Se sheet network distances are anion dependent allows a correlation to be drawn between the critical pressure and the size of the different anions. It was suggested that when the superconductors with the larger counter ions are placed under pressure the Se-Se network contracts until its geometry approximates that in $(TMTSF)_2 ClO_4$ i.e. the smaller anions mimic the effect of pressure for superconductivity.

Following the discovery of superconductivity in the $(TMTSF)_2 X$ systems, research into the area quickly diverged into studies of other potential organic donors. This led to the discovery of superconductivity in the first sulphur based donor molecule bis-(ethylene dithio)tetrathiafulvalene (BEDT-TTF) Figure 1.1.3 and the inorganic anion ReO_4^- .

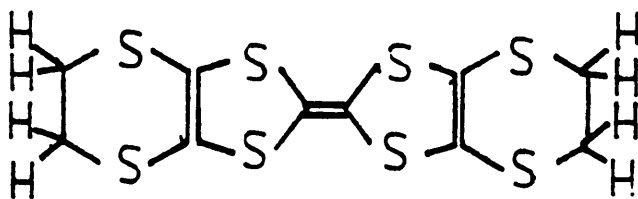


Figure 1.1.3 The donor BEDT-TTF.

Again a pressure of 4kbar, was required to suppress a metal insulator transition at 81k and prior to the onset of superconductivity at about 2K⁴⁴. In 1984, the salt β -(BEDT-TTF)₂I₃ was shown to be superconductive at ambient pressure, with the superconducting transition temperature occurring at 1.5K⁴⁵. The crystal structure reveals that it contains a 'corrugated sheet network' of short interstack S-S contacts sandwiched between linear-symmetric I₃⁻ anions⁴⁶. It was realised that the interstack S-S distances could be altered by changing the length of anion. This led to a new salt (BEDT-TTF)₂IBr₂ which superconducts at ambient pressure and at a temperature of 2.7K⁴⁷. However, a report that the salt β -(BEDT-TTF)₂I₃ becomes superconducting under slight pressure at ~7-8K due to an increased structural ordering^{45, 48} led to a series of β -(BEDT-TTF)₂X salts with linear-symmetric anions of greater length than IBr₂⁻, but shorter than I₃⁻ being synthesised. Table 1.1.3 summarises the superconducting critical temperatures T_c and critical pressures of the (BEDT-TTF)₂X salts.

<u>Salt</u>	<u>T_c(k)</u>	<u>Pressure(k bar)</u>	<u>References</u>
(BEDT-TTF) ₂ ReO ₄	~2	4	44
β-(BEDT-TTF) ₂ I ₃	1.5	10 ⁻³	45
β-(BEDT-TTF) ₂ IBr ₂	2.7	10 ⁻³	47
β-(BEDT-TTF) ₂ AuI ₂	5	10 ⁻³	49
κ-(BEDT-TTF) ₂ (Cu(NCS) ₂	10.4	10 ⁻³	50

Table 1.1.3: A summary of the properties of the (BEDT-TTF)₂X Salts

A structural-property correlation was developed for these isostructural salts⁵¹, which suggested that centro symmetric linear anions with lengths exceeding that of I_3^- would give salts with T_c 's exceeding ~8K. This resulted in an entirely new organic material $K-(BEDT-TTF)_2 Cu (NCS)_2$ ⁵⁰ which was superconducting with a T_c of 10.4K exceeding for the first time the highest T_c of the elements (9K in Nb). This new phase will hopefully promise new structural-property relationships resulting with superconductors with higher critical temperatures.

Since the first successful class of organic conductors based upon TCNQ, many hundred salts have been prepared and characterised. However, only a small percentage have appreciably high conductivity and metallic properties. The magnetic and conduction properties are discussed in sections 1.2 and 1.3 respectively.

1.2.1 Introduction

There are direct and often sensitive relationships between the magnetic properties of matter in bulk and the number and distribution of unpaired electrons in its various constituent atoms or ions.

The characteristic magnetic susceptibilities of diamagnetic and paramagnetic substances are given below in figure: 1.2.1.

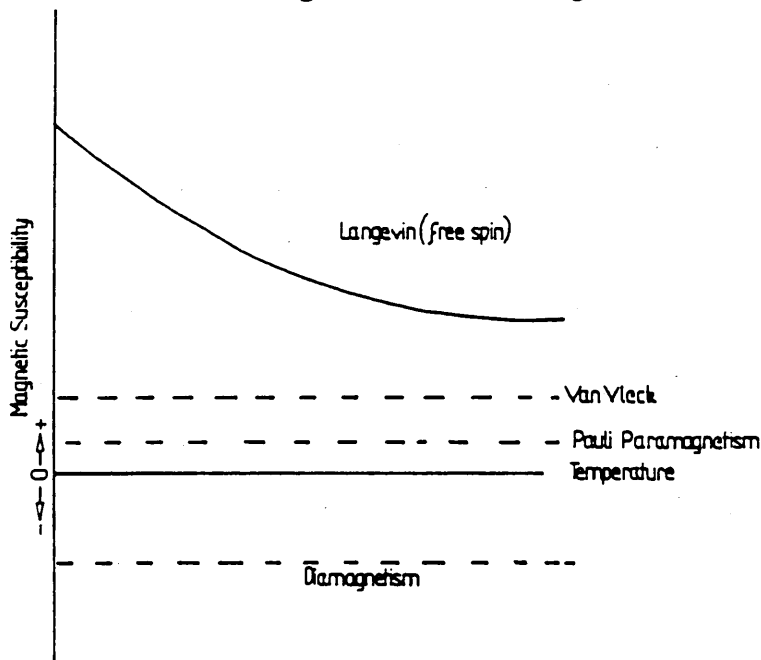


Figure: 1.2.1 The characteristic magnetic susceptibilities

The magnitude and temperature dependence of the spin susceptibility χ_s is a very useful property for characterising different classes of organic conductors⁵². The three major classes are:

1. Materials whose susceptibility increases linearly with temperature in the metallic region. However, at low temperatures there is a sharp fall at the Peierls transition followed by a small Curie tail. This behaviour is typical of uniform chain materials such as TTF-TCNO.

2. Materials which exhibit susceptibilities with a very weak temperature dependence and large upturn at low temperatures.

This is demonstrated by quinolinium $(\text{TCNQ})_2$ ($\text{Qn}(\text{TCNQ})_2$).

3. Charge transfer salts whose TCNQ molecules are grouped into diads, triads or tetrads, which exhibit an activated susceptibility with a singlet to triplet behaviour. For example triethylammonium $(\text{TCNQ})_2$ ($\text{TEA}(\text{TCNQ})_2$).

In the early 1960's Kepler⁵³ showed that the same electrons were involved in both the electrical and magnetic properties, with a close correlation being found. It was found that the materials which exhibit high conductivity for example $\text{Qn}(\text{TCNQ})_2$ were observed to have a nearly temperature independent paramagnetism between 40-300K, while at low temperatures the susceptibility begins to increase rapidly with lowering temperatures⁵³. This was interpreted as Pauli paramagnetism, which is characteristic of a system of non-interacting spins in a degenerate electron gas, such as that found in metals. However, the large low temperature upturn in susceptibility is inconsistent with the above hypothesis and would have to be explained as being extrinsic in origin. Later Bulaevskii⁵⁴ ascribed the increase in susceptibility at low temperature as an intrinsic feature where a one dimensional system of localised spins possessing an antiferromagnetic interaction decomposes into a system of virtually isolated spins at very low temperatures.

In 1984, Ashwell⁵⁵ described an organic conductor $(2,2\text{-DHPE Cl})_x (2,2\text{-DPE})_{1-x} (\text{TCNQ})$, which exhibits a temperature independent susceptibility with no Curie-tail being observed. In view of the high electrical conductivity the temperature independence was attributed to Pauli paramagnetism.

Another salt which shows temperature independent susceptibility is potassium chloranil⁵⁶. However, this material is a semiconductor and its susceptibility is, therefore, not Pauli paramagnetism but was assigned to Van Vleck paramagnetism.

The less conductive TCNQ salts, for example, $\text{TEA}(\text{TCNQ})_2$ were observed to have a temperature dependent magnetic susceptibility which passes through a maximum at a temperature which is related to the magnitude of the magnetic gap. The susceptibility was assigned by Kepler⁵³ to be activated due to a pairwise interaction of spins in which the singlet ground state and a thermally accessible triplet excited state (triplet exciton) are separated in energy by an interaction J . This was shown⁵³ to be equal to $1.61 (KT_c)$ at the temperature T_c where the susceptibility passes through a maximum.

The temperature dependent susceptibility of TTF-TCNQ above 60K is not yet fully understood⁵⁷. However, analysis of the susceptibility above 60K by a technique developed by Tomkiewicz et al⁵⁸, revealed that the contribution from the donor is nearly temperature independent, whereas the contribution from the acceptor is strongly temperature dependent, thus the spin

susceptibility is not Pauli-like. Below 60k the susceptibility becomes an activated singlet-triplet system with a singlet ground state.

The magnetic susceptibility of the superconducting (TMTSF)₂X series, for example (TMTSF)₂PF₆, shows no sharp drop at the temperature at which the salt undergoes a metal to insulator transition³⁸; this may be due to this transition not being of the Peierls-Frohlich type. However, the susceptibility has confirmed the superconducting transition temperature and the bulk nature of the superconductivity. The observation of complete expulsion (Meissner effect) is seen at the superconductive transition temperature in a number of these salts^{41,43}.

1.2.2 Basic theory of Magnetism

The basic theory of magnetism as it relates to the discussion of the results and introduction is outlined below:

The magnetic susceptibility (χ) per unit volume is defined as:

$$\chi = \frac{M}{B} \quad \text{..... Equation 1.2.2.1}$$

where B is the applied magnetic field intensity and M is the magnetic moment per unit volume.

However, there will be a positive contribution from the unpaired electrons (χ_s) and a negative contribution from the electrons in the closed shells (χ_{DIA}). Thus, the total susceptibility (χ_{TOT}) is given by the equation:

$$\chi_{TOT} = \chi_s - \chi_{DIA} \quad \text{.... Equation 1.2.2.2}$$

The diamagnetic susceptibilities (χ_{DIA}) have been determined for most atoms and the molar diamagnetic susceptibility may be calculated by summing the atomic values. The χ_s values are derived by adding χ_{DIA} to χ_{TOT} ; χ_{DIA} is assumed to be temperature independent.

When a magnetic field is applied, the unpaired electrons present in the material show a tendency to align themselves in the magnetic field and magnetization results. Increasing the temperature, acts to partially cancel the ordering effect of the applied magnetic field. If there is interaction between the spins, then $\chi \propto T^{-1}$ and Curie law is obeyed.

$$\chi = \frac{NJ(J+1)g^2\mu_B^2}{3K_B T} = \frac{C}{T} \quad \text{..... Equation 1.2.2.3}$$

where J = the total angular momentum quantum number

g = gyromagnetic ratio or magnetogyric ratio

For an electron spin $g = 2.0023$, usually taken as 2.00.

μ_B = Bohr magnetron

N = Number of spins

C = Curie Constant

Curie law behaviour is not commonly found in organic conductors and in the majority of salts the spins interact with each other with the interaction possessing some degree of anisotropy.

However, some TCNQ salts^{57,59} have been observed to show Curie law behaviour at low temperatures.

It was also observed that the magnetization of some non-ferromagnetic metals is independent of temperature. This is known as Pauli paramagnetism. The susceptibility is only 1/100th that of the expected Curie value.

The result from Curie law (equation: 1.2.2.3) tells us that the energy resisting the spin alignment to the field is KT

However, in Pauli paramagnetism the energy is the Fermi energy KT_F , where T_F is the Fermi temperature which is constant.

Hence,

$$\chi_p = \frac{N\mu_B^2}{KT_F} \dots\dots\dots \text{Equation 1.2.2.4}$$

For a system of non-interacting electrons, in a tight-binding band, the experimental χ_p values may be used to determine the transfer integral, t and therefore the electron bandwidth $4t$. The Pauli susceptibility may be represented⁵⁹.

$$\chi_p = \frac{N\mu_B^2}{t\lambda \sin(\frac{1}{2}\lambda\rho)} \dots\dots\dots \text{Equation 1.2.2.5}$$

where ρ is the number of electrons per TCNQ site.

It is also noteworthy to mention a weak paramagnetism that is independent of temperature known as Van Vleck paramagnetism⁶⁰.

This arises from a coupling of the ground state of the system with excited states of higher energy under the influence of the magnetic field. The susceptibility has been shown to vary according to the equation:

$$\chi_{VV} = \frac{2Nk_s/\mu_z \langle 0 \rangle^2}{\Delta} \dots\dots\dots \text{Equation 1.2.2.6}$$

where $\langle s/\mu_z/0 \rangle$ is the non diagonal matrix element of the magnetic moment operator, connecting the ground state 0 and the excited state s.

In addition to the simple paramagnetism discussed above, where Curie law is followed, there are more complex forms of magnetic behaviour known as ferromagnetism and anti-ferromagnetism.

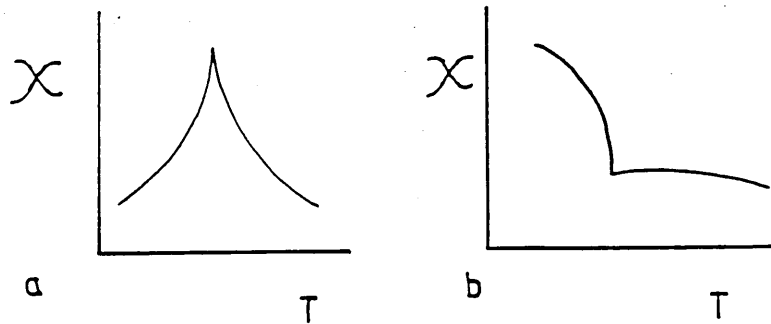


Figure: 1.2.2 Temperature dependence of magnetic susceptibility
a. antiferromagnetic b. ferromagnetic materials

A ferromagnetic interaction is one which favours the alignment of spins parallel to one another whereas antiferromagnetic materials favour antiparallel alignment of spins.

The susceptibility of a classical ferromagnet and antiferromagnet both pass through a critical temperature known respectively as: the Curie temperature T_c and the Neel point T_N . The susceptibility above these critical temperatures vary according to the Curie-Weiss law;

$$\chi = C/(T+\Theta) \dots\dots\dots \text{Equation 1.2.2.7}$$

where Θ is the Weiss constant.

The magnitude of Θ is related to the strength of the ferromagnetic and antiferromagnetic exchange interactions, thus in a Curie paramagnet $\Theta=0$. The susceptibility of many salts at low temperatures increases sharply but the temperature dependence often exhibits deviations from the Curie law behaviour due to spin-spin interactions^{57,61}, for example, Qn(TCNQ)_2 ⁶².

The large Curie tail in susceptibility at low temperatures of Qn(TCNQ)_2 was first suggested by Kepler⁵³ to be an intrinsic property rather than due to impurities or defects. Later this was ascribed to a model where the spins are localised on alternate TCNQ's in the stack and experience an antiferromagnetic interaction between them. At high temperatures the linear spin system is homogeneous in respect of the antiferromagnetic interaction. As the temperature is lowered, the spin system is decomposed into weakly interacting sub-systems which determine the low temperature susceptibility.

The susceptibility usually varies as $\chi \propto T^{-\alpha}$ where $\alpha < 1$. The model suggests that there is random variation in site energy leading to a random spin distribution along the chain⁶³ and the exchange interaction (J_m) between the neighbouring magnetic sites decays exponentially with distance between spins. This magnetic model refers to a Random Exchange Heisenberg Antiferromagnetic Chain (REHAC).

Clark et al⁶⁴ proposed a model in which every alternate J_m in the linear chain is set to zero, thus splitting up the chain into a system of interacting pairs. The susceptibility of a pair is determined by:

$$\chi = \frac{2\mu_B^2 g^2}{KT[3+\exp(J/KT)]} \dots\dots\dots \text{Equation 1.2.2.8}$$

In many other semiconductive TCNQ salts, the susceptibility passes through a maximum at a temperature which is related to the magnitude of the magnetic gap. The susceptibility exhibits a temperature dependence which may be fitted to an activation law. E.S.R.⁶⁵ and static susceptibility measurements⁵³ have shown that the susceptibility is activated due to the fact that the odd electrons with the TCNQ anion radicals are paired in quasimolecular states consisting of a ground singlet state and a thermally accessible triplet state, separated in energy by an interaction J.

In the late 1950's, Bijl, Kainer and Rose-Innes⁶⁶ examined the E.S.R. absorption of a series of charge-transfer complexes of quinones and p-phenylene diamines. In, all cases, strict conformity to a Curie law dependence was exhibited. However, they suggested that in certain salts the radicals could interact to produce magnetic states of higher multiplicity than the doublet state of single unpaired spins. The radicals were proposed to interact in pairs to form a singlet (antiparallel) state and a triplet state (spin parallel) and gave the expression for E.S.R. signal intensities to temperature as:

$$I \propto 1/T[\exp(J/kT)+3]^{-1} \dots\dots\dots \text{Equation 1.2.2.9}$$

Later Chesnut and Phillips⁶⁵ established such an interaction for TEA (TCNQ)₂, MePh₃P(TCNQ)₂ and morpholinium (TCNQ) salts and found that the J values derived from the slopes of lnIT versus reciprocal temperatures were 0.034 eV, 0.062 eV and 0.41 eV respectively.

Later, Kepler⁵³ found that the susceptibility of the materials could be fitted to the expression:

$$\chi = \frac{2Ng^2\mu_B^2}{[3+\exp(\frac{J}{KT})]KT} \dots\dots\dots \text{Equation 1.2.2.10}$$

where N is the number of the triplet levels in the sample (both vacant and occupied).

This model suggests that the spins interact into isolated pairs. However, there is a possibility of an antiferromagnetic interaction between the nearest neighbours, which can be described by the one-dimensional Heisenberg Hamiltonian.

$$\mathcal{H} = \sum_m (2J_m S_m S_{m+1} - g \mu_B H S_m^z) \dots\dots \text{Equation 1.2.2.11}$$

where J_m = the exchange interaction; the precondition for a homogeneous spin system is that the spins are spaced equally along the chain.

S_m, S_{m+1} = the spins of a pair on the magnetic sites m and m+1.

Bonner and Fisher⁶⁷, calculated that the susceptibility was related to the temperature by

$$\chi = \frac{g^2 \mu_B^2 N}{KT_{\max} \eta} \dots\dots\dots \text{Equation 1.2.2.12}$$

Bulaevskii et al⁵⁴ found that the maxima in the susceptibility of $\text{Qn}(\text{TCNQ})_2$ and $\text{Ad}(\text{TCNQ})_2$ may be fitted with the above expression with $\eta=0.1+/-0.01$. These materials must possess a homogeneous one-dimensional spin systems which may be attributable to the short, regular inter-site spacing of the TCNQ stack in homologous columns. However, as stated earlier, in intermediate conductivity complexes, the TCNQ units are grouped into diads, triads and tetrads which leads to an interaction between adjacent spin pairs and thus the alternate values of J are non zero.

For systems in which there is some interaction between adjacent pairs, the above Hamiltonian equation 1.2.2.11 has to be modified⁶⁸.

$$\mathcal{H} = \sum_m J(S_m S_{m+1} + \gamma S_m S_{m-1}) \dots\dots\dots \text{Equation 1.2.2.13}$$

where $S_m S_{m-1}$ describes the interaction between the spins on site m with spins on neighbouring sites (m-1) where the exchange interaction is $J\gamma$ (γ represents the degree of alternation between spin pairs and is known as the alternation parameter).

For the susceptibility for a linear chain of spins with values for the alternation parameter of 0 to 0.9 Bulaevskii⁶⁸ developed the equation:

$$\chi = \frac{2N\mu_B^2 g^2 a(\gamma)}{KT \exp(-J\Delta(\gamma))} \quad \text{..... Equation: 1.2.2.14}$$

where $a(\gamma)$ and $\Delta(\gamma)$ are tabulated functions of the alternation parameter.

However, when the alternate values of J are zero and $a(\gamma)$ and $\Delta(\gamma)$ are both unity then equation 1.2.2.14 reduces down to equation 1.2.2.8 where the condition $\exp(J/KT) \gg 3$ applies.

1.3 Electrical Conductivity

The charge transfer salts of TCNQ may be classified in a general way, based on both their stoichiometry and conductivity¹.

I. the simple ionic salts and charge transfer complexes, for example K TCNQ and NMQn-TCNQ, with a neutral or ionic ground state have a low conductivity $\sigma_{300} < 10^{-3} \text{ Scm}^{-1}$ and a wide band gap.

II. the simple salts which have a very high conductivity, and metallic temperature dependence, for example NMP TCNQ and TTF-TCNQ.

III. the complex salts with intermediate conductivity of 10^{-4} to 10 Scm^{-1} at room temperature, for example TEA(TCNQ)₂.

IV. the complex salts which are 'metallic' near 300K with $\sigma_{300} > 50 \text{ Scm}^{-1}$, for example Qn(TCNQ)₂.

1.3.1 Design of organic metals

A variety of features appear to be needed for the formation of a highly conducting 1-D material and can be divided into two main categories:

1. Requirements for the molecular crystal structure.
2. Requirements for the electronic structure of the component molecules and complexes.

1. Requirements for the molecular crystal structure

The fundamental requirement of the structure of an organic conductor is that the molecules are arranged to form a suitable

conduction pathway. This is usually provided by closely matching the physical dimensions of the donor and acceptor which facilitates packing in the crystal. Thus planar organic molecules have the greatest probability of permitting the close approach necessary for the achievement of strong band formation, and allowing charge transport along the columns under the influence of an applied field.

In the case of the charge transfer salts which rely for conduction on charge transport along the TCNQ stacks only, for example NMP-TCNQ, the structure consists of segregated stacks of donor and acceptor moieties with the TCNQ stacks in uniform columns with an optimum interplanar separation of $3.2 \pm 0.1 \text{ \AA}$ ^{19,30,31,34,35,24}.

The two chain conductors, have an analogous arrangement of molecules. The contribution to the conductivity is from electron and hole transport along the anion and cation stacks respectively. The sulphur or selenium donor molecules also stack in columns with a short interplanar spacing. In TTF-TCNQ⁶⁹ the inter TTF and inter TCNQ spacing are 3.74 \AA and 3.17 \AA respectively. Analogous overlaps occur in the corresponding selenium donor salts with an accompanying increase in the separation.

A lower conductivity would result when there is a discontinuity in the regular short spacing caused by the infinite stacks of the like species being divided into diads, triads or tetrads.

Steric effects also play an important role in determining the stacking characteristics of the charge transfer complexes. The TCNQ complexes of TTF⁶⁹, tetramethyl-TTF⁷⁰ and diethyl dimethyl-TTF⁷¹ have segregated structures while the complexes of tetraethyl-TTF⁷² and octamethylene-TTF⁷³ have mixed stack structures. In these complexes it is assumed that the bulky alkyl groups hinder close intercolumnar contacts between the conjugated parts of the donor and acceptor systems and thus favour the formation of the mixed-stack less conductive phase.

2. Requirements for electronic structure of the component molecules and complexes.

A major criterion for high conductivity is the presence of unpaired electrons on the donor and/or acceptor molecules in the complex⁷⁴ and incomplete charge transfer from donor to acceptor⁷⁵. The degree of charge transfer depends upon the difference (I-A) between the donor ionization potential (I) and the acceptor electron affinity (A) as well as the Madelung energy (Em)¹⁵.

As a general rule, the ionization potential of the highly conductive TCNQ complexes usually fall within the range 6.5 to 7.0 eV⁷⁶⁻⁷⁸. If the donor ionization energy is considerably higher, as for example in anthracene, than 7eV their 1:1 complexes will have a neutral ground state with $\rho=0$ whereas for the donors with a low ionization potential, for example the alkali metals, their 1:1 complexes will be ionic with $\rho=1$. However, low ionization as obtained for tetrathiatetracene ($I=4.56\text{eV}$)⁷⁹ is not necessarily a disadvantage. Donors of this size readily form 1:2 complexes with TCNQ and the higher stoichiometry yields a mean charge density of 0.5e on the lattice sites^{80,81}.

The conductivity is dependent upon the degree of charge transfer and is highest when ρ is not a simple fraction. If ρ is incommensurate the electrons can correlate their movement to avoid both the on site electron-electron coulomb repulsion energy (U_0) and the neighbouring site repulsion energy (V_1). Table 1.3.1 shows the relationship between ρ and the conductivity.

The electron-electron Coulombic repulsion in organic materials forces the electrons to stay away from each other and thus governs the ease with which carriers can migrate along the conductive chains. In the simple ionic salts it is necessary to place two electrons on the same TCNQ lattice site during the

conduction process and the conductivity is limited by the high on site electron-electron Coulomb repulsion energy - the difference U is given by:

$$U = U_0 - V_1 \quad \text{..... Equation 1.3.1}$$

U is thus the difference between the Coulomb repulsion energy (U_0) when two electrons are on the same TCNQ molecule and the repulsion (V_1) when they are on adjacent molecules. If the energy U is large (compared with $4t$) the material will be an insulator (Mott insulator).

Salt	ρ	$\sigma_{R.T.}$	Ref.
TEA(TCNQ) ₂	0.5	6.5	82
Qn(TCNQ) ₂	0.5	100	1,11
TMTSF-TCNQ	0.57	1000	37,84
TTF-TCNQ	0.59	200-600	19,20
TSF-TCNQ	0.63	1000	83,84
HMTSF-TCNQ	0.74	1500	24,84
NMQn-TCNQ	1	$\times 10^{-7}$	74,15
TEA-TCNQ	1	$\times 10^{-9}$	74,15
Na TCNQ	1	10^{-6}	85,86

*denotes powder conductivity

Table 1.3.1: The relationship between ρ and the room temperature conductivities of a number of TCNQ salts.

To overcome this problem it is necessary to reduce the mean ionic charge on the lattice sites. This can either be achieved by forming salts with a cation to TCNQ ratio greater than 1:1, for example the complex TCNQ salts (in this system conduction may occur without the need to place two electrons on the same lattice) or in the 1:1 complexes by selecting a suitable electron donor with an intermediate ionization potential of 6-7eV in order to obtain a partial charge transfer.

Torrance¹ proposed that the large conductivity of class II and IV has been achieved, not by decreasing the Coulomb and other strong interactions but by avoiding them by having ρ incommensurate.

1.3.2 One dimensional effects

A variety of features for the formation of highly conducting materials have now been discussed, and it is now appropriate to look at the problem of instabilities that limit the metallic conductivity. However, it is first necessary to discuss the general nature of 1-D systems.

A definition initially given by Heeger and Garito⁸⁷ is that a system is termed quasi-1-D if the electronic meanfree path λ_{11} along a specific direction is comparable to or greater than the lattice constant in that direction, whereas for motion perpendicular to the chosen direction, λ_{\perp} is much less than the lattice constant in that direction. There are normally strong interactions along the chains due to the intermolecular

overlap, but weak transverse interaction. As a result, the electrical conductivity is highly anisotropic. The conductivity is often of the order of few hundred times greater parallel to the chains than perpendicular, for example, TTF-TCNQ^{88,89}.

It is found, however, that at some temperature T_m , most of the quasi 1-D systems undergo a transition to an insulating state. The degree of interchain interactions have been shown to have a direct effect on the critical temperature T_m . The reasons for this transition will now be examined.

One-dimensional systems can display a wide variety of instabilities and these influence the temperature dependence of the electrical conductivity. That a 1-D metal is unstable against static lattice distortions was first pointed out by Peierls⁹⁰. He predicted that a one dimensional metallic system was liable to undergo a periodic lattice distortion leading to a localisation of charge and an insulating stage.

This can be illustrated by considering a linear array of N molecules, each of which has one valence electron (Figure 1.3.1a), for a 1-D metal the overlap integral of electron wave functions (t) on neighbouring sites is large enough to form a conduction band of width $4t$. In a nearest-neighbour tight binding approximation the band would be half-filled and if the Coulomb interactions are neglected the system may be metallic. The conduction band which results is shown in figure (1.3.1.b).

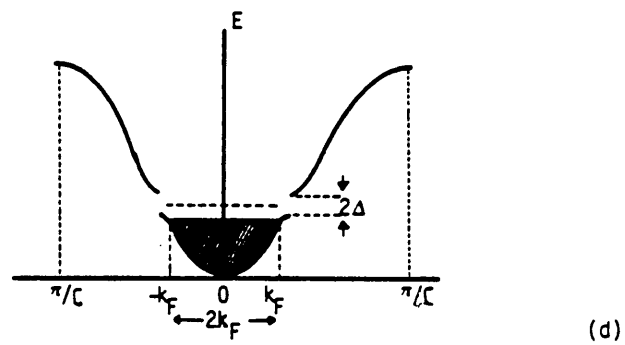
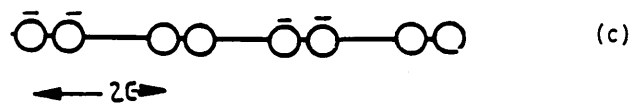
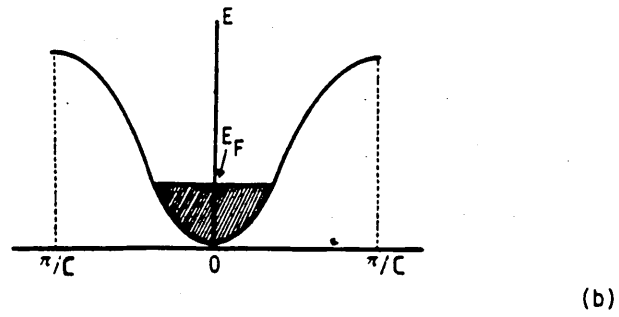
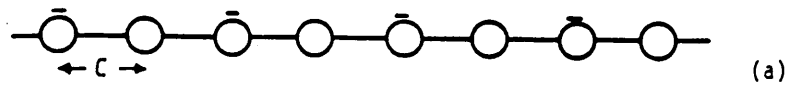


Figure: 1.3.1 Energy wave vector diagram and stacking models of a quasi-one dimensional conductor.

The Fermi wave vector of the electrons within the band is given by $\pi/2c$.

However, for a static periodic distortion (Figure 1.3.1c) the system can be viewed as a linear array of $N/2$ interacting dimers. For a given dimer, the low-lying bonding orbital that arises from the mixing of monomeric molecular orbitals will be filled. An energy gap of 2Δ will open at the Fermi level which separates the occupied orbitals from the unoccupied antibonding band. The distortion occurs with wavevector $2k_F$. This is illustrated in figure 1.3.1d.

Below the transition temperature the material exhibits an activated conductivity or, depending on the ratio $2\Delta/KT$, becomes insulating.

The temperature at which the Peierls transition occurs is usually dependent upon the strength of the transverse overlap between wave functions on neighbouring chains or to direct Coulomb interaction between charge density waves. It would be expected that the greater the coupling the higher the transition temperature.

The Peierls instability may be stabilised by the introduction of disorder into the lattice or by pressure.

The introduction of disorder by, for example doping TTF-TCNQ with tetraselenafulvalene (TSF)⁹¹ has been shown to lower the metal-insulator transition. The inclusion of the TSF into the donor stack leads to the coupling between the stacks to vary randomly in strength due to the differences in the interstack S-N and Se-N contacts. This disrupts the commensurability of the Peierls modulation and condensation of the charge density wave and inhibits the periodic ordering. Other examples of disorder stabilisation include anion ordering in the series of organic metals (TMTSF)₂X⁹² and anion disorder in the tetrathiotetracene (TTT) salts⁹³.

Modest pressure has been shown to suppress the M-I transition of the (TMTSF)₂X salts³⁸⁻⁴². The metallic state in TMTSF-DMTCNQ is stabilised³⁴.

In TMTSF-DMTCNQ the enhanced conductivity and suppression of the metal-insulator transition may arise if the wavelength of the Peierls Modulation can be varied under the influence of pressure, $2K_f$ may become incommensurate with the lattice period and the charge density wave may vary freely. The experimental evidence which supports this proposal is the observation of an increase in the anisotropy at ambient temperature⁹⁴ of 25% as the pressure is increased from 0 to 13 Kbar. The increase in the conductivity along the chains reflects the greater contribution from the depinned charge density waves.

1.3.3 The temperature dependence of conductivity

The temperature dependence of conductivity (σ) is made up of the temperature dependence of the mobility of the carriers (μ) and number of the carriers (n). This may be expressed:

$$\sigma = \sigma_0 T^{-\alpha} \exp(-\Delta/T) \dots\dots\dots \text{Equation 1.3.2}$$

where $T^{-\alpha}$ is the temperature dependence of the mobility and $\exp(-\Delta/T)$ is the temperature dependence of the carrier concentration. This relationship forms the basis of a mobility model proposed by Epstein et al¹ and is found to be a good fit to the observed conductivity over a wide temperature range for many salts.

Most of the mixed valence salts (Class III) and simple ionic salts (Class I) exhibit a strongly activated conductivity temperature dependence below room temperature and may be classed as semiconductors with intermediate and low conductivities respectively.

There have been attempts to ascribe the activation energy observed to an intrinsic semiconductor gap⁹⁵. The salt $\text{Cs}_2(\text{TCNQ})_3$ forms a segregated stack in which a trimeric modulation exists along the TCNQ stack. This introduces a band gap because the bonding overlap interactions within the trimer are larger than the interactions between molecules belonging to different trimers. If no impurities are present, the lower tight binding band is filled and the middle and upper bands are empty. In $\text{Cs}_2(\text{TCNQ})_3$, the loss of the Cs s electron leads to a closed shell configuration and there are no states available

for conductivity. Thus $\text{Cs}_2(\text{TCNQ})_3$ has only filled bands and displays semiconductor properties with a d.c. conductivity:

$$\sigma = \sigma_0 \exp(-E_a/KT) \dots\dots\dots \text{Equation 1.3.3}$$

where E_a is an apparent activation energy for the thermal generation of free electrons or holes: E_a/K is often written as Δ . Radical ion salts exhibiting a strong temperature-activated conductivity of the form given in equation 1.3.3 generally have a room temperature conductivity of 10^{-6} - 10 Scm^{-1} depending on the magnitude of E_a . For the transverse direction, the weak interactions between TCNQ orbitals suggest transport is apt to be hopping-like.

Activated hopping has been proposed for several class III salts. The observation of a temperature independent thermoelectric power has led to a hopping description for the conductivity in $\text{TEA}(\text{TCNQ})_2$ ^{96,97} for $T > 200\text{k}$. In this salt, the observed activation energy is thought to be derived from a gap due to Coulomb interactions. Above 300k the observation of curvature in the $\ln \sigma$ vs reciprocal temperature plot for $\text{TEA}(\text{TCNQ})_2$ has been attributed to the onset of a semiconductor to a metal transition⁹⁸. This implies a gap in the low temperature state which is renormalized to zero about 300k. This has been previously proposed for the semiconductor to metal transition for the class II, NMP-TCNQ salt at 200k⁹⁹.

The class II materials can be divided into two categories.

1. Those compounds that have a broad weak maximum in their conductivity, (T_m) for example NMP-TCNQ. The maximum variation in $\sigma_{(T_m)}/\sigma_{(285)} < 2$ and σ_{300} is generally about 10^2 Scm^{-1} .
2. The salts which generally have conductivities with $\sigma_{RT} = 4 \times 10^2$ to 10^3 Scm^{-1} the majority of which upon cooling undergo metal to insulator transitions at T_m , signalling the onset of a Peierls instability, for example TTF-TCNQ. In most cases $\sigma_{(T_m)}/\sigma_{(295)} > 2$.

The best fit for the conductivity for class II, salts and also the class (IV) salts, for example $\text{Qn}(\text{TCNQ})_2$, have been made using the mobility model of Epstein¹. The temperature dependence of the conductivity for these salts approximately obeys the relationship:

$$\sigma_{(T)} = AT^{-\alpha} \exp(-E_a/KT) \dots \text{Equation 1.3.4}$$

where α is a sample dependent constant and A is fixed by setting σ_{295} .

For NMP-TCNQ, $E_a = 900\text{k}$ and $\alpha \sim 4$. Epstein et al¹ have interpreted equation 1.3.4 in terms of the product of an activated carrier concentration dependence $n \propto \exp(-E_a/KT)$ and a large strongly temperature-dependent mobility $\mu \propto T^{-\alpha}$. The product of $n(T)$ and $\mu(T)$ has a maximum at $T_m = E_a/\alpha$. The conductivity of TTF-TCNQ can also be fitted to the equation where $E_a/K = 0$ and $\alpha = 2.3$.

In the metallic region the conductivities of the highly conductive class II (2) salts often give a reasonable fit to the expression³³

$$\sigma^{-1} = \rho_R + \lambda T^n \dots\dots\dots \text{Equation 1.3.5}$$

where ρ_R is the temperature-independent resistivity, λ and n are sample independent with λ being constant, $n \sim 2$. Groff³¹ has determined α to be between 2.23 to 2.40 with a value of 2.33 representing the majority of samples for TTF-TCNQ.

The difference in the conductivity temperature dependence between the two categories of class II salts can be explained if it is assumed that there is an energy gap E_a/k , persistent at all temperatures for the less conductive class II(1) and a zero gap for the highly conductive salts of class II(2).

In summary, if the charge transfer is complete a semiconductive class I and III radical ion is produced. In this case Δ/α is large, since Δ is large and α is small, implying a weakly temperature dependent mobility. For the class IV and class II (1) salts, for example NMP-TCNQ where $\rho=0.67^{100}$ the materials are best characterized as band semiconductors with large onsite Coulombic repulsions and carrier mobilities that are strongly temperature dependent. For the class II (2) salts where $\rho=0.5$ they display metallic conductivity since the lower density of electrons minimizes the effects of the Coulombic repulsive interactions. At temperatures below T_m there is a metal to insulator transition as a result of the onset of a Peierls instability.

1.4 REFERENCES

1. Synthesis and Properties of Low-dimensional Materials, Annals N.Y. Acad. Sci. 313 (1978).
2. Proceedings of the International Conference of Low-dimensional Synthetic Metals (Helsinki), Chemica Scripta, 17 (1981).
3. Proceeding of the International Conference of Low-dimensional Conductors (Boulder); Mol. Cryst. Liq. Cryst. 86, (1982).
4. Electrical and Related Properties of Organic Solids (ERPOS4-Zamek Ksiaz), Materials Science, X (1984).
5. G.J. Ashwell, D.D. Eley and M.R. Willis; Nature, 259, 201 (1976).
6. G.J. Ashwell, Nature, 290, 686, (1981).
7. G.J. Ashwell, Mol. Cryst. Liq. Cryst., 86, 1887 (1982).
8. P. Cassoux, L. Valade, M. Bousseau, J. P. Legros, M. Garbauskas and L. Interrante; Mol. Cryst. Liq. Cryst., 120, 377 (1985).
9. G.W. Crabtree, K. D. Carlson, L. N. Hall, P. T. Copps, H. H. Wang, T. J. Emge, M. A. Beno and J. M. Williams; Phys. Rev; B30, 2958 (1984).
10. H. Akamata, H. Inokuchi, Y. Matsunaga; Nature, 173, 168 (1954).
11. D. S. Acker, R. J. Harder, W. R. Hertler, W. Mahler, L. R. Melby, R. E. Benson and W. E. Mochel; J.Am.Chem.Soc., 82 6408 (1960).
12. D. J. Dahm; P. Horn, G. R. Johnson, M. G. Miles and J. D. Wilson; J. Cryst Mol. Struct 5, 27, (1975).
13. L. B. Coleman, S. K. Khanna, A. F. Garito, A. J. Heeger and B. Morosin; Phys. Lett. 42A, 15 (1972).
14. G. J. Ashwell; Phys. Stat. Sol. (b), 86, 705 (1978).
15. J. B. Torrance; Acc. Chem. Res., 12, 79 (1979).
16. W. A. Little, Phys. Rev.; 134, 6A, A1416 (1964).
17. F. Wudl, G. M. Smith, E. J. Hafnagel; Chem. Commun., 1435, (1970).

18. F. Wudl, D. Wobschull, E. J. Hafnagel; J.Am.Chem.Soc., 94, 670 (1972).
19. J. Ferraris; D. O. Cowan, J. V. Walat ka and J. H. Perlstein; J.Am.Chem.Soc., 95, 948 (1973).
20. R. Comes; Chemistry and Physics of one-dimensional Metals 25 NATO Advanced study Institutes series (B-Physics) Plenum Press, N.Y. Ed H. J. Keller, (1977).
21. J. P. Ferraris, T. O. Poehler, A. N. Bloch and D. O. Cowan; Tetrahedron lett, 2553 (1973).
22. W. R. Hurtley and S. Smiles; J.Chem.Soc., 1821 (1976).
23. E. Engler and V. V. Patel; J.Am.Chem.Soc., 96, 7376, (1974).
24. A. N. Block ; Phys. Rev lett, 34, 1561, (1975).
25. F. Wudl and E. Aharon-shalom; J.Am.Chem.Soc., 104, 1154, (1982).
26. K. Lerstrup, D. Talham, A. Bloch, T. Poehler and D. Cowan; J.C.S. Chem. Commun., 336, (1982).
27. M. R. Bryce; Aldrichimica Acta, 18, 73 (1985).
28. A. Krief; Tetrahedron, 42, 1209 (1986).
29. T. Sugimoto, H. Awaji, I. Sugimoto, Y. Misaki and Z. Yoshida; Synthetic Metals, 19, 569 (1987).
30. L. B. Coleman, M. J. Cohn, D. J. Sandman, F. G. Yamagishi, A. J. Garito and A. J. Heeger; Solid state commun 12, 1125 (1973).
31. R. P. Groff, A. Suna and R. E. Merrifield; Phys. Rev lett, 33, 418 (1974).
32. E. M. Engler and V. V. Patel; J. Org. Chem., 40, 387 (1975).
33. S. Etemad, T. Penny, E. M. Engler, B. A. Scott and P. E. Seiden; Phys. Rev. Lett 34, 741 (1975).

34. C. S. Jacobsen, K. Mortensen, J. R. Andersen and K. Bechgaard;
Phys. Review, B18, 905 (1978).
35. R. Schumaker, M. Ebenhaln, G. Castro, R. L. Greene; Bull. Am.
Phys. Soc. II, 20, 495 (1975).
36. S. Yamaguchi and T. Hanafusa; Chemlett, 689, (1985).
37. C. S. Jacobson, K. Mortensen, J. R. Andersen, K. Bechgaard; Phys.
Rev. B: Condens. Matter, 18, 905 (1978).
38. K. Bechgaard, C. S. Jacobsen, K. Mortensen, H. J. Pedersen and
N. Thorup; Solid State Commun., 33, 1119, (1980).
39. D. Jerome, A. Mazaad, M. Ribault, K. Bechgaard; J. Phys.lett, 41,
L195 (1980).
40. M. Ribault, J. P. Pouget, D. Jerome and K. Bechgaard; C. R. Acad.
Sci. Paris, 291, B145 (1980).
41. K. Bechgaard, K. Carneiro, F. B. Rusmussen, M. Olsen, G. Rindor ,
C. S. Jacobsen, H. J. Pesersen and J. C. Scott; J.Am.Chem.Soc.,
103, 2440 (1981).
42. S.S.P. Parkin, M. Ribault, D. Jerome and K. Bechgaard, J.Phys.C.
Solid State Phys. 14, 5305 (1981).
43. K. Andres, F. Wudl, D. B. McWhan and A. L. Stevens, Phys. Rev
lett, 45, 1449 (1980).
44. S.S.P. Parkin, E. M. Engler, R. R. Sch maker, R. Lagier, V. Y.
Lee, J. C. Scott and R. L. Greene; Phys. Rev. lett, 50, 270
(1983).
45. E. B. Yagubskii, I. F. Shchegolev, V. N. Laukhin,
P. A. Kopnonovich, M. W. Karatsovnik, A. V. Zvarykina and L. I.
Buravov; Pis'Ma Zh. Eksp. Teor. Fiz. 39, 12 (1984), JETP Lett
(Engl. Transl.) 39,12 (1984).

46. J. M. Williams, T. J. Emge, H. H. Wang, M. A. Beno, P. T. Copps, L. N. Hall, K. D. Carlson and G. W. Crabtree. *Inorg. Chem.* 23, 2558 (1984).
47. J. M. Williams, H. H. Wang, M. A. Beno, T. J. Emge, L. Sowa, P. T. Copps, F. Behrooz, L. N. Hall, K. D. Carlson and G. W. Crabtree; *Inorg., Chem.* 23, 3839 (1984).
48. K. D. Carlson, G. W. Crabtree, M. Choi, L. N. Hall, P. Copps, H. H. Wang, T. J. Emge, M. A. Beno and J. M. Williams; *Mol. Cryst. Liq. Cryst.* 119, 351, (1985).
49. H. H. Wang, M. A. Beno, U. Geiser, M. A. Firestone, K. S. Webb, L. Nuniz, G. W. Crabtree, K. D. Carlson, J. M. Williams, L. J. Azeredo, J. F. Kwak, and J. E. Schirber; *Inorg. Chem.* 24, 2465 (1985).
50. H. Urayama, H. Yamochi, G. Saito, K. Nozawa, J. Sugano, M. Kinoshito, S. Sato, K. Oshima, A. Kawamoto and J. Tanuka; *Chem. lett*, 55 (1988).
51. J. M. Williams, H. H. Wang, T. J. Emge, U. Geiser, M. A. Beno, P.C.W. Leung, K. D. Carlson, R. J. Thorn, A. J. Schultz and M. H. Whangbo; *Prog. Inorg. Chem.*, 35, 51 (1987).
52. J. J. Andre, A. Bieber and F. Gautier, *Ann. Phys.*, 1,145, (1976).
53. R. G. Kepler; *J. Chem. Phys.* 39, 3528 (1963).
54. L. N. Bulaevskii, A. V. Zvarykina; Yu S Karimar, R. B. Lyubovski and I. F. Shehegolev; *Sov. Phys. (JETP)*, 35,384 (1972).
55. G. J. Ashwell; *Phys. stat. sol(a)* 81, 361, (1984).
56. T. Sugano, T. Ohta and H. Kurocla; *Chem. Phys. lett*, 34, 164 (1975).
57. J. R. Cooper, M. Mijak and B. Korin; *Chemica Scripta*, 17, 79, (1981).

58. Y. Tomkiewicz, A. R. Taranko and J. B. Torrance; Phys. Rev. Letts, 36, 757 (1976).
59. L. C. Isett; Phys. Rev. B 18, 439, (1978).
60. J. H. VanVleck, Electric and Magnetic susceptibilities; (Oxford University Press London 1932) p145.
61. I. F. Shchegolev; Phys. Stat. Sol; 12, 9 (1972).
62. L. C. Tippie and W. G. Clark; Phys. Rev. B, 23, 8846, (1981).
63. A. N. Bloch, R. B. Weisman and C. S. Varma, Phys. Rev. Lett, 28, 753 (1972).
64. W. G. Clark, J. Hammann, J. Sanny and L. C. Tippic, Proceedings of International Conference on 1-D conductors, Dubrovnik, (1978).
65. D. B. Chesnut and W. D. Phillips; J.Chem.Phys., 35, 1002, (1961).
66. D. Bijl, H. Kainer and A. C. Rose-Innes; J.Chem.Phys. 30, 765 (1959).
67. J. C. Bonner and M. E. Fischer; Phys. Rev. A, 135, 640, (1964).
68. L. N. Bulaevskii, Sov. Phys. JETP 17, 684 (1963).
69. T. J. Kistenmacher, T. E. Phillips and D.O. Cowan; Acta Cryst., B30, 763 (1974).
70. T. E. Phillips, T. J. Kistenmacher, A. N. Bloch, J. P. Ferraris and D. O. Cowan; Acta Cryst, B33, 422 (1977).
71. G. Keryer, P. Delhaes, J. Amiell, S. Flandrois and B. Tissier, Phys. Stat. Sol. (b) 100, 251 (1980).
72. J. L. Galigne, J. M. Fabre and L. Giral; Acta. Cryst, B33, 3827, (1977).
73. D. Chasseau and D. Gaultier; Acta. Cryst., B38, 1632 (1982).
74. L. R. Melby, R. J. Harder, W. R. Hertler, W. Mahler, R. E. Benson and W. E. Mochel; J.Am.Chem.Soc., 84, 3374 (1962).
75. A. F. Garito and A. J. Heeger; Acc. Chem. Res., 7,232, (1974).

76. R. Gleiter, E. Schmidt, D. O. Cowan and J. P. Ferraris; J. Electron. Spectrosc., 2, 207, (1973).
77. V. Kamper et al; Zh. Obshch. Khim, 48, 647 (1978)
78. K. Bechgaard, D. O. Cowan and A. N. Bloch; Proceedings of the IV international symposium of the organic solid state (Bordeau), 71, (1975).
79. H. Inokuchi, M. Kochi and Y. Horada; Bull. Chem. Soc. Japan, 40, 2695, (1967).
80. A. W. Hanson; Acta Cryst; B24, 768 (1968).
81. L. I. Buravov, O. N. Eremenko, R. B. Lyubkovskii, L. P. Rozenburg, M. Khidekel, R. P. Shibaeva, I. F. Shchegolev and E. B. Yagubskii, J.E.T.P. Lett, 20, 208, (1974).
82. W. J. Siemons, P. E. Bierstedt and R. G. Kepler; J.Chem.Phys., 39, 3523 (1963).
83. S. Etemad; Phys. Rev. B, 13, 2254 (1976).
84. S. Mazumdar and A. N. Bloch; Phys. Rev. Lett., 50, 207 (1983).
85. M. Konno and Y. Saito; Acta. Cryst. B30, 1295 (1974).
86. H. Afifi, F. M. Abdel-Kerim, H.F. Aly and A. A. Shabaka; Z. Naturforsch, 33a, 344, 91978).
87. A. J. Heeger and A. F. Garito, Low-Dimensional Cooperative phenomena (Ed. H. J. Keller), Plenum Press, N.Y. 89 (1975).
88. M. J. Cohen, L. B. Coleman, A. F. Garito and A. J. Heeger; Phys. Rev. B, 10, 1298 (1974).
89. D. E. Schafer, F. Wudl, G. A. Thomas, J. P. Ferraris and D. O. Cowan; Sol. St. Comm., 14, 347 (1974).
90. R. E. Peierls; Quantum Theory of Solids, Oxford Press, London, 108, (1955).

91. S. Etemad, E. M. Engler, T. D. Schulz, T. Penney and B. A. Scott; Phys. Rev. B.17 513, (1978).
92. J. P. Pouget, R. Monet, R. Comes, K. Bechgaard, J. M. Fabre and L. Giral; Mol. Cryst. Liq. Cryst., 79, 129 (1982).
93. K. Kamaras, G. Mihaly, G. Gruner and A. Janossy; J.Chem.Soc.Chem.Comm., 974, (1978).
94. A. Andrieux, P. M. Chaikin, C. Duroure, D. Jerome, C. Weyl and K. Bechgaard; J.Phys.(Fr) 40, 1199, (1979).
95. G. J. Ashwell, D. D. Eley, S. C. Wallwork and M. R. Willis, Proc. Roy. Soc. A, 343, 461 (1975).
96. J. P. Farges and A. Brau, Phys. Stat. Sol. (b), 64, 269, (1974).
97. A. Brau and J. P. Farges; Phys. Stat. Sol. (b), 61, 257, (1974).
98. S. Bouffard, M. Ribault, R. Brusetti, D. Jeromeand, K. Bechgaard, J. Phys. C. 15,2951 (1982).
99. A. J. Epstein, S. Etemad, A. F. Garito and A. J. Heeger; Phys. Rev. B. 5, 952, (1972).
100. J. P. Pouget, S. M. Shapiro, G. Sherane, A. F. Garito and A. J. Heeger; Phys. Rev. B19, 1792, (1979).

It is more than half a century since Michaelis¹ first reported on the electrochemical behaviour of a class of compounds which he christened the 'viologens', but which are also known as 1,1'-disubstituted 4,4'-bipyridinium salts (Figure 2.0.1).

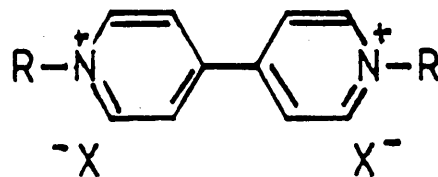


Figure 2.0.1: A 1,1'-disubstituted 4,4'-bipyridinium salt

The viologens were originally investigated as redox indicators in biological studies¹. Subsequently they were found to have practical applications as herbicides for example paraquat². Soon after their herbicidal properties were first recognized, their ability to form complexes attracted attention.

The dialkyl 4,4'-bipyridinium salts are electron acceptors³ and can form complexes with many electron donor molecules:

- i. With neutral organic molecules, for example, amines, phenols and acetic acid⁴. This was established by White⁵ when spectroscopic measurements showed that the absorptions were frequently displaced to wavelengths longer than the parent absorptions. This was attributed to the intermolecular charge transfer with the bipyridinium salt acting as the electron acceptor and the neutral molecule as the electron donor⁵.

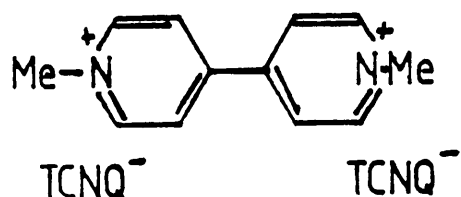
Later it was suggested that the charge-transfer transitions resulted from favourable orbital overlap as a consequence of dipole-dipole interactions. This was supported by the particularly favourable interaction of the closely matched molecular geometries of paraquat and 4,4'-dihydroxy biphenyl⁶.

ii. With non-metal anions, as demonstrated by Nakahara and Wang⁷. They observed that crystals of paraquat dichloride appeared almost white with the absorption maxima at 260nm and 377nm, those of the bromide were light yellow with the absorption maxima at 265nm and 387nm and those of the iodide were red with absorptions at 277, 285 and 475nm. Since neither the bipyridinium dication nor the halide ion in the ordinary ionic crystals absorb in the visible region, the absorption bands at the longer wavelengths were attributed to charge-transfer transitions. Qualitatively, the longest wavelength of the charge transfer band for the iodide crystal was consistent with the strongest electron-donor property of the iodide ion.

iii. With metal species addition complexes have been reported between the bipyridinium salts and various heavy metal salts for example silver iodide and copper chloride^{8,9}. Charge transfer complexes with high conductivities have also been reported from the anions obtained from metal cations and halides, for example, FeCl_4^{2-} and CuCl_6^{2-} ¹⁰. E.s.r. measurements indicate that the complexes contain some reduced paraquat cation and some oxidised anion.

iv. With TCNQ. In the early 70's the paraquat di-cation was observed to form two types of electrically conducting salts (Figure 2.0.2).

a)



b)

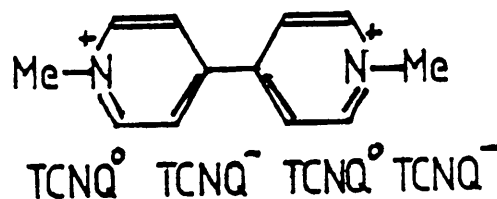


Figure 2.0.2 The two types of electrically conducting salts of paraquat

The dramatic increase in conductivity of complex (b) compared to complex (a) was attributed to the enhanced electron transport in the presence of neutral TCNQ¹¹.

In the middle 70's to early 80's, the versatile chemistry of the bipyridinium cation made it a popular candidate to investigate the relationship between the structure and electrical properties of TCNQ salts. Its size, geometry and rigidity may be varied simply by changing the quaternary groups and/or the link between the pyridinium rings. By systematically increasing the cation length it is possible to influence the stoichiometry. Cation to TCNQ ratios of 1:2 to 1:6 have been obtained¹²⁻¹⁶.

The crystal structures of the ordered bipyridinium TCNQ salts show three common features:

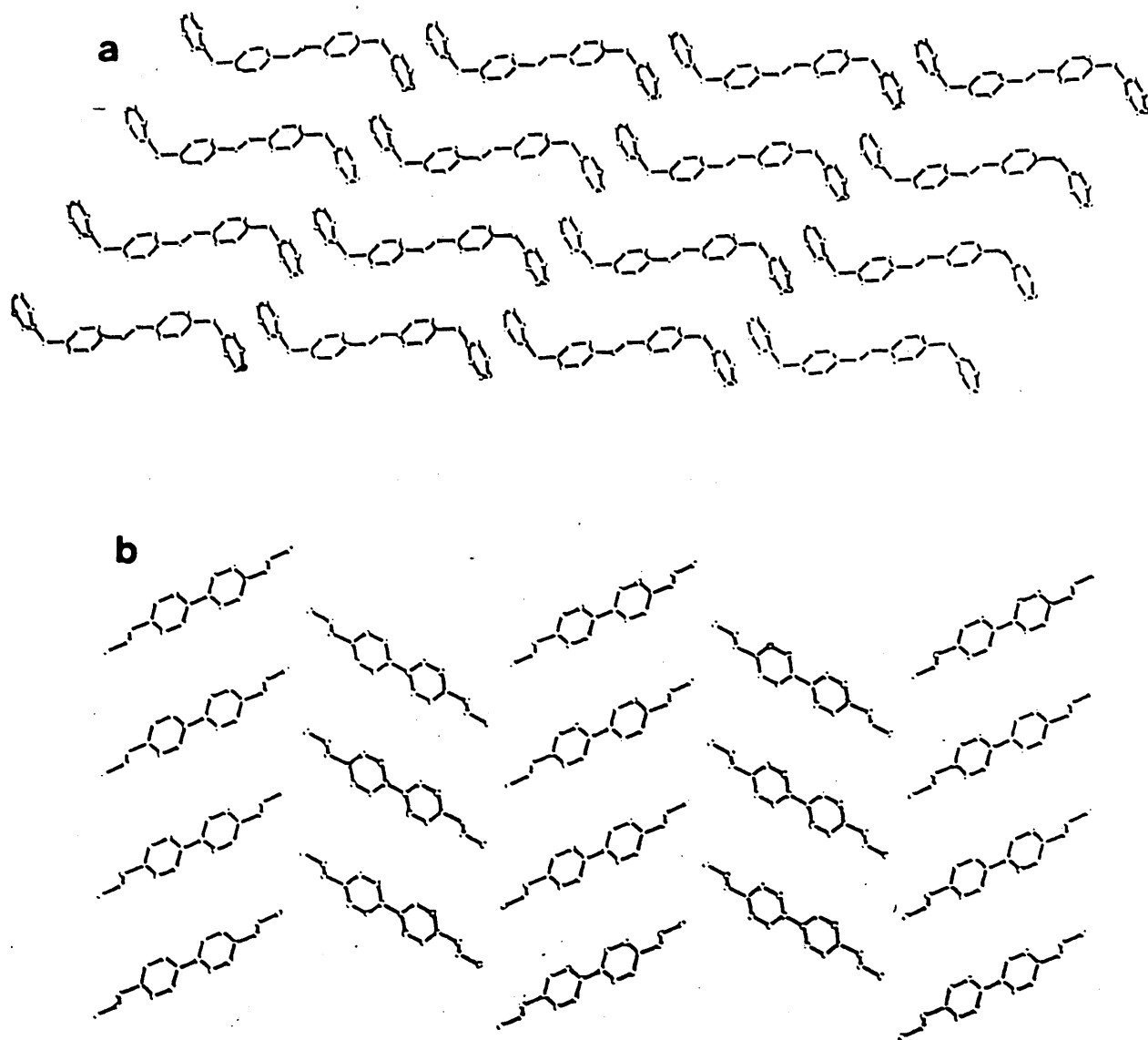
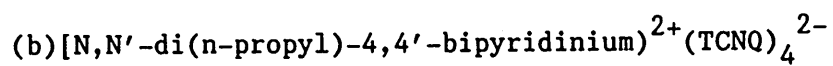
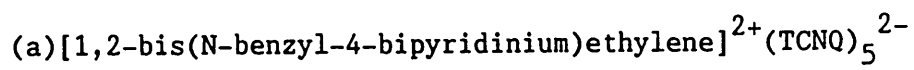


Figure 2.0.3 Cation arrangement in



(1) the TCNQ's stack in a plane to plane manner, within the stoichiometric unit, in a direction parallel to the length of the dication;

(2) the adjacent columns are held together by Van der Waals forces and so form two dimensional arrays parallel to the crystallographic axis;

(3) the arrays are interleaved along the third axis by sheets of the dications.

The properties of the complex bipyridinium TCNQ salts are dependent upon the stacking characteristics and the salts vary from small band gap semiconductors to semimetals. The stacking within the TCNQ arrays depends upon the ability of the cation to align in columns. Benzyl quaternary groups facilitate column formation as shown by N,N'-dibenzyl-4,4'-bipyridinium cation¹⁷. The adjacent cations are held together in columns by Van der Waals forces between the partially overlapping phenyl rings (Figure 2.0.3). However, with alkyl quaternary groups, for example N,N'-di(n-propyl)-4, 4'-bipyridinium¹⁸ the cations form a 'zig-zag' pattern (Figure 2.0.3).

The TCNQ molecules stack in stoichiometric groups of three, four, or five, and compete to make the closest contacts. As a general rule, the charges localise on the TCNQ's which make the closest contact with the quaternary cations.

In the early 80's the high conductivity observed for the simple salt (4,4'-bipyridinium)²⁺(TCNQ)₂²⁻¹² renewed interest in the bipyridinium salts.

Rembaum et al^{11,19} have shown that the H-quaternised bipyridinium salts are unstable and have suggested that they react with TCNQ⁻ to give the unquaternised base, H₂TCNQ and neutral TCNQ¹⁹. The mechanism has been adapted for the pyridinium salts and is shown in Figure 2.0.4.

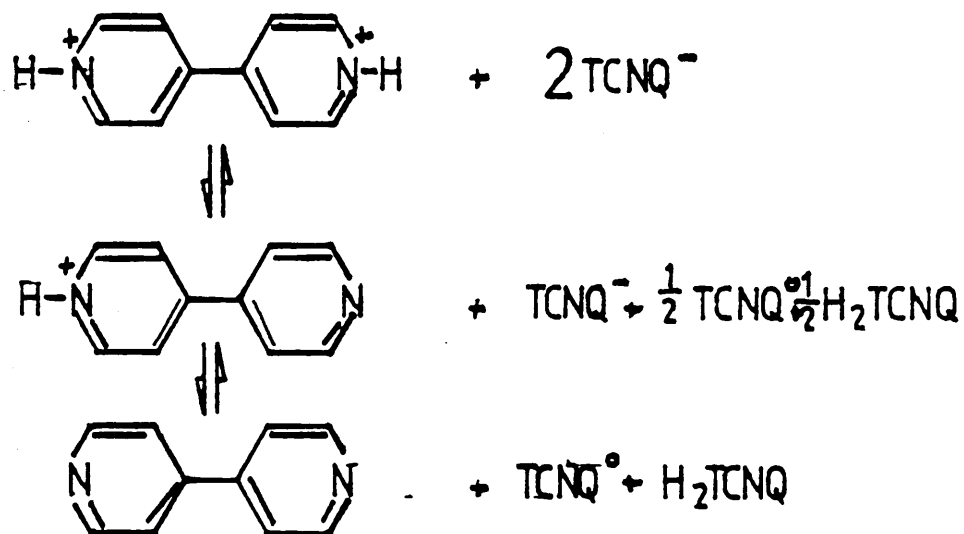


Figure 2.0.4: Proton transfer mechanism in acetonitrile solution

Anomalous properties of the $(4,4'\text{-bipyridinium})_2^{2+}(\text{TCNQ})_2^{2-}$ have therefore been attributed to a small but significant filling of the dication sites by either neutral 4,4'-bipyridyl or the 4-pyridyl-4'-pyridinium monocation which are formed during the reaction^{19,20}. This causes the average charge on the TCNQ sites to become non-integral and removes the need for double occupancy during conduction.

Other hydro-quaternised cations have been shown to give conductive salts. They include the 1:3 complex salt 1,2-bis(4-pyridinium)ethane²¹ which is a small band gap semiconductor with a room temperature conductivity of 10 Scm^{-1} and the 1,2-bis-(2-pyridinium)ethylene chloride)_{0.7} (1,2-bis(2 pyridyl)ethylene)_{0.3} TCNQ salt which was shown to be a Pauli paramagnet with a conductivity of 10 to 70 Scm^{-1} at 300K²². However, not all the hydro quaternised cations give conductive salts the 1,2-bis(4-pyridinium)ethane simple salt being a diamagnetic insulator²¹, with the charge on the TCNQ moiety estimated to be 1e. The crystal structure reveals that between the TCNQ diads there is no direct plane to plane overlap and the molecules are arranged in sheets²¹. In this salt, the molecular parameters result in its low conductivity.

More recently the effect of solvent inclusion on the behaviour of the bis-pyridinium TCNQ salts has been studied^{23,24}.

Differential scanning calorimetry was used to investigate the solvent inclusion. Many of the samples recrystallised from acetonitrile showed the distinctive double transition close to

229 and 214 K, whereas the samples recrystallised from acetone, ethanol and ethyl acetate showed no transition.

The electrical behaviour of the solvated TCNQ salts 1,4-bis(N-pyridinium methyl)benzene-TCNQ₄ and N,N'-bis(p-cyanophenyl)-4,4'-bipyridinium exhibit a slight change in slope centred at 229 K and a pronounced transition respectively. Hysteresis was observed for the latter salt. The transitions were attributed to the localised structural distortions as the trapped solvent contracts upon freezing. The different behaviour of the two salts at the melting point may be explained by the differing TCNQ stacking characteristics²⁴.

In the mid 60's attempts to incorporate TCNQ or its anion into polymeric structures were reported^{25,26}. It was found that soluble, high molecular weight, electrically conducting polymers of 10^{-3}Scm^{-1} could be obtained by combining polycations with TCNQ anions and adding neutral TCNQ to such systems²⁷. The polycations employed were derived from the quaternization of a polymeric amine with an alkyl halide or sulphate²⁷. This discovery prompted the synthesis of new polyelectrolytes with ammonium groups in the backbone termed ionenes^{28,29} (Figure:2.0.5).

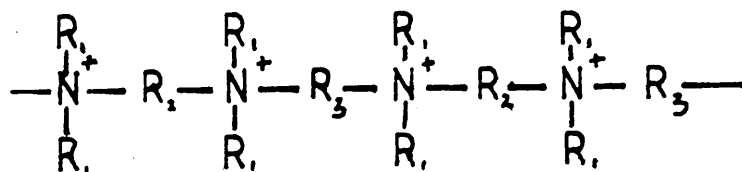


Figure 2.0.5: An ionene

The early studies dealt mainly with the ionenes composed of flexible polymethylene chains with different distribution of donor centres in the main chain i.e. bromides of x,y ionenes^{28,29,30}. Their complexes were shown to have an electrical conductivity of the order of 10^{-3} Scm^{-1} ^{28,29,30}.

Ionenes containing aromatic rings have also been studied³¹. The rigidity of the chains from the presence of the aromatic systems has been shown to be an important factor in their electrical properties³¹. Comparing an analogous class of TCNQ complexes containing bromides e.g. x,y ionenes, and the complexes with the aromatic rings, shows the latter to have considerably lower values of resistivity³¹.

In 1971, Factor and Heinsohn reported, the preparation of a novel class of ionene termed polyviologens³² (figure 2.0.6) formed by the Menschutkin reaction between 4,4'-bipyridine and dihaloalkanes and dihaloarylalkanes.

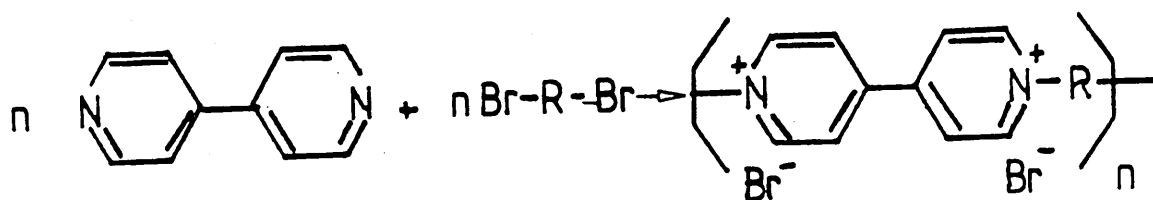


Figure 2.0.6: The formation of a polyviologen via the Menschutkin reaction

Their conducting polymers containing neutral TCNQ were shown to have conductivities analogous to those prepared by Kopple, Lupurski²⁷ and Hertz²⁷.

The 4,4'-bipyridinium in the polyviologens maintain the interval between N^+ atoms in the main chain to 6-8 Å by their rigid ring structure. This allows the complex formation of $[\text{TCNQ}^\bullet/\text{TCNQ}^-]=1.0$ ^{33,34}. This brings about the simultaneous lowering of the Coulomb repulsion between the carrier electrons and an increase in the overlap of π of the TCNQ molecules³⁴. This has contributed to the polyviologens having the highest conductivities among the polycation-TCNQ complex salts^{35,36}.

However, their films made by casting techniques are brittle and lack mechanical strength as polymeric materials. To overcome this problem polyamides containing bipyridiniums³⁷ and polymerisation of a prepolymer with 4,4'-bipyridyl or 1,2-bis(4-pyridyl)ethylene have been studied³⁸.

2.1 AIM

The design of highly conductive TCNQ salts of quaternary organic cations is inhibited by the requirement that the conduction electrons localise on those TCNQ molecules closest to the positive charges and the electrostatic interactions lead to the formation of a periodically distorted TCNQ lattice. To stabilise a uniform lattice it is necessary to delocalise the positive charge. However, the charge is localised on the quaternary nitrogen, therefore stabilisation may only be achieved by introducing some lattice disorder. This can be seen in NMP-TCNQ³⁹ and acridinium-TCNQ₂⁴⁰; these planar cations may take one of two orientations within the stack. This disorder effectively cancels out the periodic potential of the cation lattice and stabilises the TCNQ stack in these salts.

Attempts have been made to introduce disorder in bis-pyridinium cations by using an alkane or alkene bridge between the two rings. This will allow some, although restricted, freedom of rotation. Many of these salts have disordered cation lattices and show favourable TCNQ stacking.

We thought it might be possible to introduce disorder by using the unsymmetrical bipyridinium, N-methyl-N'-(p-methyl phenyl)-4,4'-bipyridinium (2.1.1) (Figure 2.1.1).

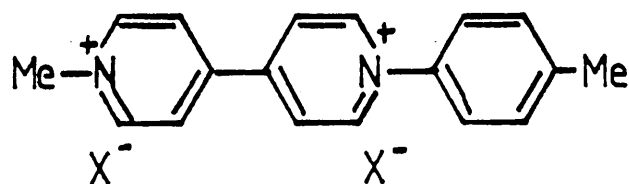


Figure 2.1.1 The unsymmetrical, N-methyl-N'-(p-methylphenyl)-4,4'-bipyridinium

It was thought that this planar molecule might be able to take at random one of two alternative orientations (Figure 2.1.2) and therefore smear out the periodic potential and stabilise the TCNQ column.

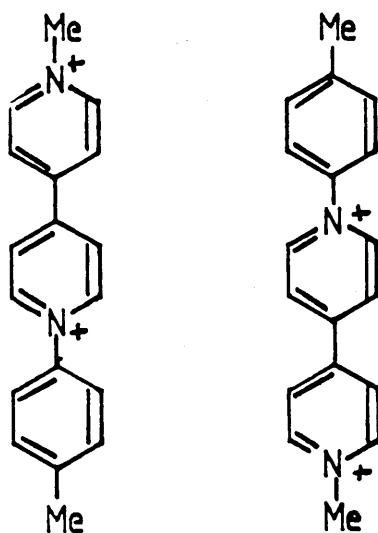


Figure: 2.1.2: The possible orientations of N-methyl-N'-(p-methylphenyl)-4,4'-bipyridinium in the crystal lattice

An attempt was also made to affect the stoichiometry and introduce disorder by synthesising the bipyridinium derivative (2.1.2) (Figure 2.1.3)

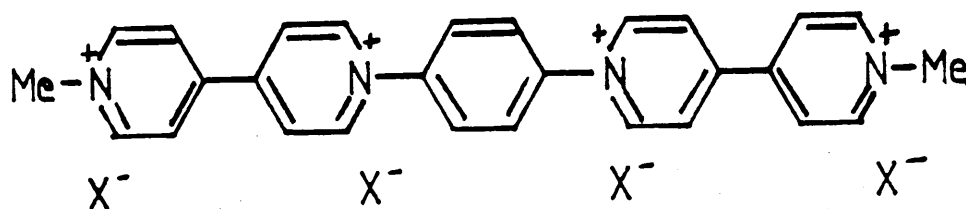


Figure: 2.1.3: The target bipyridinium derivative (2.1.2)

The stoichiometry should be increased due to the length of the cation and the phenyl bridge unit between the two bipyridinium portions should allow some degree of rotation.

The conductivities of the ionene and polyviologen salts of TCNQ have been found to be high (see introduction). It was therefore proposed to investigate the synthesis and conductivity of a novel cationic redox polymer, polyviologen (2.1.3) (Figure: 2.1.4)

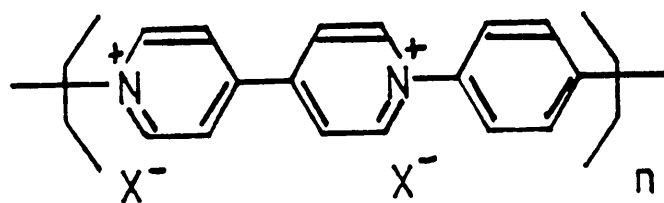
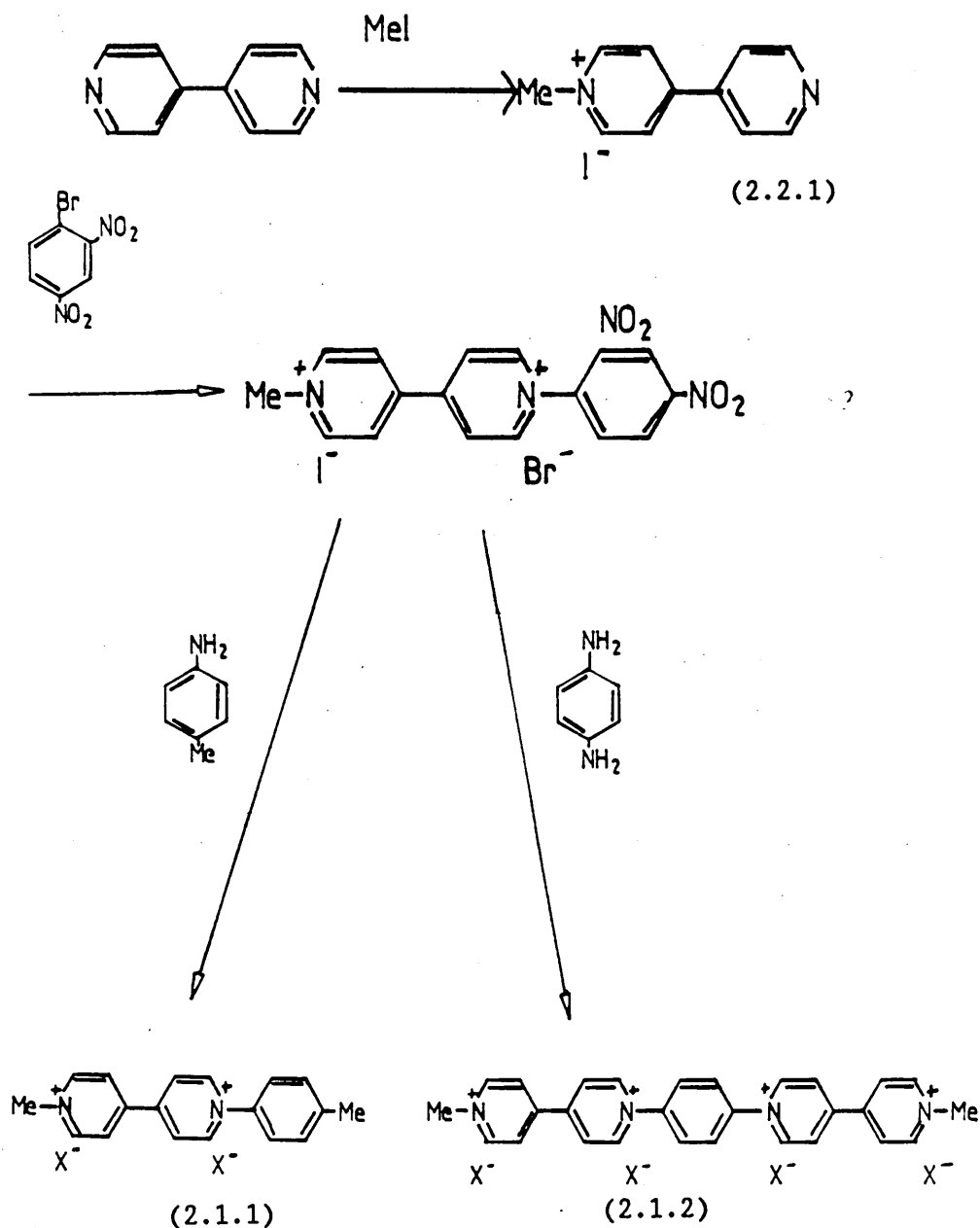


Figure: 2.1.4: The proposed polyviologen

2.2 SYNTHESIS

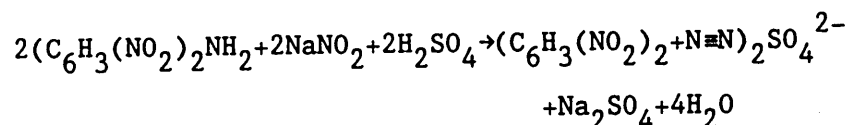
The proposed synthetic pathway for the preparation of the bipyridinium target molecules (2.1.1) and (2.1.2) is given below:



An increase in the yield for the quaternisation of the bipyridyl was found using a short reflux in ethanol. The colour change between yellow monoquaternised iodide (2.2.1) and the red diquaternised iodide enabled monitoring of the reaction and the isolation of the monoquaternised product (2.2.1) in good yields.

The quaternisation of the N-methyl bipyridinium (2.2.1) with 2,4-dinitrobenzene produced two precipitates, a red one which was the diiodide and a yellow one which could be either a mixed counterion species of bromide and iodide or the dibromide. To remove the possibility of the differing counterions and hopefully reduce the reaction times and increase the yield, it was proposed to synthesise 2,4 dinitroiodobenzene.

The diazotization of the primary aromatic amine 2,4-dinitroaniline was carried out by adding an aqueous solution of sodium nitrite to a suspension of the amine hydrogensulphate in an excess of sulphuric acid which was cooled in an ice bath (Equation 2.2.1).



Equation 2.2.1

The aromatic iodide was prepared by treating a solution of potassium iodide with a solution of the diazonium salt. The iodide was formed in good yields.

The quaternisation with 2,4 dinitroiodobenzene in methanol was attempted, but with the desired product only being produced with long reflux times and poor yields. Efforts were directed towards reducing the time taken and increasing the yields by using higher boiling solvents for example ethanol 78°C and ethylene glycol 194°C.

The diquaternised salt was produced with an improved yield and shorter reflux time, 49% and 4 days compared with 24% and 8 days, using ethanol. The reaction with ethylene glycol failed. Allen et al⁴¹ found that similar reactions could be conveniently carried out at a temperature at which the reflux of the solvent occurs, but preferably not higher than about 160°C. The boiling point of ethylene glycol is 194°C.

The preparations of the bipyridinium target molecules (2.1.1;2.1.2) were investigated on a small scale with the reactions being monitored for the production of the by product 2,4-dinitroaniline (Figure 2.2.1) by thin layer chromatography.

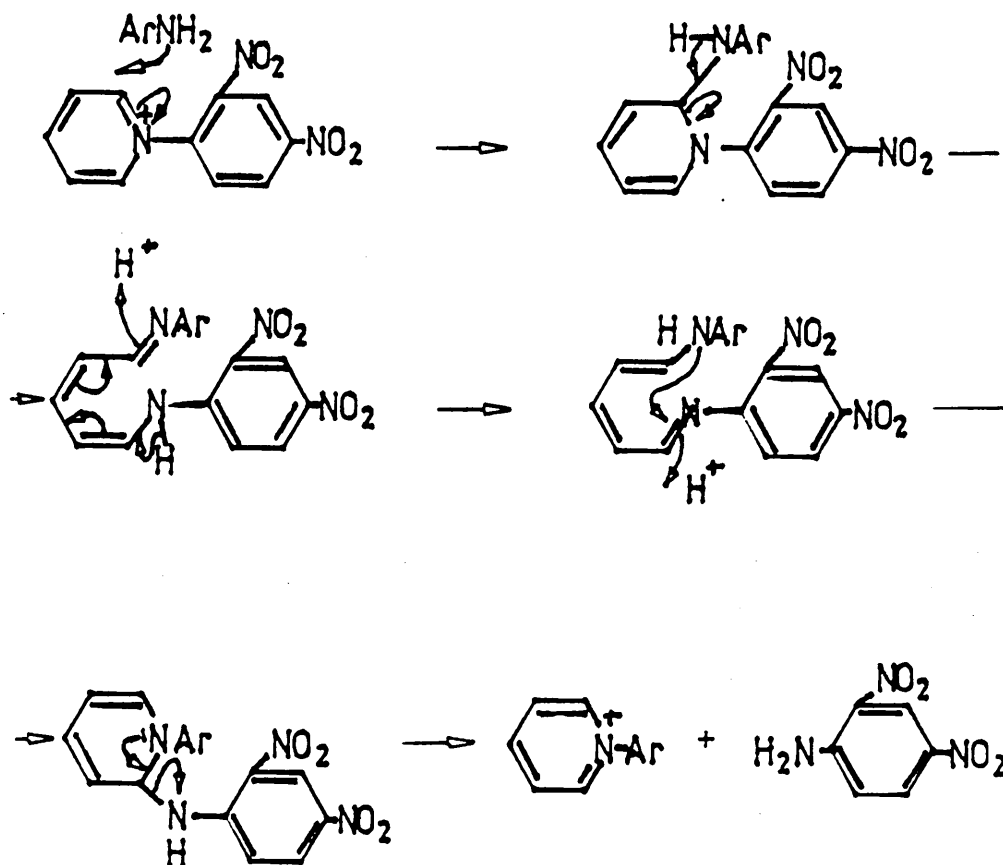


Figure 2.2.1: Mechanism for the production of the byproduct
2,4-dinitroaniline

The N-methyl-N'-2,4 dinitrobenzene bipyridinium was refluxed with either p-toluidine or p-phenylene diamine in ethanol. However, under these conditions the desired three ring product (2.1.1) was only produced in very low yields and the isolation of the five ringed target molecule (2.1.2) proved to be unsuccessful.

The low yields of the former reaction prompted the use of longer reflux times, but this only resulted in a slight improvement. The reaction was repeated using higher boiling solvents for example water and ethylene glycol. The reaction using water produced comparable yields, but with shorter reflux times. However, the reaction in ethylene glycol failed, with no observation of the byproduct 2,4 dinitroaniline on t.l.c. The failure of the reaction could be due to the high boiling point of the ethylene glycol ⁴¹.

Efforts to repeat the reaction with p-phenylene diamine using water as the solvent also proved to be unsuccessful. The failure and low yields of the above reactions could be explained by the autoxidation of the aromatic amines to be a relatively stable cation (Figure 2.2.2).

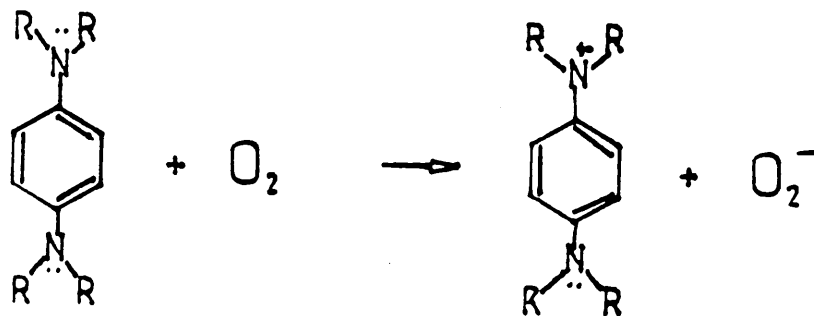


Figure: 2.2.2: The autoxidation of aromatic diamines

The effect could be catalysed by the iodide ions associated with the diquaternised bipyridinium. Iodide ions have been shown to cause oxygen activation⁴², which is probably related to the good electron donor ability of I⁻ ion⁴² observed even towards oxygen. The complexation accelerates the autoxidation of the diamines⁴².

The p-phenylene diamine may also undergo polymerisation to form an aromatic azo polymer by oxygenation⁴³ (Figure 2.2.3).

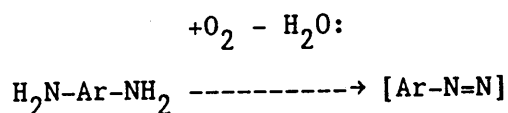


Figure: 2.2.3: Oxidative coupling of primary diamines to prepare an aromatic azo polymer.

To remove the possibility of polymerisation a control reaction was tried. The diamine was refluxed in water for 4 days. The product isolated was a mixture of starting material and a highly polar solid, presumably from the oxidation of the aromatic diamine.

To reduce the problem of autoxidation the aromatic amines were recrystallised and sublimed and the synthesis was carried out under an inert atmosphere. A substantial increase in the yield was observed for the three ringed target molecule (2.1.1). However, all attempts to isolate the five ringed targeted molecule (2.1.2) failed.

The presence of the byproduct 2,4-dinitroaniline, observed by thin layer chromatography, indicated the desired reaction was taking place. The microanalytical data suggested that the product isolated was a 1:1 complex of p-phenylene diamine and the bipyridinium target molecule (see table 2.2.1). Complex formation was confirmed from the observation of an NH_2 absorption in the infra-red spectra of the isolated products, which t.l.c. evidence suggested was not associated with the p-phenylene diamine starting material.

The p-phenylene diamine molecule is an electron donor with it being the best donor among the three isomers of phenylene diamine⁴⁴. The phenylene diamines have been shown to form charge transfer complexes with electron acceptors for example, iodine, chloral, tetracyano ethylene, and TCNQ^{44,45}.

The quaternary salts of 4,4'-bipyridine are electron acceptors and have been found to form complexes with many electron donor molecules⁴⁶. They have been shown to form addition products with amines (see introduction). In the mid 70's the x-ray diffraction analysis of the 1:1 complex between paraquat and hydroquinone indicated that charge transfer existed between both the hydroquinone and the iodide anions as donors and the bipyridinium ion as an acceptor⁴⁷.





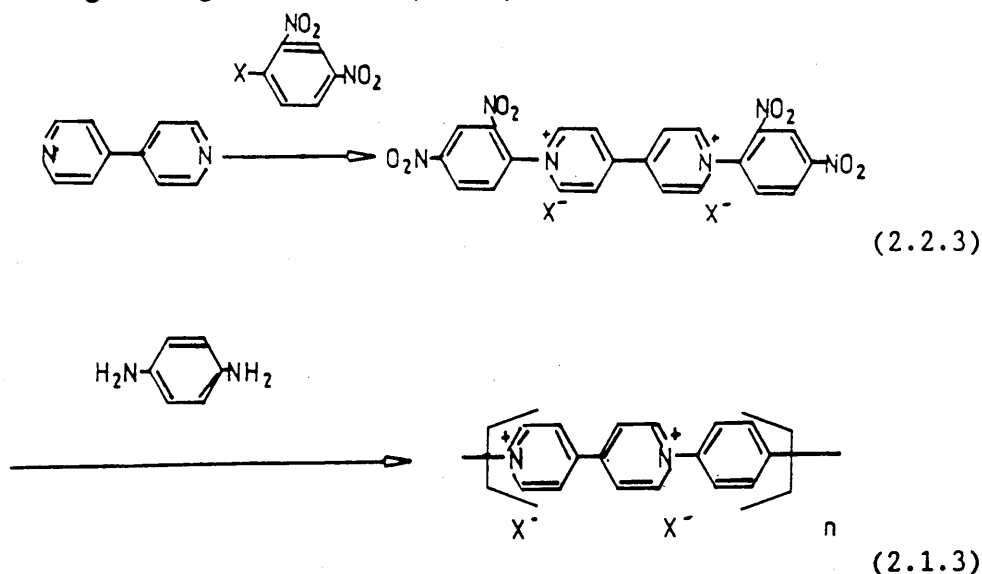
REACTION CONDITIONS	MICROANALYTICAL DATA									
	FOUND					BIPYRIDINIUM TARGET MOLECULE (2.1.2) THEORY				
	C	H	N	C	H	N	C	H	N	1.1 COMPLEX
SOLVENT: ETOH RATIO BIPYRIDINIUM	2	39.65	3.25	8.15	36.31	2.82	39.45	3.29	8.12	
NH ₂  NH ₂	1									
SOLVENT: ETOH RATIO BIPYRIDINIUM	2	39.44	3.18	8.11	36.31	2.82	39.45	3.29	8.12	
NH ₂  NH ₂	2									
SOLVENT: H ₂ O BIPYRIDINIUM	2	39.71	3.22	7.93	36.31	2.82	39.45	3.29	8.12	
NH ₂  NH ₂	1									
SOLVENT: H ₂ O BIPYRIDINIUM	2	39.52	3.16	8.01	36.31	2.82	39.45	3.29	8.12	
NH ₂  NH ₂	2									

Table 2.2.1 Microanalytical data for the isolated products of the reaction
p-phenylene diamine and N-methyl-N'-2,4 dinitrobenzene bipyridinium

It is proposed that the bipyridinium target molecule (2.1.2) was produced but then reacted further to form a 1:1 charge transfer complex with the remaining p-phenylene diamine. This is supported by t.l.c, infra-red and microanalytical data.

The charge transfer complex of the three ringed target molecule (2.1.1) with TCNQ was prepared. A solution of the bipyridinium salt in acetonitrile was added to a refluxing solution of neutral TCNQ in acetonitrile. After cooling black hairs of the charge transfer complex were recovered.

The proposed synthetic pathway for the preparation of the polyviologen target molecule (2.1.3) was as follows:



The problems for the diquaternisation were again the length of reflux and poor yields. Efforts were immediately directed to optimizing the reaction, with a significant improvement in the yield being afforded by reference to an I.C.I. patent⁴¹. It stated that further refluxing of the filtrate produced a further crop of the desired product.

The initial low yield for the formation of the polymer (2.1.3) can again be attributed to the problems associated with phenylene diamine e.g. autoxidation (see earlier). The synthesis carried out under an inert atmosphere with the amine being recrystallised and sublimed gave a substantial increase in the yield.

The presence of the byproduct 2,4-dinitroaniline, observed by t.l.c., the insolubility of all the samples in a variety of polar solvents for example, water, acetonitrile, methanol, ethanol and their high melting points indicated that the desired reaction had possibly taken place. The observation of NH_2 and NO_2 absorptions in the infra-red spectra of the isolated products suggests that they could be associated with the termination groups in the polymer (Figure: 2.2.4).

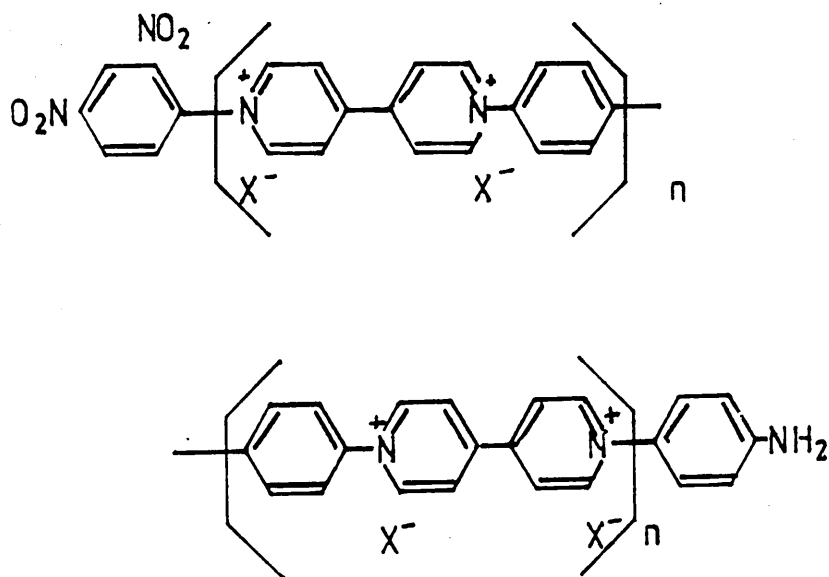


Figure 2.2.4 Termination groups associated with the polymer

The microanalytical data for the samples show a large deviation when compared to the calculated value for $\text{C}_{16}\text{H}_{12}\text{N}_2\text{X}_2$ but does not suggest that a 1:1 complex with p-phenylenediamine is formed. The termination groups could account for this deviation if the molecular mass of the polymer was low. However, if the molecular mass of the polymer was high, the end groups would become insignificant and could not account for this deviation.

2.3 OPTICAL STUDIES

The stoichiometry of the TCNQ complex with the target molecule (2.1.1) was determined by employing a spectrophotometric method first used by Rembaum¹¹ in a study of back charge transfer in bipyridinium TCNQ salts.

The TCNQ radical anion, TCNQ^- , absorbs strongly at 842nm and at 395nm, while neutral TCNQ, TCNQ^0 , absorbs only at 395nm. Rembaum et al plotted the ratio of TCNQ^- to TCNQ^0 , versus the peak intensity at $\lambda_{\text{max}} 395\text{nm}/\lambda_{\text{max}} 842\text{nm}$. It was seen that Beer's Law is obeyed for only a limited composition corresponding to $\text{TCNQ}^0:\text{TCNQ}^-$ ratios <1 . Similar behaviour has been observed by Ashwell et al⁴⁸ for the stoichiometry of bipyridinium TCNQ salts (Figure: 2.3.1). However, it is possible to use the technique in support of other methods of determining the stoichiometry and of ρ .

The complex was finely ground to ensure that the bulk properties were represented and a few mg's were dissolved in spectroscopic grade acetonitrile (10ml) with dilution as necessary to bring the largest peak on scale. Analysis was made using a Perkin-Elmer Lambda 7 uv/vis spectrophotometer with heterosil cells (10mm path length; range 190-1000nm).

The absorption spectrum showed major maxima at 842.5, 742.9, 393.3, and 198.7nm. (Figure 2.3.2)

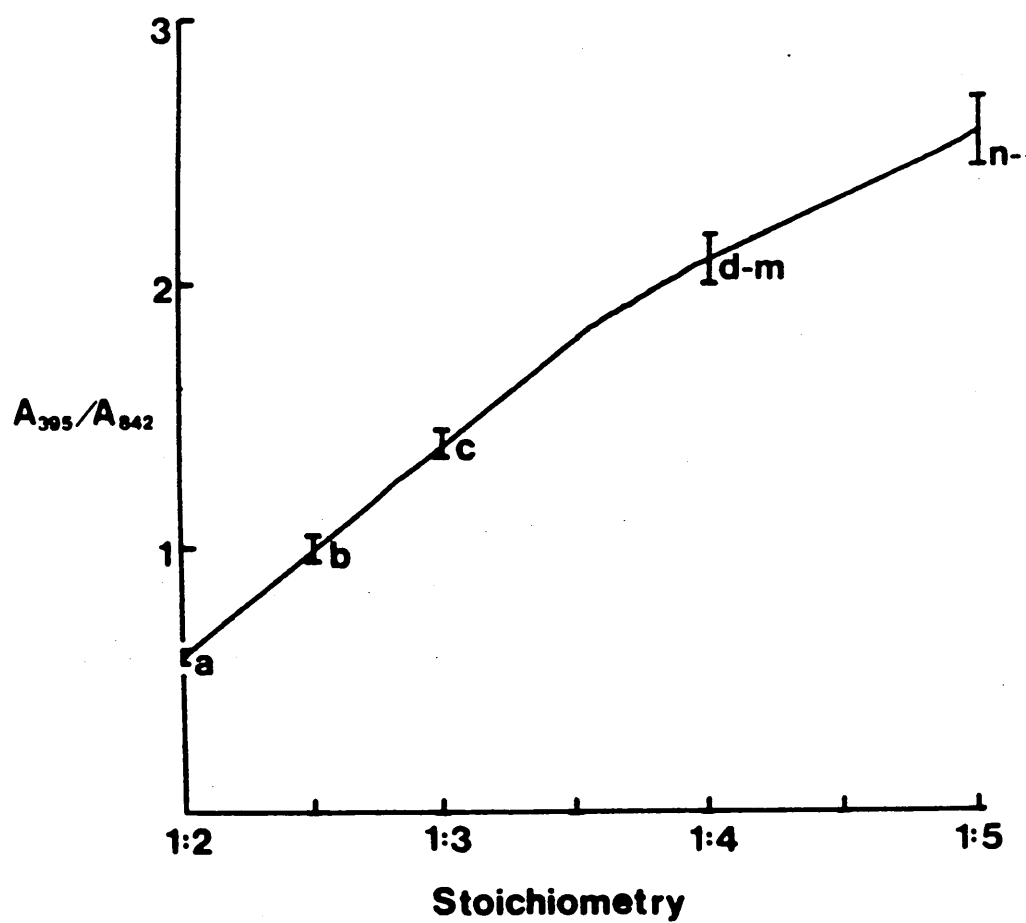
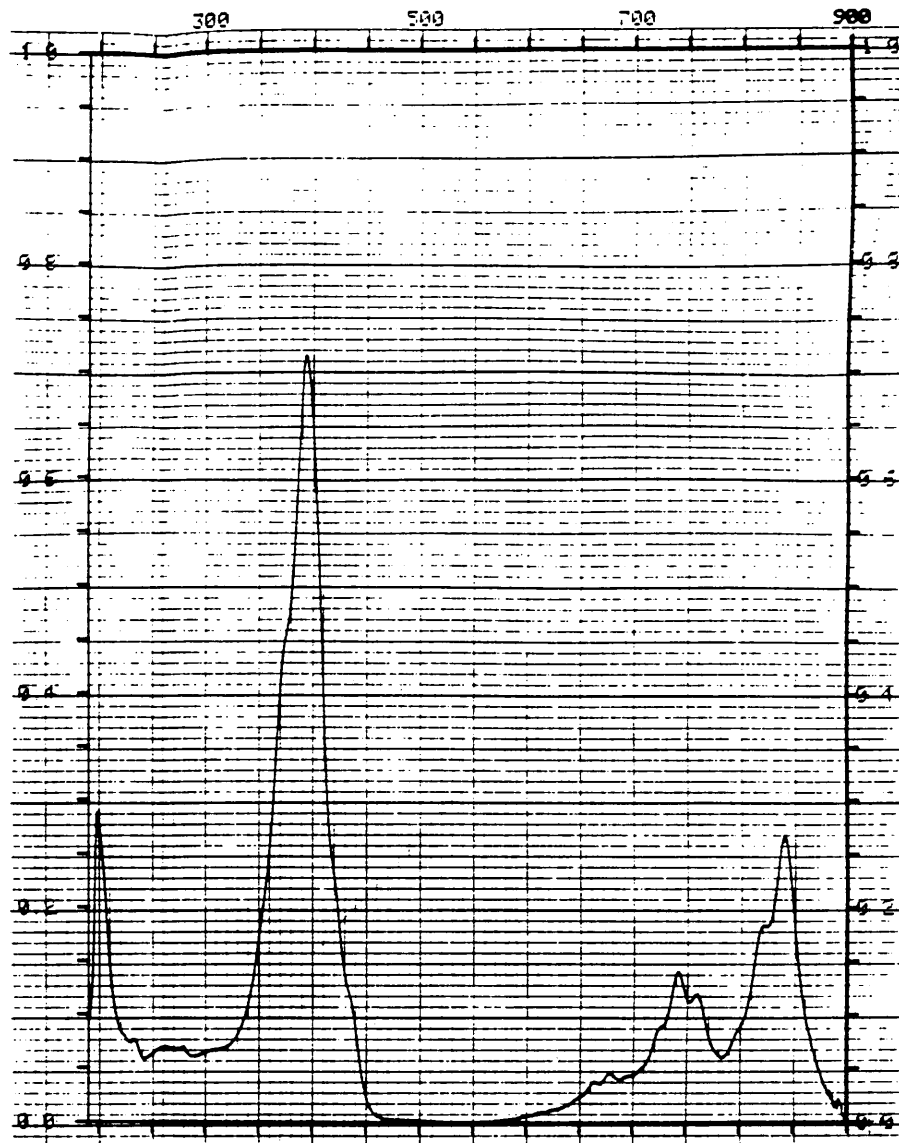


Figure 2.3.1: Ratio of the molar absorption coefficients at 395 and 842nm vs stoichiometry for fifteen bipyridinium salts



Wavelength

Absorbance

842.5nm

0.268A

742.9nm

0.142A

393.3nm

0.713A

198.7nm

0.290A

Figure 2.3.2 The absorption spectrum of the TCNQ complex with the bipyridinium (2.1.1)

The ratio of the molar absorption coefficients at 395 and 842nm = 2.66. This value compares favourably with those obtained for [1,2-bis(1-benzyl-4-pyridinium)ethylene](TCNQ)₅ and [1,2-bis(1-benzyl-4-pyridinium)ethane](TCNQ)₅, whose structures are known. This value is characteristic of a TCNQ⁻:TCNQ^o ratio of 1½:1 and a stoichiometry of 1:5. This is in agreement with the elemental analysis data.

2.4 ELECTRICAL AND MAGNETIC PROPERTIES

The room temperature conductivity of the three ringed bipyridinium TCNQ complex is $1.31 \times 10^{-3} \text{ Scm}^{-1}$ with its magnetic susceptibility showing it to be a Curie-Weiss paramagnet.

The conductivity temperature dependence ($\log \sigma$ versus $10^3/T$) for the salt is shown in figure 2.4.1. The conductivity exhibits semiconducting behaviour. The 1:5 salt shows an activated behaviour over the narrow temperature range between 300-200K. However, at lower temperatures the $\log \sigma$ versus reciprocal temperature plots exhibit curvature. Within a very narrow temperature range, the data gave a reasonable fit to the expression:

$$\sigma = \sigma_0 \exp(-E_a/KT) \quad \text{Equation - 2.4.1}$$

Over a wider temperature range the correlation is poor, which suggests that either E_a or σ_0 is temperature dependent. However, attempts to fit the conductivity data using a temperature-dependent pre-exponential factor $\sigma_0 = AT^x$ in equation 2.4.1 was unsuccessful.

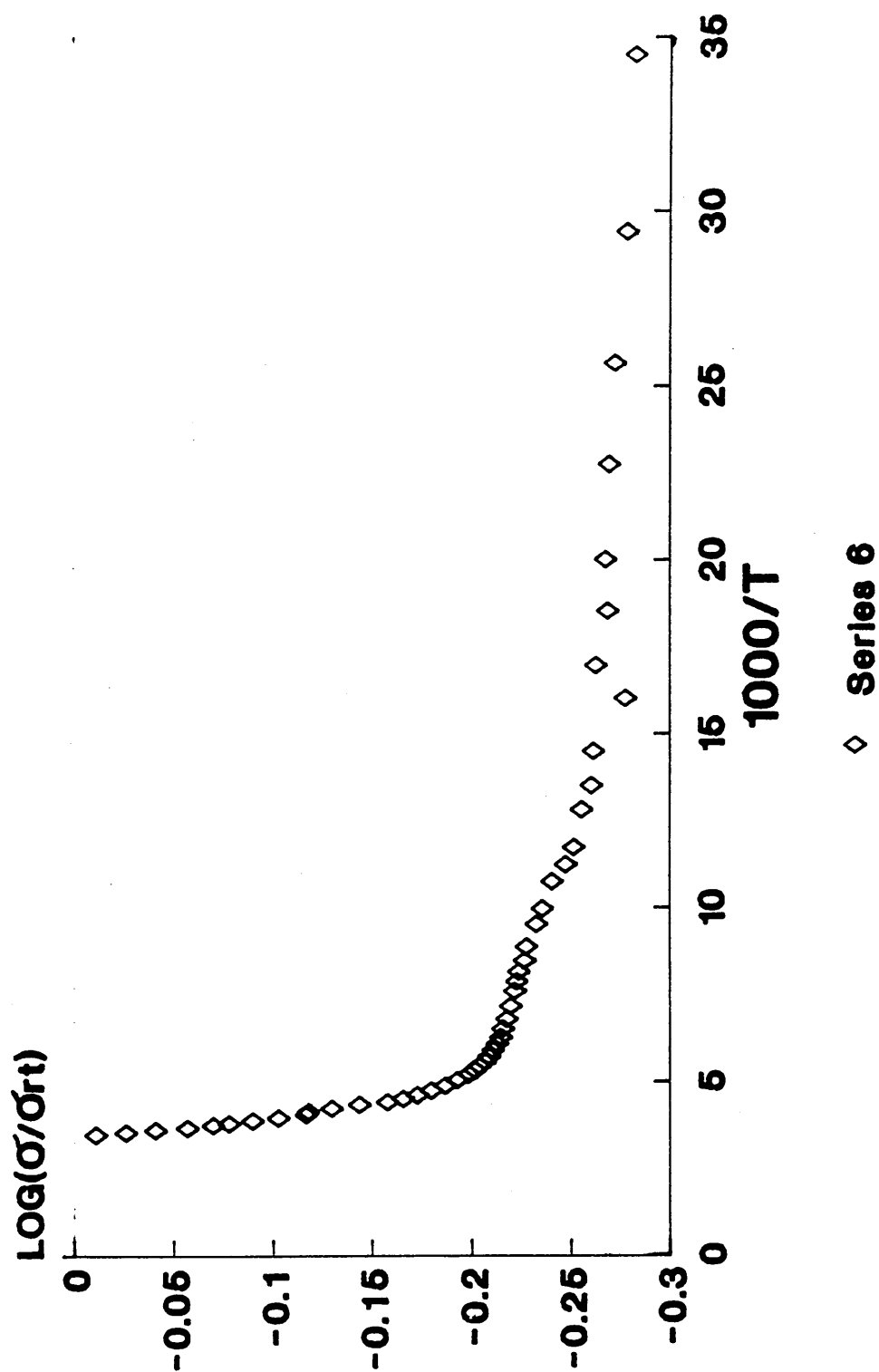


Figure: 2.4.1: Log normalised conductivity versus reciprocal temperature

one dimension⁴⁹:

$$\sigma = \sigma_0 \exp(-\Delta/T)^{1/2}$$

Equation - 2.4.2

was also unsuccessful.

In this case the curvature is attributed to the onset of low temperature extrinsic behaviour due to impurities or defects.

The activation energy derived from the $\log \sigma$ versus reciprocal temperature plot at high temperature is given in table 2.4.1. The salt may be classified as a small band gap semiconductor.

σ (Scm ⁻¹) RT	Ea(eV)	Magnetic Susceptibility
1.31×10^{-3}	0.037	Curie-Weiss $\Theta=160K$ $\mu_{eff}=2.62$

Table 2.4.1: The electrical and magnetic properties of the complex TCNQ salt of the three ringed bipyridinium cation

The temperature dependence of the magnetic susceptibility corrected for core diamagnetism for the 1:5 salt is given in figures 2.4.2 and 2.4.3. The $1/x$ versus T plot is linear in the

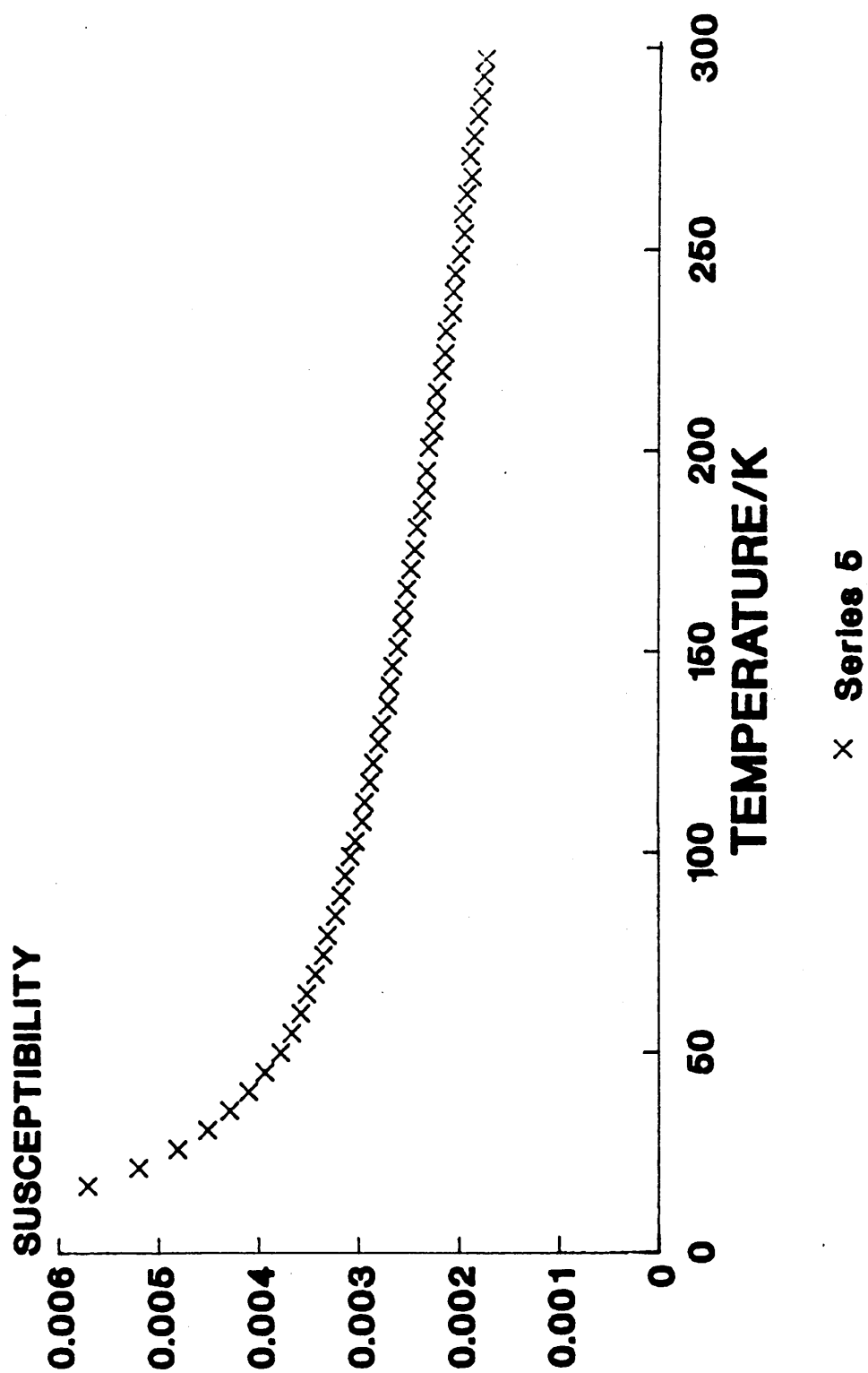


Figure: 2.4.2: The susceptibility, corrected for core diamagnetism versus temperature

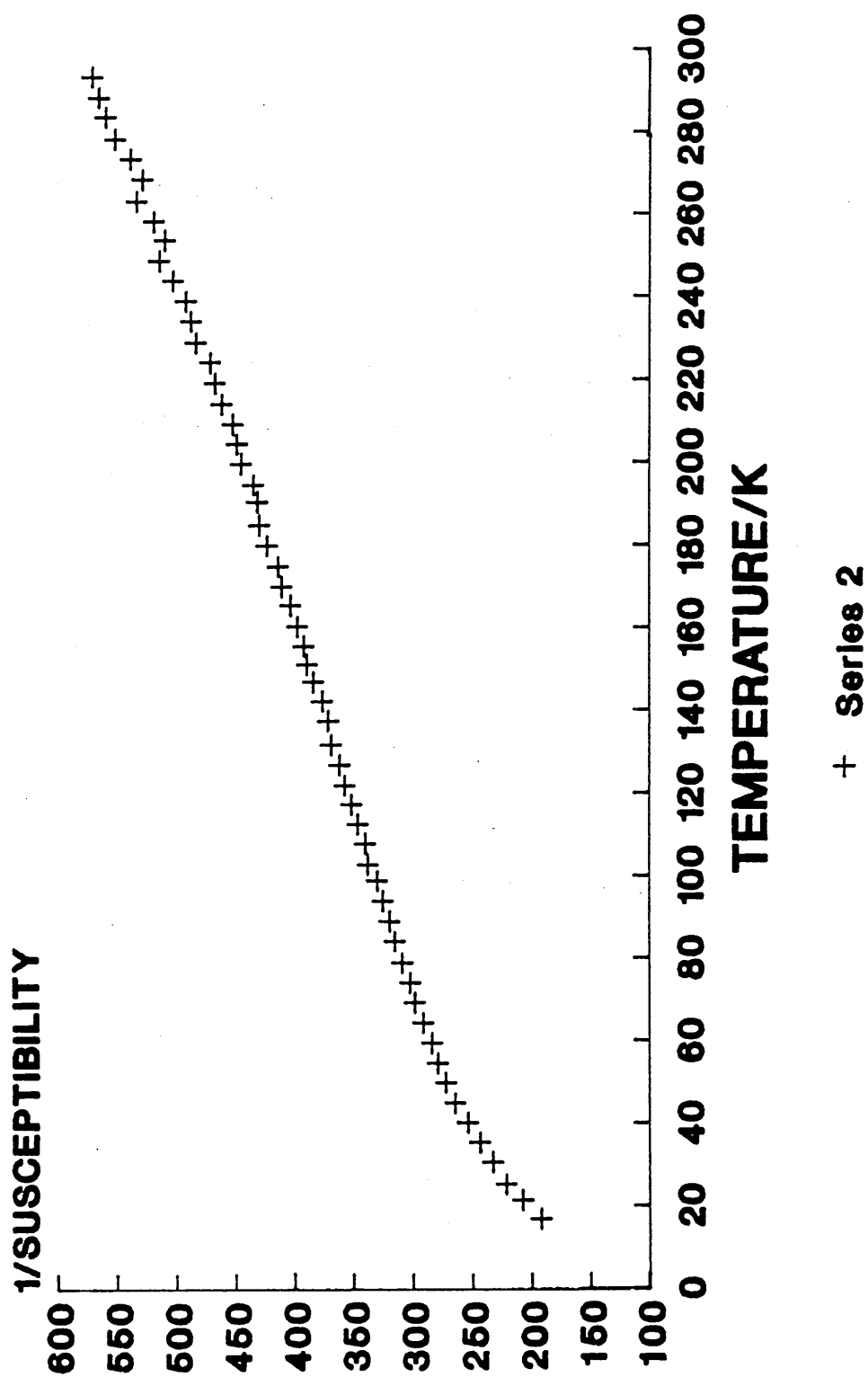


Figure: 2.4.3: The reciprocal susceptibility versus temperature

range 25-300K showing the salt to be a Curie-Weiss paramagnet where the susceptibility varies as:

$$\chi = \frac{C}{(T+\theta)} \quad \text{Equation 2.4.3}$$

From the slope of the $1/\chi$ versus T plot figure 2.4.3

$$C=0.85 \text{ emu mol}^{-1}\text{K and } \theta = 160\text{K}$$

The effective magneton number, μ_{eff} may be determined from:

$$\mu_{\text{eff}} = (3K/N\mu_B^2)^{1/2} C^{1/2} = 2.84C^{1/2} \quad \text{Equation 2.4.4}$$

For the experimental value, $C=0.85$, $\mu_{\text{eff}} = 2.62$

Using the "spin only" formula

$$\mu_{\text{eff}} = [n(n+2)]^{1/2} \quad \text{Equation 2.4.5}$$

where n is the number of free spins per mole,

$\mu_{\text{eff}} = 2.83$ for two free spins (electrons) per mole and agrees well with the experimental value. Thus the mean ionic charge on each TCNQ moiety in the complex is of the order 0.4e. This value is in good agreement when compared with the expected mean ionic charge 0.4e from the formula; (bipyridinium)²⁺(TCNQ)₅²⁻.

The absorbance ratio A_{395}/A_{842} , derived from the visible spectrum obtained from crystals dissolved in acetonitrile is 2.66. This corresponds to a mean ionic charge on the TCNQ's of approximately 0.4e.

The magnetic susceptibility measurements support the determination of the mean ionic charge on the TCNQ species made from spectral methods. The salt possesses a lower room temperature conductivity than would be expected for a salt in which the TCNQ stack is regular and in which the ionic charge per site is less than 1. This suggests that the TCNQ's may stack in stoichiometric groups with no direct overlap between the adjacent groups.

2.5 EXPERIMENTAL

2.5.1 General Information

For the general experimental information (see Appendix 1)

2.5.2 Experimental Methods

N-Methyl-4,4'-bipyridinium iodide⁵⁰ (2.2.1)

4,4-bipyridyl (35g; 0.22 moles) was dissolved in ethanol (100ml) and methyl iodide (31g; 0.22 moles) added in one portion. The resulting solution was refluxed for 15 minutes. The solution was cooled. The resulting solid was filtered and re-crystallised from aqueous ethanol. A yellow precipitate of the desired bipyridinium (2.2.1) was obtained.

35g; 53%; mp: 243-245°C

I.R.(KBr): 2980; 2900; 1605; 1510; 780; 795:

¹H NMR(D₂O): 9.1-7.9 (m, 8H); 4.7 (s, 3H):

Microanalysis: Found: C, 44.45%; H, 3.67%; N, 9.29%:

C₁₁H₁₁N₂I requires: C, 44.32%; H, 3.72%; N, 9.40%:

N-methyl-N'-(2,4 dinitrophenyl)-4,4'-bipyridinium iodide
bromide (2.2.2)

N-methyl-4,4'-bipyridinium iodide (2.2.1) and
2,4-dinitrobromobenzene (5g; 0.02 moles) were dissolved in
methanol (100ml). The resulting solution was refluxed for 8
days. The solution was cooled and the methanol was removed
under reduced pressure to yield a solid. The solid was
recrystallised from an acetone/water mixture. A red
crystalline precipitate of the diiodide was obtained
1.4g; 24%

IR(KBr): 2980; 2900; 1605; 1510; 1310; 780; 795; 720:

^1H NMR(D_2O): 9.5-8.0(m, 11H); 4.5(s, 3H):

Microanalysis: Found: C, 34.45%; H, 2.75%, N, 9.40%

$\text{C}_{17}\text{H}_{14}\text{N}_4\text{O}_4\text{I}_2$ requires: C, 34.46%; H, 2.36%; N, 9.46%:

A yellow brown precipitate was also obtained

0.5g; 9%

IR(KBr): 2980; 2910; 1600; 1515; 1330; 780; 790; 720:

^1H NMR(D_2O): 9.5-8.1(m, 11H); 4.3(s, 3H):

Microanalysis: Found: C, 37.48%; H, 2.61%; N, 10.34%:

$\text{C}_{17}\text{H}_{14}\text{N}_4\text{O}_4\text{Br.I}$ requires: C, 37.43%, H, 2.57%, N, 10.28%

2,4-Dinitroiodobenzene⁵¹ (2.5.1)

A mixture of 2,4-dinitroaniline (13.94g; 0.08 moles),
concentrated sulphuric acid (200ml) and water (150ml) was
heated to 100°C for one hour. The mixture was then cooled to
0-5°C and diazotised with a solution of sodium nitrite (5.24g;
0.08 moles) in water (25ml).

The cold solution was filtered, and the filtrate was added with stirring to a solution of potassium iodide (30g; 0.18 moles) in water (150ml). The precipitate was filtered and re-crystallised from methanol.

9.3g; 40%:

IR(KBr): 3010; 1605; 1510; 1340; 780; 730:

Microanalysis: Found: C, 24.84%, H, 1.00%; N, 9.20%:

$C_6H_3N_2O_4I$ requires: C, 24.51%; H, 1.02%; N, 9.52%:

N-methyl-N'-(2,4-dinitrophenyl)-4,4'-bipyridinium diiodide

(2.5.2)

To a refluxing stirred solution of (2.2.1) (4g; 0.01 moles) in ethanol (100ml) was added 2,4-dinitroiodobenzene (5g; 0.02 moles) in ethanol (50ml) over a period of half an hour. The solution was refluxed for 4 days. The solution was cooled and the ethanol was removed under reduced pressure to yield a solid. The solid was recrystallised from an acetone/water mixture. A red crystalline precipitate of the bipyridinium diiodide was obtained.

2.9g; 49%: mp:>300°C

IR(KBr): 2980; 2900; 1605; 1510; 1310; 780; 795; 720:

1H NMR (D_2O): 9.5-8.0(m,11H); 4.5(s,3H):

Microanalysis: Found: C, 34.63%; H,2.78%; N,9.45%:

$C_{17}H_{14}N_4O_4I_2$ requires: C, 34.46%; H,2.36%; N,9.46%:

N-methyl-N'-(p-methylphenyl)-4,4'-bipyridinium di-iodide

(2.1.1)

To a refluxing stirred solution of (2.5.2) (0.54g; 0.92 mmoles) in water (50ml) under nitrogen was added p-toluidine (0.53g; 5.0 mmoles) in water (25 ml) over a period of half an hour. The resulting solution was refluxed for a further 4 days. The water was removed under reduced pressure to yield a solid. The solid was recrystallised from an acetone/water mixture to yield a red crystalline precipitate.

0.19g; 40%: mp:>300°C

IR(KBr): 3100; 2990; 2910; 1640; 1490; 820:

Microanalysis: Found: C,41.83%; H,3.48%; N,5.58%:

$C_{18}H_{18}N_2I_2$: requires: C, 41.88%; H,3.51%; N, 5.43%:

The attempted preparation of the bipyridinium Tetraiodide

(2.1.2)

To a refluxing stirred solution of (2.5.2) (0.54g; 0.92 mmoles) in water (50ml) under nitrogen was added p-phenylenediamine (0.05g; 0.46 mmoles) in water (25 ml) over a period of half an hour. The resulting solution was refluxed for further 4 days. The water was removed under reduced pressure to yield a solid. The solid was re-crystallised from an acetone/water mixture to yield a red solid.

0.23g: mp:>300°C

IR(KBr): 3500; 3410; 3100; 2980; 2905; 1630; 1510; 830; 790:

Microanalysis: Found: C,39.65%; H,3.25%; N,8.15%:

$C_{28}H_{26}N_4I_4$: requires: C,36.31%; H,2.82%; N,6.04%

N-methyl-N'-(p-methylphenyl)-4,4'-bipyridinium-(TCNQ)5

To a boiling solution of TCNQ (0.24g; 1.2 mmoles) in acetonitrile (100ml) was added a solution of (2.1.1)(0.61g; 1.2 mmoles) in acetonitrile (10ml). The resulting solution was refluxed for a further 21 hours. The reaction mixture was allowed to cool. Black needle crystals were filtered and washed with toluene and ether.

0.15g; 12%

IR(KBr): 3100; 2980; 2910; 2250; 2220; 1630; 1500; 820:

Microanalysis: Found: C, 72.82%; H, 2.98%, N, 23.43%

C₇₈H₃₈N₂₂: requires: C, 73.01%; H, 2.96%; N, 24.02%:

UV/visible spectroscopy (CH₃CN): A₃₉₅/A₈₄₂ = 2.66

N,N'-bis(2,4-dinitrophenyl)-4,4'-bipyridinium di-iodide⁴¹

(2.2.3)

To a refluxing stirred solution of 2,4-dinitroiodobenzene (5.82g; 0.02 moles) in methanol (50ml) under an inert atmosphere was added 4,4'-bipyridyl (1.55g; 0.01 moles) in methanol (25ml) over a period of half an hour. The resulting solution was refluxed for a further 5 days. The methanol was removed under reduced pressure to yield a solid. the precipitate was re-crystallised from an acetone/water mixture.

4.3g; 57%; mp: >300°C

IR(KBr): 2980; 2900; 1605; 1510; 1310; 795; 780; 720:

Microanalysis: Found: C, 35.40%, H, 1.79%; N, 11.21%

C₂₂H₁₄N₆O₈I₂ requires: C, 35.48%, H, 1.88%; N, 11.29%:

N,N'-bis(2,4-dinitrophenyl)-4,4'-bipyridinium di-Chloride

(2.2.3)

The bipyridinium was prepared from 2,4-dinitrochlorobenzene (5.5g; 0.03 moles) and 4,4'-bipyridyl (2.1g; 0.01 moles) using the method described above.

3.3g; 59%; mp:218-220°C(lit mp:220-223°C)⁴¹

IR(KBr): 2970; 2910; 1630; 1520; 1305; 795; 780; 720:

Microanalysis: Found: C,47.31%; H,2.53%; N,14.97%

$C_{22}H_{14}N_6O_8Cl_2$: requires: C,47.06%; H,2.50%; N,14.97%:

N,N-bis(2,4-dinitrophenyl)-4,4'-bipyridinium dibromide (2.2.3)

The bipyridinium was prepared from 2,4-dinitrochlorobenzene (5.35g; 0.02 moles) and 4,4'-bipyridyl (1.67g; 0.01 moles) from the method described above.

3.91g; 56%; mp:272-275°C

IR(KBr): 2980; 2910; 1605; 1520; 1305; 790; 785; 730:

Microanalysis: Found: C,40.53%; H,2.09%; N,12.90%:

$C_{22}H_{14}N_6O_8Br_2$: requires: C,40.62%; H,2.15%; N,12.92%

Polyphenylviologen diiodide (2.1.3)

To a refluxing stirred solution of p-phenylene diamine (0.18g; 0.17 mmoles) in water (50ml) under an inert atmosphere was added N,N-bis(2,4-dinitrophenyl)-4,4'-bipyridinium (1.23g; 0.17 mmole) in hot water (25ml) over a period of half an hour. The resulting reaction mixture was refluxed for a further 14 days. The water was removed under reduced pressure to yield a solid. The solid was washed with water (100ml) and chloroform (100ml).

IR(KBr): 3440, 3300, 1600, 1560, 1330, 830, 740:

Microanalysis: Found: C,41.07%; H,2.58%; N,6.89%:

$C_{16}H_{12}N_2I_2$ requires: C,39.51%; H,2.45%; N,5.76%:

Polyphenylviolgen dibromide (2.1.3)

The p-phenyldiamine (0.53g; 0.49 mmoles) was allowed to react with N,N'-bis(2,4 dinitrophenyl)-4,4'-bipyridinium dibromide (3.17g; 0.49 mmoles) using the method described above.

IR(KBr): 3420; 3315; 1630; 1500; 1580; 1330; 830:

Microanalysis: Found: C,50.01%; H,3.14%; N,8.33%:

$C_{16}H_{12}N_2Br_2$ requires: C,48.98%; H,3.06%; N,7.14%:

Polyphenylviolgen dichloride (2.1.3)

The p-phenyldiamine (0.54g 5 mmoles) was allowed to react with N,N'-bis(2,4 dinitrophenyl)-4,4'-bipyridinium dichloride (2.73g; 4.9 mmoles) using the method described above.

IR(KBr): 3400; 3315; 1600; 1510; 1330; 830; 740:

Microanalysis: Found: C,61.31%; H,3.89%; N,10.26%:

$C_{16}H_{12}N_2Cl_2$ requires: C,63.37%; H,3.96%; N,9.24%:

2.6 REFERENCES

1. L. Michaelis and E. S. Hill: J. Gen. Physiol, 16, 59 (1933)
2. W. R. Boon: Outlook Agric, 4, 163-170 (1964)
3. A. J. Macfarlane and R. J. P. Williams: J.Chem.Soc.(A) 1577 (1964)
4. B. Emmert and N. Roh: Ber, 58B, 503 (1925)
5. B. G. White: Trans Faraday Soc., 65, 2000, (1969)
6. A. Ledwith and H. Woods: J.Chem.Soc.(C), 1422 (1970)
7. A. Nakahara and J. H. Wang: J.Phys.Chem., 67, 496 (1963)
8. B. Emmart and H. Lauritzen: Ber, 71B, 240 (1938)
9. M. S. Novakovskii, V. N. Voinova; N. S. Pivnenko and N. F. Kozarinova; Zh. Nerogan khim, 11, 1738 (1966) (Chem abstr., 65, 18143, (1966))
10. A. J. Macfarlane and R. J. P. Williams: J.Chem.Soc.(A), 1517 (1969)
11. A. Rembaum, V. Hadek and S. P. S. Yen: J.Am.Chem.Soc., 93, 2532 (1971)
12. G. J. Ashwell and J. G. Allen: J.de Physique, 44, 1261 (1983)
13. G. J. Ashwell: Phys. stat. sol. (b), 86, 705 (1978)
14. G. J. Ashwell: Phys. stat. sol. (b), 109, K89 (1982)
15. G. J. Ashwell, D. D. Eley, S. C. Wallwork and M. R. Willis: Acta Cryst, A31, 5205 (1975)
16. G. J. Ashwell, S. C. Wallwork and P. J. Rizkallah: Mol.Cryst.Liq.Cryst. 43, 731 (1983)
17. G. J. Ashwell and K. Osborne: Phys. stat. sol. (a), 79, K35 (1983)

18. G. J. Ashwell and S. C. Wallwork: Z.Naturforsch, 40a, 726: 1974
19. R. Somoano, V. Hadek, S.P.S. Yen, A. Rembaum and R. Deck:
J.Chem.Phys, 62, 1061 (1975)
20. G. J. Ashwell, D. D. Eley and M. R. Willis: J.Chem.Soc.
Faraday Trans II, 71, 1227 (1975)
21. G. J. Ashwell, J. G. Allen, G. H. Cross and I. W. Nowell:
Phys. stat. sol. (a) 79, 455 (1983)
22. G. J. Ashwell: phys. stat. sol. (a), 81, 361 (1984)
23. G. J. Ashwell, I. M. Sandy, A. Chyla and G. H. Cross: Syn
Metals 19, 463 (1987)
24. G. J. Ashwell, A. T. Chyla, I. M. Sandy, M. T. Jones,
J. Roble and J. G. Allen: Mol. Cryst. Liq. Cryst., 137, 191
(1986)
25. A. Mizoguchi, H. Moriga, T. Shimidzu and Y. Amano: Natl.
Techn. Rept. (Matsushita Electro. Ind. Co. Osaka) 9, 407
(1963)
26. M. Hatano, H. Nomori and S. Kambara. Rept. Progr. Polymer
Phys. Japan 7, 321 (1964); (see also: Polymer Preprints,
American CHEMSOC Division of Polymer Chemistry p.849 (Sept.
1964)
27. J. H. Lupinskiĭ, K. D. Kopple and J. J. Hertz: Journal of
Polymer Science, Part C 16, 1561, (1967)
28. A. Rembaum, W. Baumgartner, A. Eisenberg: Polymer letters, 6,
159 (1968)
29. H. Noguchi, A. Rembaum: Polymer letters, 7, 383 (1969)
30. A. Rembaum: J. Macromol Sci. Chem., A3, 87 (1969)

31. W. Ciesielski; J. Pecherz and M. Kryszewski: *Acta Polymerica* 33, 318 (1982)
32. A Factor and G. E. Heinsohn: *Polymer letters*, 9, 289 (1971)
33. K. Mizoguchi, S. Kajiura, A. Nakano, E. Tsuchida and I. Shinohara: *Nippon Kagaku Kaishi*, 1404 (1975)
34. T. Kamiya and I. Shinohara: *J. Polym. Sci., Polym. Lett. Ed.* 17, 641 (1979)
35. T. Kamiya, K. Goto and I. Shinohara: *J. Polym. Sci. Polym. Chem. Ed.*, 17, 561 (1979)
36. T. Kamiya, M. Watanabe, K. Goto and I. Shinohara *Polym., Prepr. Jpn.*, 27, 944 (1978)
37. M. S. Simon and P. T. Moore, *J. Polymer Sci.*, 13,1, (1975)
38. M. Watanabe, N. Toneaki and I. Shinohara: *Polymer Journal*, 14, 189 (1982)
39. C. J. Fritchie: *Acta Cryst.*, 20, 892 (1966)
40. H. Kobayashi: *Bull. Chem. Soc. Japan*, 47, 1346 (1974)
41. J. G. Allen: *British Patent* 1399 595 (1971)
42. C. Cilento and K. Zinner: *Arch. Biochem. Biophys.* 120(1), 244, (1967)
43. H. C. Bach: *Am Chem. Soc. Div. Polymer Chem. Preprints*, 7(2), 576 (1966)
44. H. Kusakawa and S. Nishizaki: *Bull. Chem. Soc. Japan*, 38(12), 2201 (1965)
45. M. Ohmasa, M. Kinoshita, M. Sano and H. Akamatu: *Bull. Chem. Soc. Japan*, 41, 1998 (1968)
46. L. A. Summers: *The bipyridinium Herbicides*, Academic Press, London (1980)

47. M. M. Mahmoud and S. C. Wallwork: Acta. Cryst. (B), 32, 440,
1976
48. G. J. Ashwell, S. C. Wallwork and P. J. Rizkallah: Mol.
Cryst. Liq. Cryst. 91, 359, (1983)
49. N. F. Mott and E. A. Davies, Electronic Processes in non
crystalline materials Oxford University Press 1979
50. G. J. Ashwell, D. D. Eley, M. R. Willis, and J. Woodward: J.
Chem. Soc. Faraday II 1785 (1975)
51. Vogel's textbook of practical organic chemistry 4th edition:
Revised by B. S. Furniss, A. J. Hannaford, V. Rogers,
P. W. G. Smith, A. R. Tatchell: IV, 79, 696

Typically organic and inorganic anisotropic compounds with high 'metal-like' conductivity have one donor and one acceptor. However, in 1976, Cougrand et al¹ reported the first example of a ternary quasi-one dimensional molecular conductor between trimethyl ammonium (TMA) iodide and TCNQ. Extensive studies showed the large highly conducting metallic green appearing crystals to be $(\text{TMA}^+)(\text{I}_3^-)_{1/3}(\text{TCNQ})^{2/3-}$ with both the TCNQ and iodine forming segregated linear stacks and a conductivity (σ) that is high at room temperature and is strongly temperature dependent¹⁻³.

The structure from X-ray experiments can be explained by considering two interpenetrating lattices; the main lattice is due to TMA and TCNQ while the second lattice is of the iodine atoms. Two kinds of samples have been characterized, one where the I_3^- sublattice is disordered (D)⁴ and one where the TMA ions interact with the TCNQ molecules through hydrogen bonds with the iodine arrays organised in I_3^- chains alternating with the TCNQ stacks⁵. This was termed ordered (O).

In disordered samples, the conductivity along the chain axis always decreases with temperature ($\sigma_{300} \sim 30 \text{Scm}^{-1}$) while the ordered samples show a broad maximum at $T_m 240\text{K}$ ($\sigma_{TM}/\sigma_{300} = 1.08$)⁶. It then decreases until $\sim 160\text{K}$ ⁶ where both kinds of sample exhibit an abrupt change. This has been attributed to a 'metal to insulator' transition (Peierls distortion)⁷. For ordered samples this 150K anomaly is also present in the magnetic susceptibility and paramagnetic resonance curves^{8,9}.

In addition, anomalies at about 89K, have been observed in the Young's Modulus and microwave dielectric constants¹ and this has been associated with the freeze out of the methyl groups¹⁰.

Ashwell et al¹¹ have also proposed that the above transitions may be attributed to trapped solvent, namely acetonitrile.

As stated earlier the magnetic susceptibility gives an estimate for the metal-insulator transition temperature which is in agreement with that of the resistivity measurements. For the ordered samples a drop in the susceptibility is observed at the metal-insulator transition and an activated region is found below this temperature. The susceptibilities are remarkably similar for both the ordered and disordered samples above 150K. Below this temperature a phase transition is only observed for the ordered compound. At low temperatures a Curie law is obeyed.

In 1984, Lequan et al¹² reported the synthesis of a new series of ternary complexes based upon trimethyl sulphonium iodide, and dimethyl ethyl sulphonium iodide with TCNQ. The complexes $(\text{Me})_3 \text{S}^+(\text{TCNQ-I})^-$ and $(\text{Me})_2\text{Et} \text{S}^+(\text{TCNQ-I})^-$ were semiconductors with room temperature conductivities of 40 and 90 Scm^{-1} , and metal-insulator phase transitions at 138K and 216K respectively¹³. The structures are isostructural with the ammonium complexes¹⁴.

Recently, Barraud et al¹⁵ have reported the formation of a conducting Langmuir-Blodgett film of a ternary TCNQ salt, octadecyl sulphonium-TCNQ iodide.

3.1 Solvent Inclusion in the Sulphonium Ternary Salts

3.1.1 Introduction

Little is known of the solvent inclusion in highly conducting TCNQ salts and its effect on the electrical and magnetic properties, although it has been well established that crystals grown from solution often contain pockets of trapped solvent¹⁶. In 1974 Flandrois et al¹⁷ obtained evidence of acetonitrile in TCNQ salts by mass spectrometry and more recently Lindeguaard-Anderson et al¹⁸ observed solvent inclusions and other growth defects by X-ray topography.

The properties and transitions of acetonitrile have been summarised by Michel and Lippert¹⁹: Acetonitrile melts at 229K and undergoes a solid state endothermic transition at 214K. Differential scanning calorimetry (D.S.C.) studies also show a transition in the range 170 to 200K. In addition Jacobsen and Mikawa²⁰ have reported the existence of another phase below 100K.

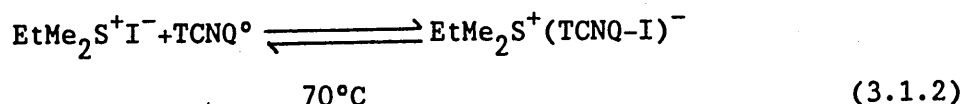
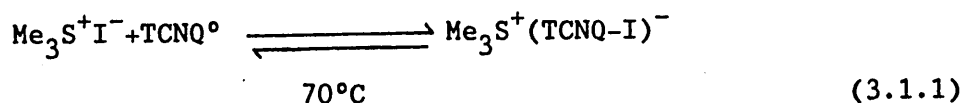
Many highly and less conductive TCNQ complexes show anomalous electrical and magnetic behaviour within the narrow temperature range 200 to 240K^{3,21-23}.

As stated earlier, Ashwell et al¹¹ have interpreted the transitions of $(\text{TMA}^+)(\text{I}_3^-)_{1/3}(\text{TCNQ}^{2/3-})$ to be solvent induced.

The sulphonium ternary salts $\text{Me}_3\text{S}^+(\text{TCNQ-I})^-$ (3.1.1) and $\text{EtMe}_2\text{S}^+(\text{TCNQ-I})^-$ (3.1.2) have a broad maximum conductivity $T_m \sim 250\text{K}$ and metal-insulator phase transition at 216K respectively^{13,14}. It was planned to synthesise the above salts from a variety of differing solvents and to observe their D.S.C. traces and magnetic susceptibilities to determine whether transitions are intrinsic or solvent induced.

3.1.2 Synthesis

Crystals of the ternary complexes were synthesised using the methods of Lequan et al¹⁴ from acetonitrile, ethanol and methanol.



3.1.3 Differential Scanning Calorimetry Studies

The D.S.C. trace of spectrophotometric grade acetonitrile shows a distinctive broad double exothermic transition (Figure: 3.1.1) with $\Delta H = 8.3\text{KJ mol}^{-1}$ at 229K and $\Delta H = 0.80\text{KJ mol}^{-1}$ at 214K ¹¹. The transitions have been attributed to the melting point and a structural modification respectively.

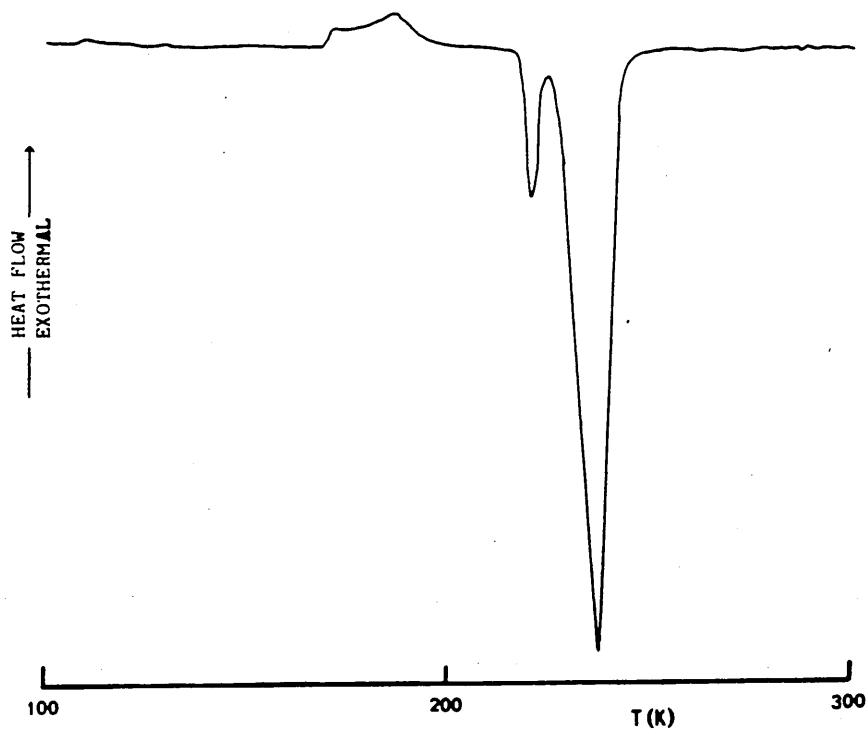


Figure: 3.1.1: D.S.C. Trace of Acetonitrile

The D.S.C. studies were carried out on 15 to 20mg samples using a Mettler T.A. 3000 thermal analysis system. The temperature was increased from 100K to 400K at a rate of 5K per minute.

The D.S.C. trace for a number of samples of the ternary complex $\text{EtMe}_2\text{S}^+(\text{TCNQ-I})^-$ (3.1.2) prepared from acetonitrile showed no characteristic double transition only a small enthalpy change at ~250K. This was also observed in the other samples prepared from methanol and ethanol.

The D.S.C. traces of the $\text{Me}_3\text{S}^+(\text{TCNQ-I})^-$ (3.1.1) complexes from the varying solvents showed no transitions in the region 100K to 400K.

The results seem to support the argument that these complexes either have no, or only a small amount of, solvent inclusion associated with them and the observed electrical transitions are intrinsic in nature.

3.1.4 Magnetic Studies

The Faraday method was employed for the determination of the magnetic susceptibility using a C.I. Robel microbalance.

The ternary complexes of $\text{Me}_3\text{S}^+(\text{TCNQ-I})^-$ (3.1.1) synthesised from the varying solvents showed very similar behaviour (Figures 3.1.2; 3.1.3). A drop in the magnetic susceptibility is observed for all the samples at $\sim 130\text{K}$, the metal-insulator transition, and below this temperatures an activated regime is found. At low temperature a 'Curie tail' is detected due to impurities. At higher temperatures a temperature independent susceptibility is observed, which may be interpreted as Pauli paramagnetism.

The $\text{EtMe}_2\text{S}^+(\text{TCNQ-I})^-$ (3.1.2) salts show exactly the same behaviour. The temperature dependences of the magnetic susceptibility, corrected for core diamagnetism are given in Figures: 3.1.4 and 3.1.5. The $1/\chi$ versus T plot is linear in the range 300 to 25K, showing the salt to be a Curie -Weiss paramagnet where the susceptibility varies as $\chi = C(T + \theta)$. A transition for the ternary salts is observed at $\sim 252\text{K}$ which is in agreement with the results obtained from the D.S.C. studies.

In conclusion the physical properties of the ternary complexes have been shown not to be solvent induced. The D.S.C. and magnetic susceptibility studies show that their transitions are intrinsic.

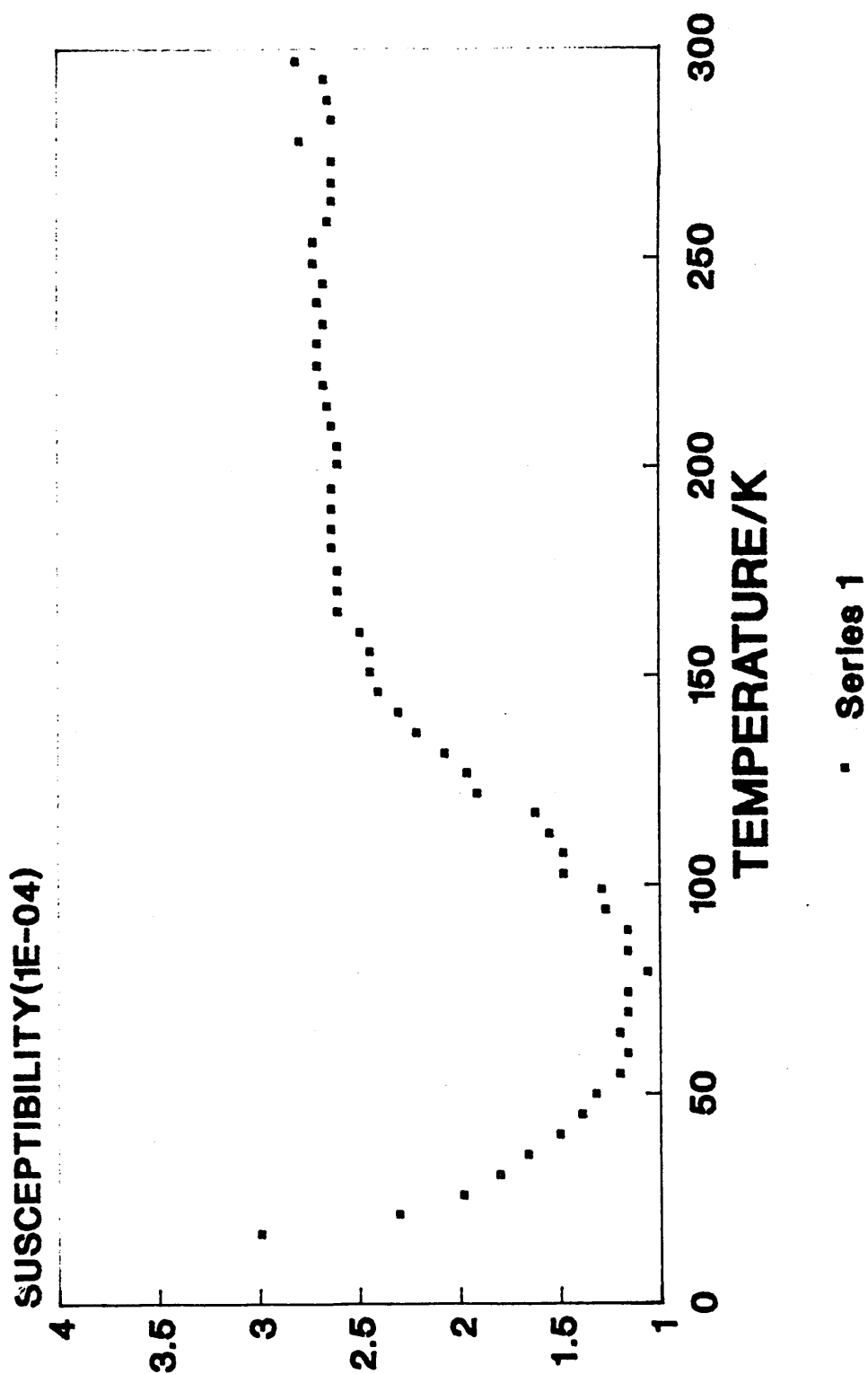


Figure: 3.1.2: The Magnetic Susceptibility Temperature dependence of $\text{Me}_3\text{S}^+(\text{TCNQ-I})^-$ Synthesised from acetonitrile

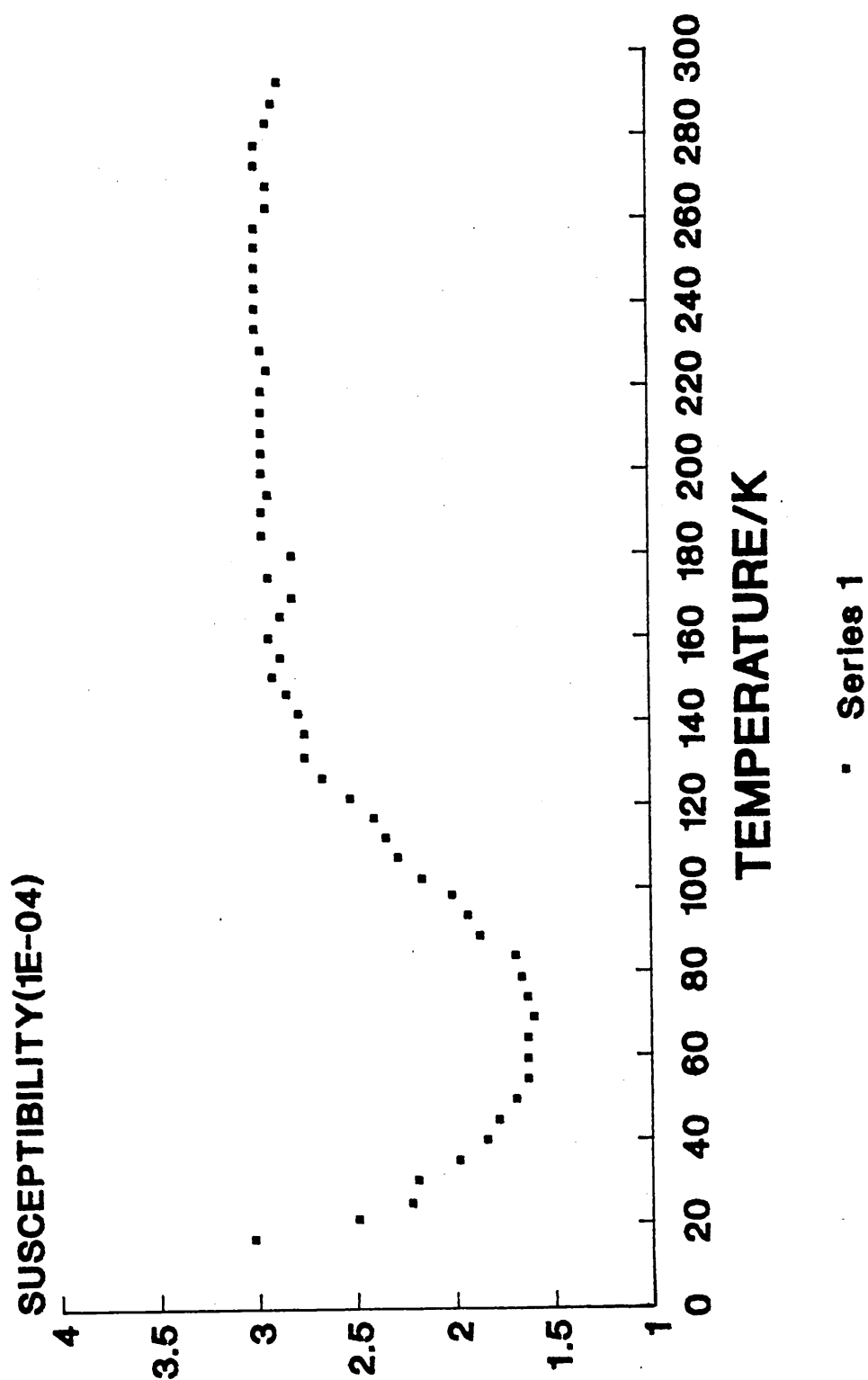


Figure: 3.1.3: The Magnetic Susceptibility Temperature dependence of $\text{Me}_3\text{S}^+(\text{TCNQ-I})^-$ Synthesised from ethanol.

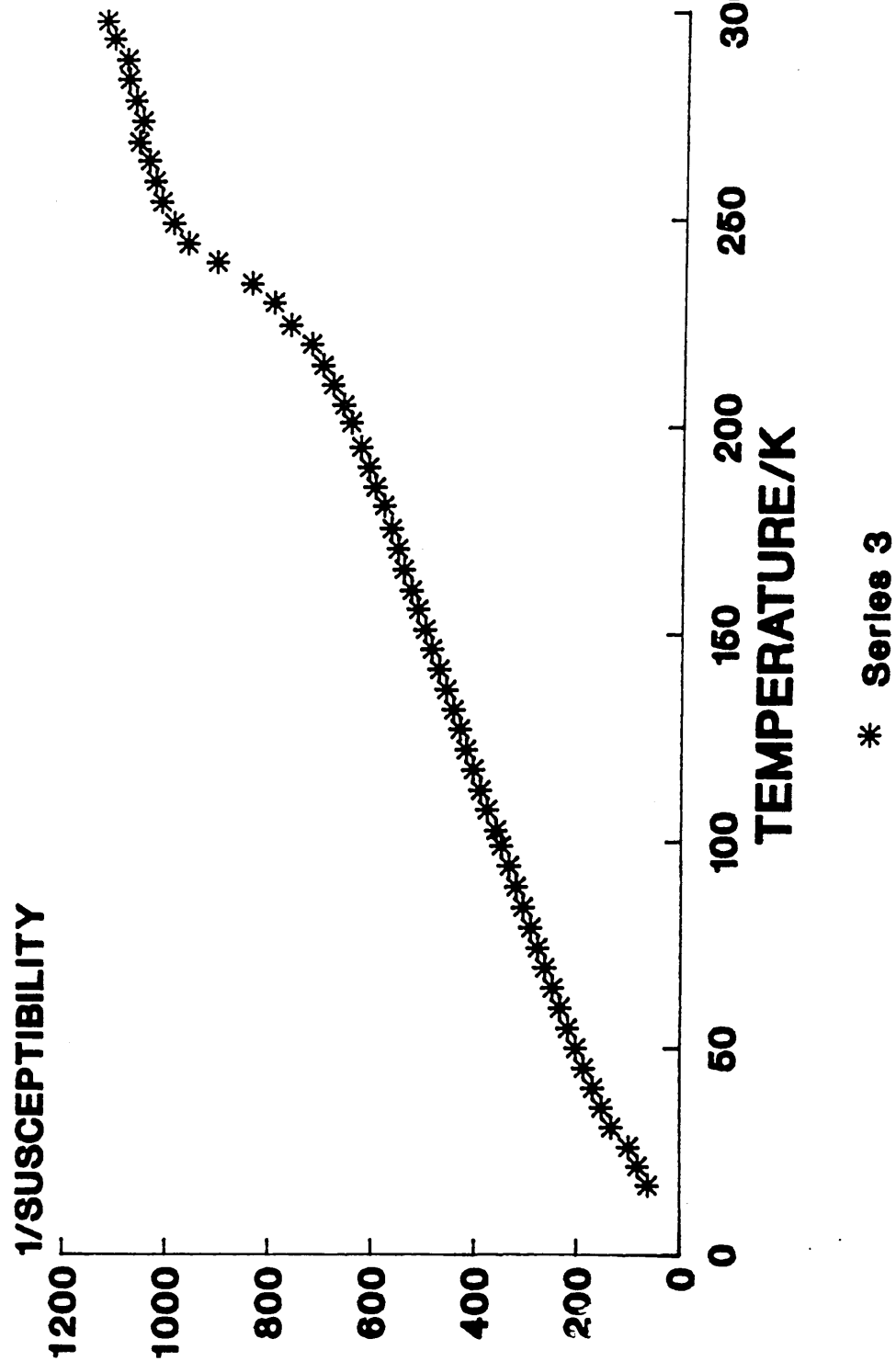


Figure: 3.1.4: The Magnetic Susceptibility Temperature dependence of $\text{EtMe}_2\text{S}^+(\text{TCNQ-I})^-$ Synthesised from acetonitrile

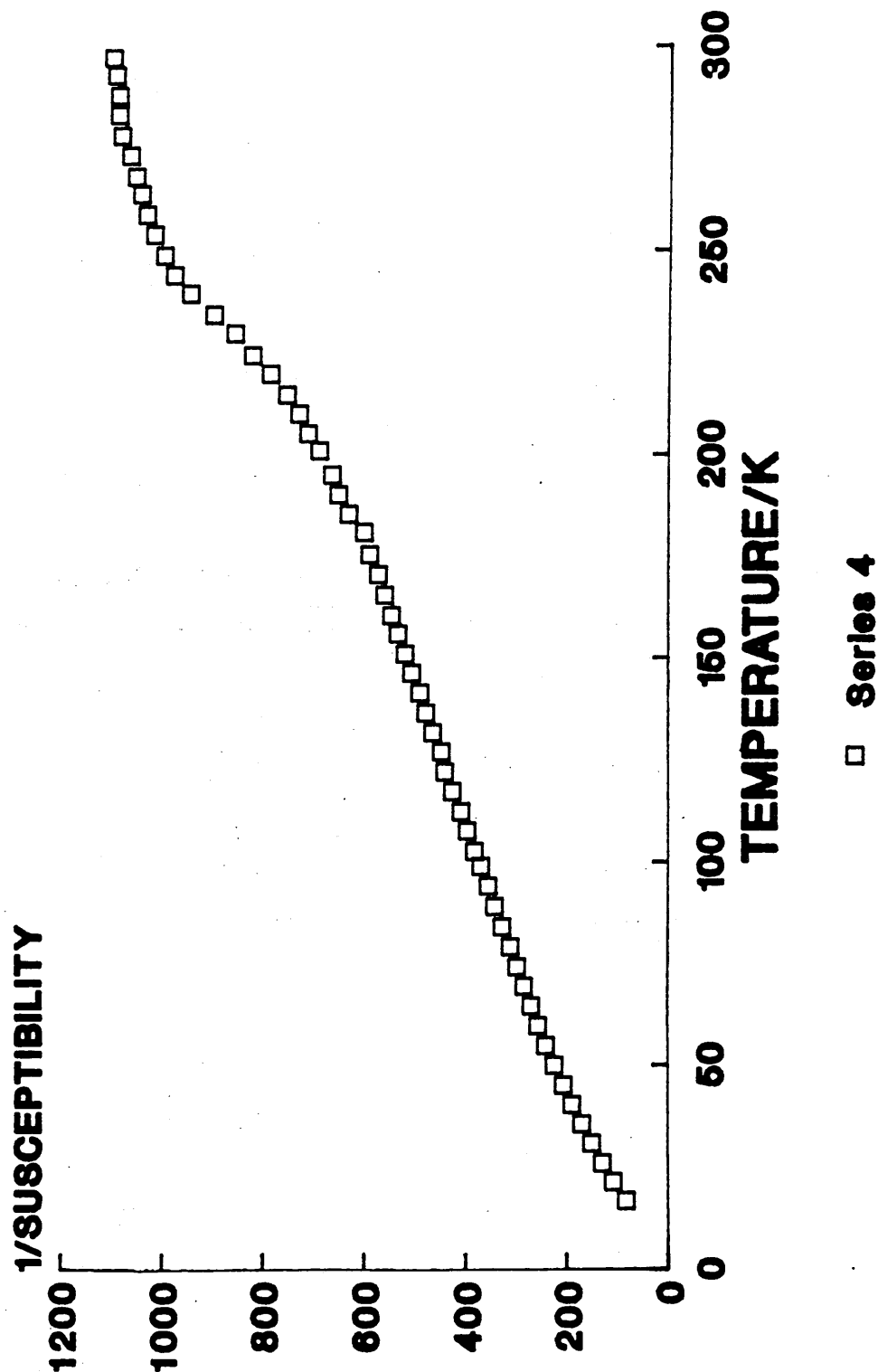


Figure: 3.1.5: The Magnetic Susceptibility Temperature dependence of $\text{EtMe}_2\text{S}^+(\text{TCNQ-I})^-$ Synthesised from Methanol

3.2 Dipyrrylmethene ternary complexes

3.2.1 Introduction

The ternary complex of TCNQ with 3,4,5,3',4'-pentamethyl-dipyrrylmethene hydrobromide (3.2.1Br) (Figure: 3.2.1) was observed to have no absorption in its ultra violet/visible solid state spectra at 842nm, indicating the absence of the radical anion TCNQ^- . However, this neutral molecule has a conductivity at 300K of $2.3 \times 10^{-4} \text{ Scm}^{-1}$ ²⁴.

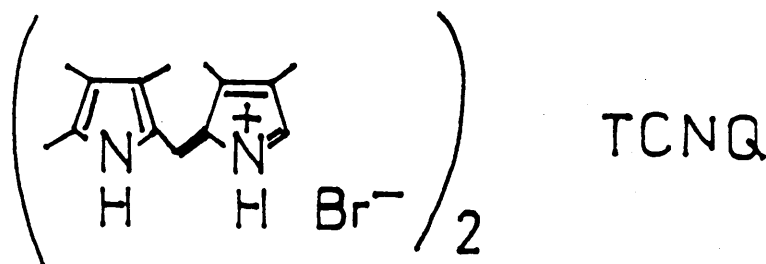
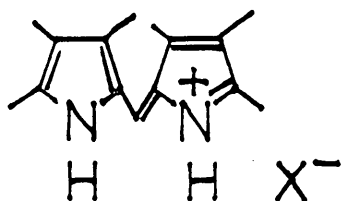


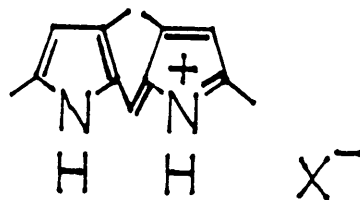
Figure: 3.2.1: The ternary complex (3,4,5,3',4'-pentamethyl-dipyrrylmethene hydrobromide)₂ TCNQ

It was proposed to re-synthesise the above complex and to investigate the effect on the degree of charge transfer of varying the anion and of systematically varying the number of methyl groups (Figure: 3.2.2).

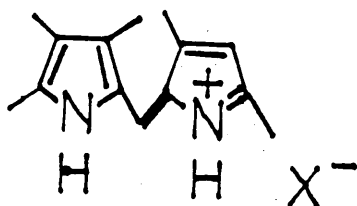
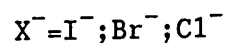
The target molecules were:



(3.2.2)



(3.2.3)



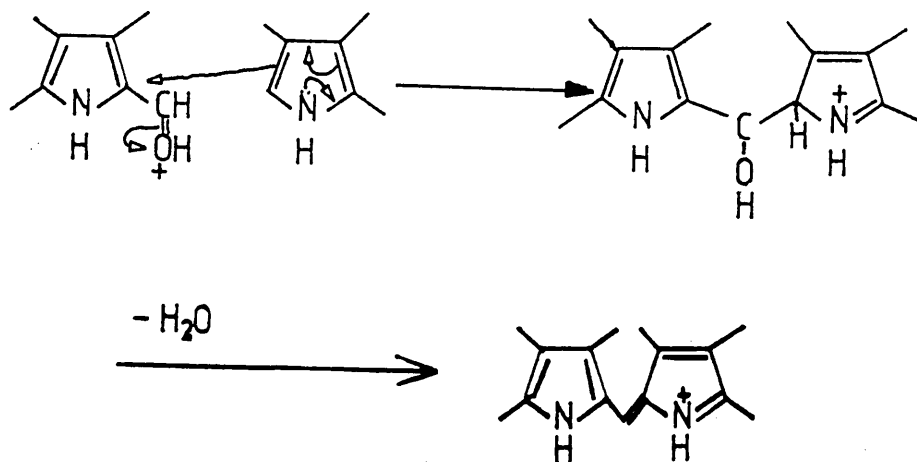
(3.2.4)

Figure: 3.2.2: The proposed donor molecules

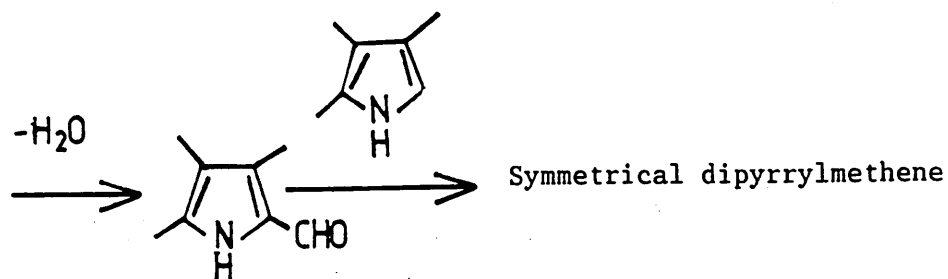
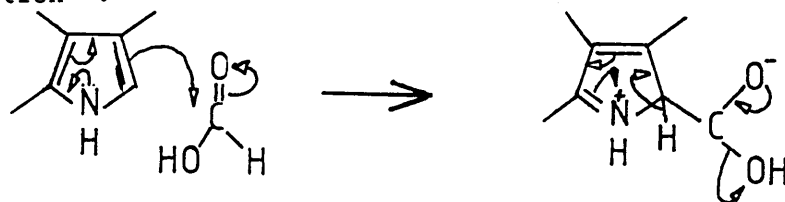
Dipyrromethenes are mainly used in chemistry as intermediates for the synthesis of porphyrins²⁵⁻²⁷. The porphyrin skeleton is usually constructed from four individual pyrroles by first bringing these units together in pairs to give two dipyrromethenes and then joining the pairs.

The four main methods for synthesizing these important molecules are reviewed below:

1. A pyrrole-2-aldehyde can be treated with a 2-unsubstituted pyrrole in an acid solution²⁸. The acid increases the reactivity of the aldehyde group towards nucleophiles with the reaction proceeding via a dipyrromethanol.



2. The preparation of a pyrrole-2-aldehyde may be by-passed if a symmetrical dipyrromethene is required. A 2-unsubstituted pyrrole can be treated with formic acid in the presence of an acid to form a pyrrole-2-aldehyde which in turn can condense with an unreacted pyrrole to produce a dipyrromethene cation²⁹.



3. A 2-methyl pyrrole containing a free-5-position e.g. kryptopyrrole can be treated with bromine in acetic acid. A benzylic-type bromide is formed by one of the pyrrole units and this reacts with the second pyrrole at the 5-position to give a dipyrromethene³⁰.
4. Finally dipyrromethanes can be oxidised to their corresponding dipyrromethenes³¹.

3.2.1.1 Properties and reactions

They are intensely coloured compounds with their salts being more stable than their corresponding free bases on account of the fuller resonance in the symmetrical cation (Figure: 3.2.2)

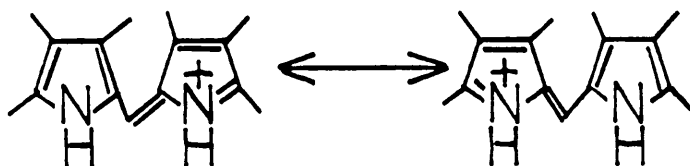


Figure: 3.2.2: The resonance of the symmetrical cation dipyrromethene

The dipyrromethenes are very susceptible to attack by nucleophiles at the methine carbon atom. For example Brunings and co-workers³² observed that the co-valent bromo dipyrromethene (Figure 3.2.3) was isolated rather than the dipyrromethene hydrobromide.

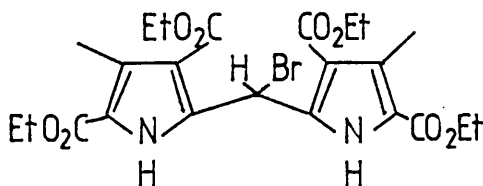


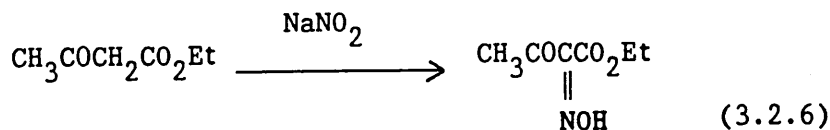
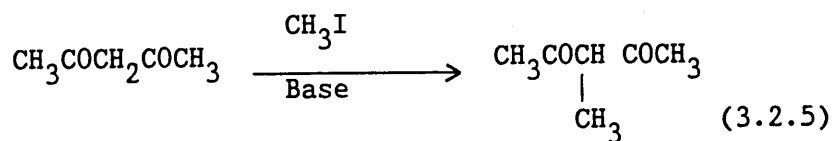
Figure: 3.2.3: The co-valent bromo dipyrromethene.

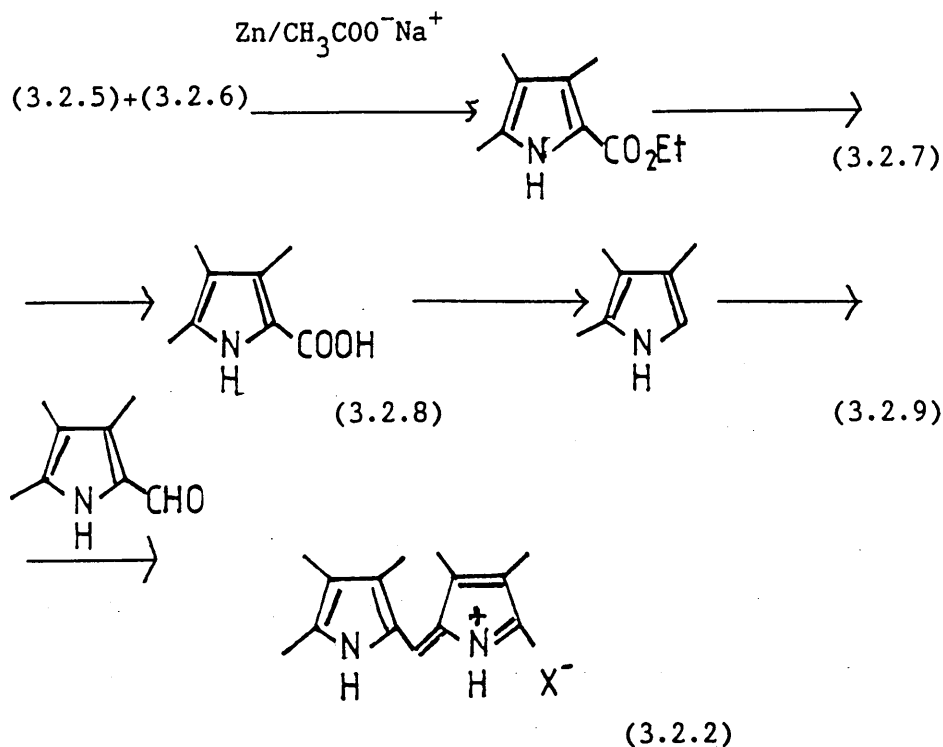
The only other noteworthy reaction of the simple dipyrromethenes is their formation of a variety of fairly stable metal complexes, for example with cobalt, nickel, copper and zinc³³.

3.2.2 Synthesis

3.2.2.1 Preparation of 3,4,5,3',4',5'-hexamethyl dipyrromethene hydrobromide

The proposed reaction scheme for the synthesis of the hexamethyl dipyrromethene donor molecule (3.2.2) is given below:





The pyrrole ester (3.2.7) was obtained in high yields comparable with the published work³⁴⁻³⁶.

3.2.2.2 Hydrolysis of 2-ethoxycarbonyl-3,4,5-trimethyl pyrrole

This reaction was investigated on a small scale, but all attempts to isolate the desired pyrrole acid (3.2.8) proved to be unsuccessful.

The first method attempted was a base catalysed hydrolysis using sodium hydroxide in ethanol at room temperature followed by acidification of the anion. However, thin layer chromatography confirmed that the starting material remained unreacted.

The failure of the above reaction prompted the use of methods with more vigorous conditions. The above reaction was repeated, but at an elevated temperature. However, this reaction was unsuccessful. Two procedures which increase the basicity of the OH^- were tried. The first as described by Gassman et al³⁷, for the base promoted hydrolysis of hindered esters, using potassium tert-butoxide in anhydrous ether. Thin layer chromatography again confirmed the failure of the reaction. The second method³⁸ uses potassium hydroxide, dicyclohexyl 18-crown-6 and toluene as the solvent. The complexation of K^+ by the crown ether renders the OH^- more basic. However, this reaction was unsuccessful.

The methyl ester pyrrole (Figure: 3.2.4) was prepared because of the increased number of methods available in the literature for hydrolysis of methyl esters compared to ethyl esters.

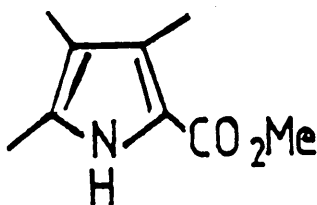


Figure: 3.2.4: 2-methoxycarbonyl-3,4,5-trimethyl pyrrole

Two methods^{39,40} for the conversion of sterically hindered methyl esters to their corresponding acids were tried, the first³⁹ using chlorotrimethyl-silane in the presence of anhydrous sodium iodide. The trimethylsilyl pyrrole ester should then be susceptible to reaction with water to produce the corresponding acid. The second⁴⁰ involves the heating of the pyrrole methyl ester with lithium iodide in dimethylformamide. The mechanism involved the nucleophilic attack by the halide ion on the methyl carbon. However, attempted isolation of the desired product failed.

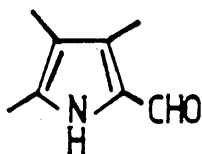
Thin layer chromatography of the above reactions revealed a spot for the starting material and a spot which was not representative of the pyrrole acid. It is worth noting that Fischer and Walach⁴¹ observed that the related 3-ethyl-4,5-dimethyl pyrrole-2-carboxylic acid was extremely unstable.

However, the need to prepare the carboxylic acid was removed when a new synthetic approach was found in the literature²⁹. The pyrrole ester (3.2.7) was refluxed with formic acid and either hydrobromic, hydrochloric or hydroiodic acid to give the appropriate symmetrically substituted dipyrromethene. The reaction proceeds via the in situ hydrolysis and decarboxylation of the pyrrole ester (3.2.7), to form a 2-unsubstituted pyrrole. This forms the desired product in the way detailed earlier (see 3.2.1 Introduction). The acid catalyses the processes involved.

3.2.2.3 Penta and tetramethyl dipyrromethenes

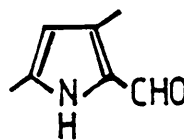
The penta and tetramethyl dipyrromethene target molecules (3.2.4, 3.2.1, 3.2.3) were synthesised from the following precursors:

1.



(3.2.10)

2.



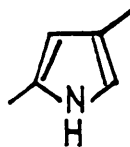
(3.2.11)

3.



(3.2.12)

4.



(3.2.13)

The pyrrole-2-carboxaldehyde precursor 1 (3.2.10) was prepared via a Vilsmeier-Haak reaction⁴³ of 3,4,5-trimethyl pyrrole obtained from the hydrolysis and in situ decarboxylation of 2-ethoxycarbonyl 3,4,5-trimethyl pyrrole (3.2.7)⁴².

Precursor 2 (3.2.11) was obtained from the Vilsmeier-Haak reaction⁴³ of 2,4-dimethyl pyrrole. The 2-unsubstituted pyrrole forms a pyrrolyl dimethyliminium ion salt which is reacted with aqueous hydroxide solution to produce the desired aldehyde (Figure 3.2.5).

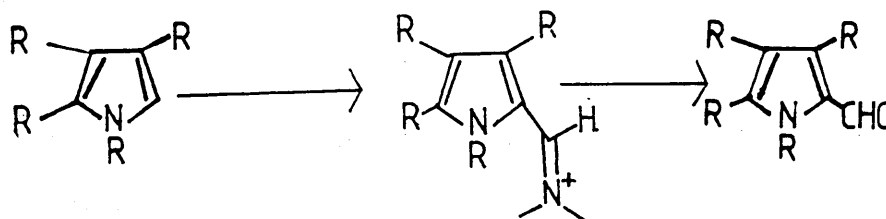


(Figure: 3.2.5) The Vilsmeier-Haak reaction

The 3,4-dimethylpyrrole (3.2.12), precursor 3, was prepared from the lithium aluminium hydride reduction of 1,3,4-triscarbomethoxypyrrole (Figure: 3.2.6)⁴⁴.

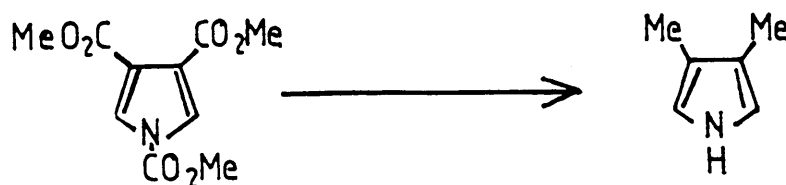


Figure: 3.2.6: The preparation of precursor 3 from the reduction of 1,3,4-triscarbomethoxypyrrole.

Precursor 4, the 2,4-dimethyl pyrrole (3.2.13), was prepared from the hydrolysis and in situ decarboxylation⁴² of 3,5-dimethyl-2,4-diethoxycarbonyl pyrrole⁴⁵ (Figure: 3.2.7).

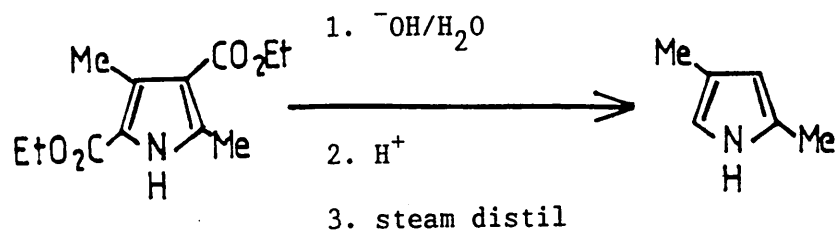
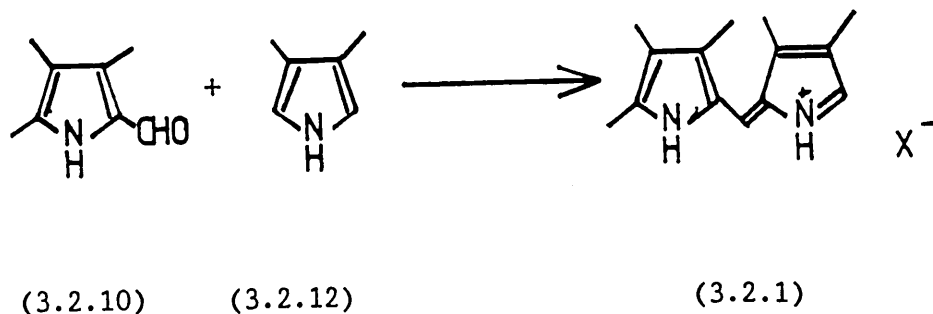
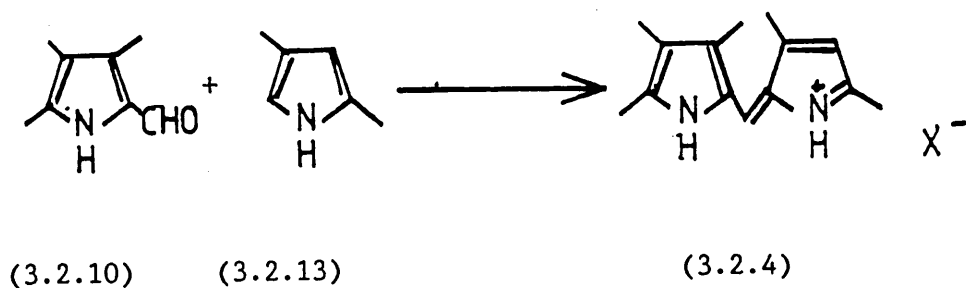


Figure: 3.2.7: The preparation of precursor 4

The pyrrole-2-aldehydes (3.2.10, 3.2.11) were treated with the 2-unsubstituted pyrroles (3.2.12, 3.2.13) in acidic solution to give the desired donors (3.2.4, 3.2.1, 3.2.3) (Figure: 3.2.8).



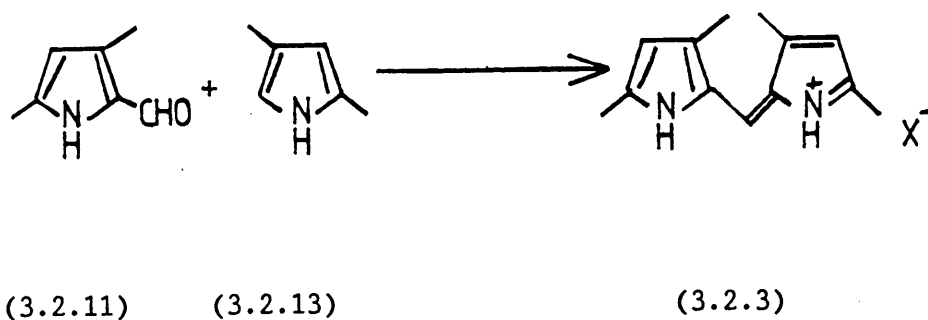


Figure: 3.2.8: The synthesis of the desired donor molecules

3.2.2.4 Preparation of the charge transfer complexes of TCNQ with dipyrromethenes

The normal conditions for the synthesis of the charge transfer complexes with TCNQ consist of a short reflux in acetonitrile. However, under these conditions no complex was observed with hexamethyl dipyrromethene (3.2.2). Attempts to prepare the charge transfer complex by increasing the reflux time also failed. Efforts were directed towards modifying the above method with the charge-transfer complex only being isolated at room temperature in a solvent mixture of acetonitrile and chloroform. However, the penta and tetramethyl dipyrromethenes (3.2.1, 3.2.4, 3.2.3) formed complexes with TCNQ both in refluxing acetonitrile and at room temperature in the solvent mixture.

Investigations of the charge-transfer complex of the hexamethyl dipyrromethene (3.2.2) showed that this was very unstable, compared with both the tetra and pentamethyl dipyrromethene (3.2.1,3.2.4,3.2.3) complexes. Ultra-violet/visible spectrophotometric techniques revealed that it breaks down to its constituent components in solution or upon heating. Steric hindrance could be a possible explanation. Crystallographic studies have shown the structure of dipyrromethene to be that in figure 3.2.9⁴⁶⁻⁴⁸.

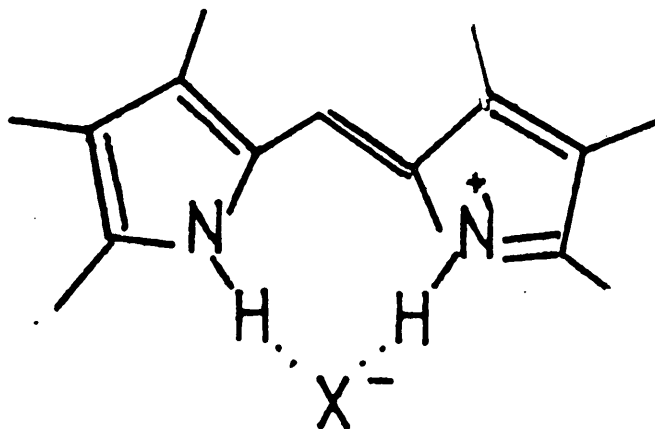


Figure: 3.2.9: The structure of the dipyrromethene donor molecule.

The extra methyl(s) could hinder the close approach of the TCNQ molecule and thus weaken the electrostatic forces between the TCNQ and the dipyrromethene, facilitating the break down of the complex. This observation is confirmed by the failure of the hydroiodide dipyrromethenes to form complexes with TCNQ in all cases. The increased size of the iodide compared to the chloride and bromide (table 3.21) is thought to hinder the

close approach of the TCNQ molecule with the result that no complex is formed.

Element	Crystal Radius X^- (Å)
Cl	1.70
Br	1.87
I	2.12

Table: 3.21: The size of the various counter anions

3.2.3 Stoichiometry

The ultra-violet/visible spectra of the dipyrromethene TCNQ complexes provided structural information on the salts. The absence of a strong absorption at λ_{\max} 840nm confirmed that the ternary salts were essentially neutral complexes (a typical spectrum is shown in Figure 3.2.10). However, the infra-red spectra for the complexes of pentamethyl dipyrromethene (3.2.1 Br) and hexamethyl dipyrromethene (3.2.2 Br) with TCNQ exhibit a very small absorption centred around 2175 cm^{-1} , which is characteristic of the TCNQ radical anion (see later).

The stoichiometries were determined by elemental analysis. This gave a 2:1 stoichiometry of dipyrromethene: TCNQ (table 3.22). However, it must be remembered that this technique is insensitive to small changes in the ratio of donor to TCNQ.

To remove any ambiguity the stoichiometries were also sought from the structural determination of the salts, using the equation:

$$\rho = \frac{Z}{V \times 0.6022} \frac{M_r}{\text{Equation 3.21}}$$

where ρ = density

Z = No. of molecules in the unit cell

M_r = relative molecular mass.

V = Volume of unit cell

Elongated brown plates of the charge-transfer complexes between TCNQ and hexamethyl dipyrromethene (3.2.2 Br) and pentamethyl dipyrromethene (3.2.1 Br) were obtained from the reaction mixture and the slow evaporation of a saturated solution respectively. However, the oscillation and zero-level Weissenberg photographs indicated that the 'single crystals' were twinned i.e. existence of two different orientations of a lattice in what is apparently one crystal⁴⁹⁻⁵¹. The elucidation of the unit cell and thus the stoichiometry proved to be impossible.

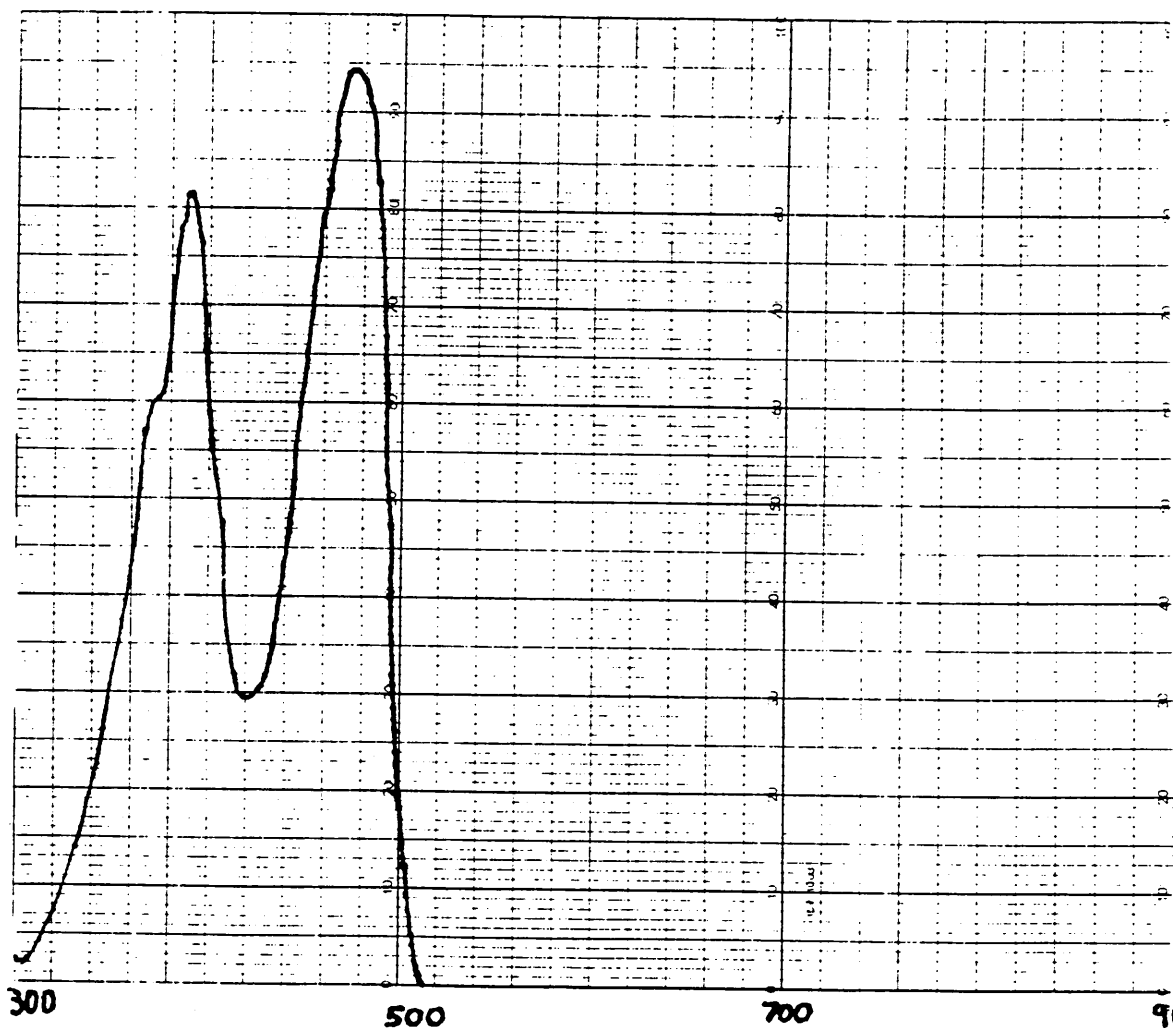


Figure: 3.2.10: Typical spectrum of dipyrrylmethene
TCNQ complex

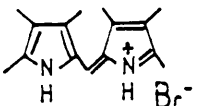
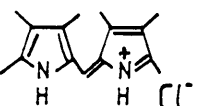
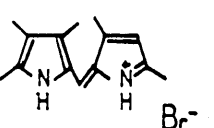
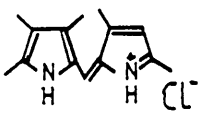
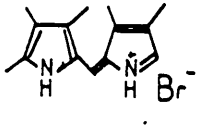
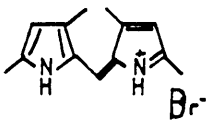
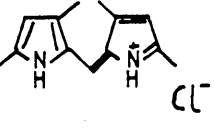
TCNQ		Ratio			
Complex of:		Elemental Analysis			Dipy:TCNQ
		C	H	N	
	calc	61.32	5.64	13.62	2 : 1
	found	61.12	5.65	13.51	
	calc	68.75	6.32	15.27	2 : 1
	found	68.70	6.25	15.26	
	calc	60.46	5.32	14.10	2 : 1
	found	60.28	5.31	14.07	
	calc	68.18	5.97	15.91	2 : 1
	found	67.93	5.91	15.83	
	calc	60.46	5.32	14.10	2 : 1
	found	60.98	5.51	13.98	
	calc	59.53	4.99	14.61	2 : 1
	found	59.42	4.93	14.61	
	calc	67.35	5.65	16.53	2 : 1
	found	67.25	5.59	16.45	

Table 3.22: The stoichiometry of dipyrromethene: TCNQ

3.2.4 Electrical Conductivity and Magnetic Susceptibility

Measurements

The electrical and magnetic properties of the series of TCNQ salts were measured using a two point probe and Faraday methods respectively.

The room temperature conductivities show that all but one of the complexes are insulating ($<10^{-7} \text{ Scm}^{-1}$). The conductivity of the pentamethyl dipyrromethene (3.2.1 Br) complex is $1.32 \times 10^{-4} \text{ Scm}^{-1}$.

The magnetic properties of the complexes show a close correlation with the above conductivities. The total susceptibilities of the TCNQ complexes with the hexamethyl (3.2.2 Cl), tetramethyl (3.2.3, Br, Cl) and pentamethyl (3.2.4 Br Cl) dipyrromethenes are all diamagnetic. However, the hexamethyl (3.2.2 Br) and pentamethyl (3.2.1 Br) dipyrromethene TCNQ complexes (Figure: 3.2.11) are weakly paramagnetic with their susceptibilities being independent of temperature in the range 295 to 25K (Figure: 3.2.12).

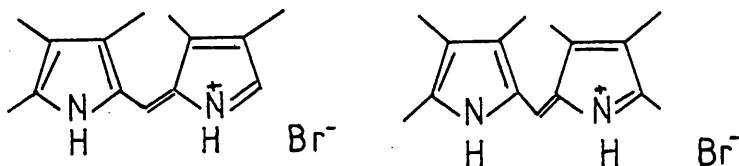


Figure: 3.2.11: The structures of the hexa and pentamethyl dipyrromethenes.

The total susceptibilities (χ_{TOT}) of the pentamethyl (3.2.1 Br) and the hexamethyl (3.2.2 Br) dipyrromethene complexes have values of $6.76 \times 10^{-4} \text{ emu mole}^{-1}$ and $1.62 \times 10^{-4} \text{ emu mole}^{-1}$ respectively. When the correction is made for a molar diamagnetic susceptibility $\chi_{DIA}=4.886 \times 10^{-4} \text{ emu mole}^{-1}$ (for the pentamethyl) and $\chi_{DIA}=5.132 \times 10^{-4} \text{ emu mole}^{-1}$ (for the hexamethyl), a value for the spin susceptibility (χ_S) of $1.15 \times 10^{-3} \text{ emu mole}^{-1}$ is obtained for the pentamethyl dipyrromethene TCNQ salt and $6.75 \times 10^{-4} \text{ emu mole}^{-1}$ for the hexamethyl dipyrromethene salt. These small positive values, independent of temperature within the experimental temperature range, could be interpreted as a Van Vleck type paramagnetism where, in the presence of a magnetic field, an excited state, separated from the ground state by an energy large compared to KT is mixed with the ground state giving it a magnetic moment. The other possibility is a Pauli paramagnetism, which is characteristic of a degenerate electron gas. However, Pauli paramagnetism is normally associated with high conductivity⁵². Therefore, the temperature independent paramagnetism could only possibly be due to Van Vleck paramagnetism⁵².

3.2.5 Infra-red studies

The visible spectrum obtained from crystals dissolved in acetonitrile suggests that there is no mean ionic charge on the TCNQ moiety and this is in agreement with the magnetic studies for the hexamethyl (3.2.2 Cl), pentamethyl (3.2.4 Br Cl) and tetramethyl (3.2.3 Br Cl) dipyrromethene complexes. To enhance conductivity it would be necessary to introduce an integral charge on the TCNQ lattice sites.

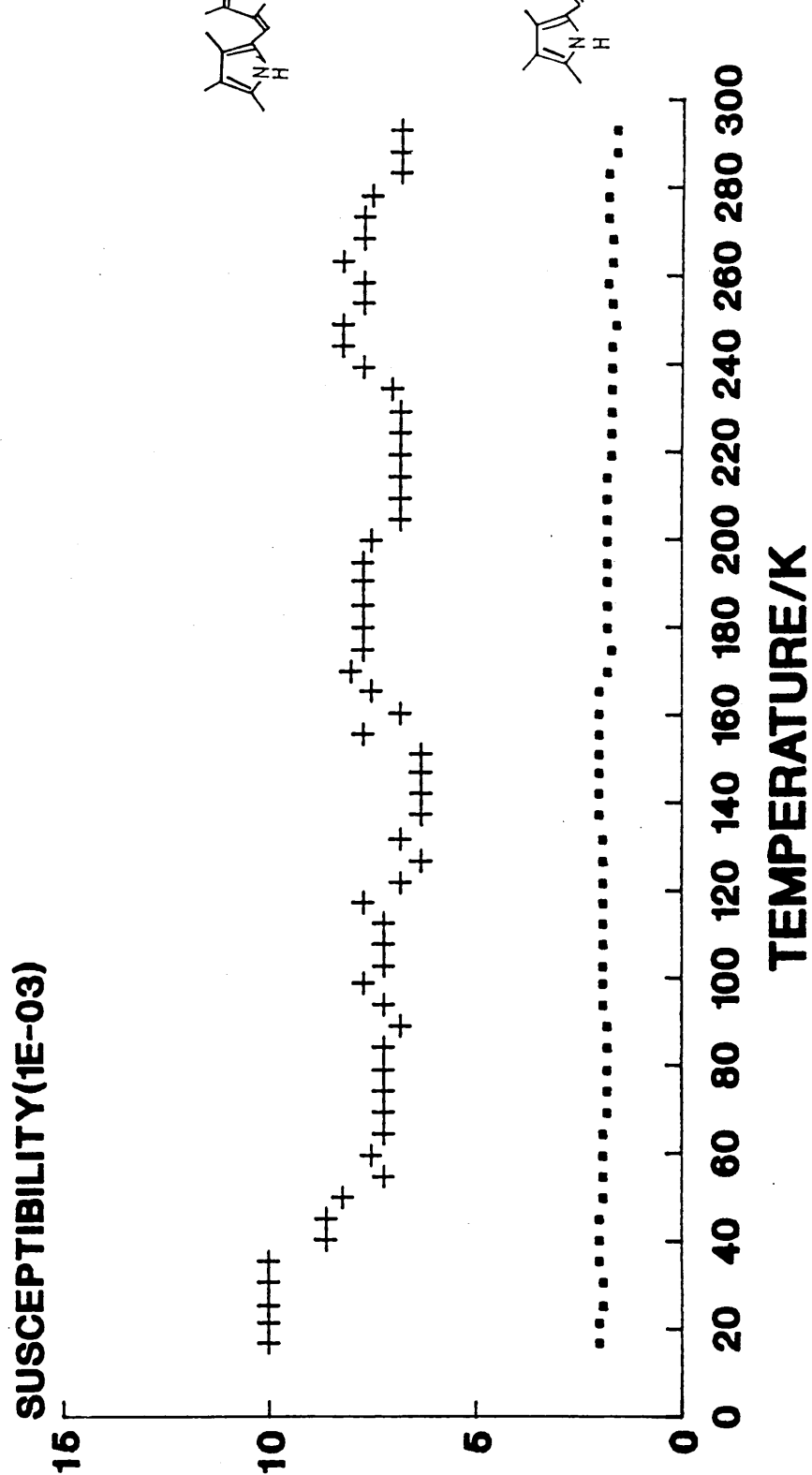


Figure: 3.2.12: The magnetic susceptibility temperature dependence of the hexamethyl (3.2.2 Br) and Pentamethyl (3.2.1 Br) dipyrromethene TCNQ complexes.

On close examination of the infra-red spectra particularly the region between 2250 and 2150 cm^{-1} , the TCNQ complexes of the hexamethyl (3.2.2 Br) and pentamethyl (3.2.1 Br) dipyrromethenes exhibit two definite absorption bands, derived from the nitrile groups of TCNQ at 2211 cm^{-1} , 2175 cm^{-1} and 2211 cm^{-1} and 2179 cm^{-1} respectively (Figure: 3.2.13). However, the other complexes only exhibit one absorption band centred around 2210 cm^{-1} (Figure: 3.2.14).

The relative intensities of the absorptions for the pentamethyl complex is ≈ 2 compared with ≈ 1 for the hexamethyl complex. Bloch and co-workers⁵³ have demonstrated that the degree of charge transfer (ρ) in TCNQ salts shows a linear dependence upon the nitrile stretching frequency, ν_{max} 2225 cm^{-1} and 2180 cm^{-1} being characteristic of TCNQ⁰ and TCNQ⁻ respectively⁵³. For the penta and hexamethyl complexes the absorptions at 2179 cm^{-1} and 2175 cm^{-1} are clearly indicative of TCNQ⁻, while the peaks at 2211 for both complexes are characteristic of a TCNQ molecule bearing a fractional anionic charge of approximately 0.4e. This is in agreement with the magnetic studies which show the two complexes to be weakly paramagnetic.

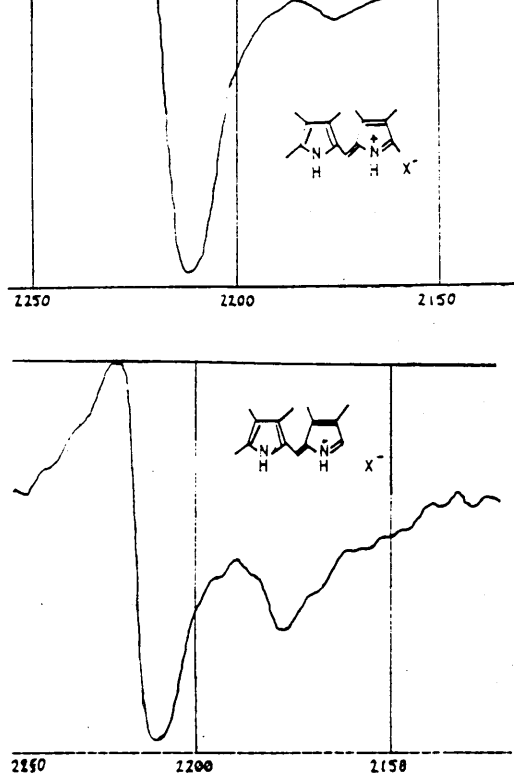


Figure: 3.2.13: The Infra-red spectra of the hexa (3.2.2 Br) and the pentamethyl (3.2.1) dipyrromethene TCNQ complexes.

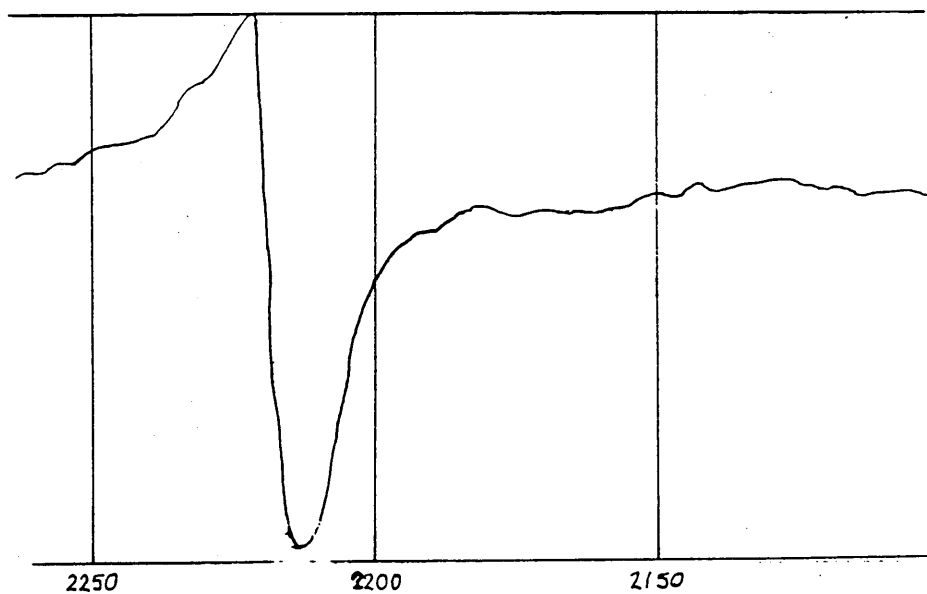


Figure: 3.2.14: The Infra-red spectra of the hexa (3.2.2 Cl) and penta (3.2.4) and tetra methyl (3.2.3) dipyrromethene TCNQ complexes.

The effect on the degree of charge transfer of varying the anion of the dipyrromethene can clearly be seen by comparing the infra-red spectra of the TCNQ complexes with hexamethyl hydrobromide and hydrochloride. As stated earlier the hexamethyl hydrobromide complex exhibits an absorption for TCNQ^- whereas the hexamethyl hydrochloride does not, suggesting significantly more charge transfer. If the accepted electronegativities of 2.85 for chlorine and 2.75 for bromine are compared, it indicates that Cl is a stronger acceptor than Br. This could possibly lead to more electron transfer occurring from TCNQ^- to the chloride than the bromide. This 'back' electron transfer would result in the oxidation of the TCNQ^- to TCNQ^0 and therefore would be responsible for the diamagnetic behaviour of the hexamethyl dipyrromethene hydrochloride complex and also the absence of a TCNQ^- absorption in its infra-red spectrum.

The reduced number of methyl groups of the tetramethyl dipyrromethenes (3.2.3) leads to a reduction in the electron density in the rings. This significantly lowers the charge transfer between the TCNQ moiety and the donor and results in an insulating salt being obtained.

The increased paramagnetic value and the larger intensity for the TCNQ^- absorption compared with the other complexes, suggests there is significantly more charge transfer between the TCNQ acceptor and the pentamethyl dipyrromethene donor (3.2.1 Br). As stated earlier, a major condition for high

conductivity is the stacking characteristics of the donor and acceptor molecules. Steric effects play an important role in determining the stacking characteristics of charge-transfer complexes (see Chapter one). The structure of the dipyrromethene donor molecule is shown below (Figure: 3.2.15)⁴⁶⁻⁴⁸.

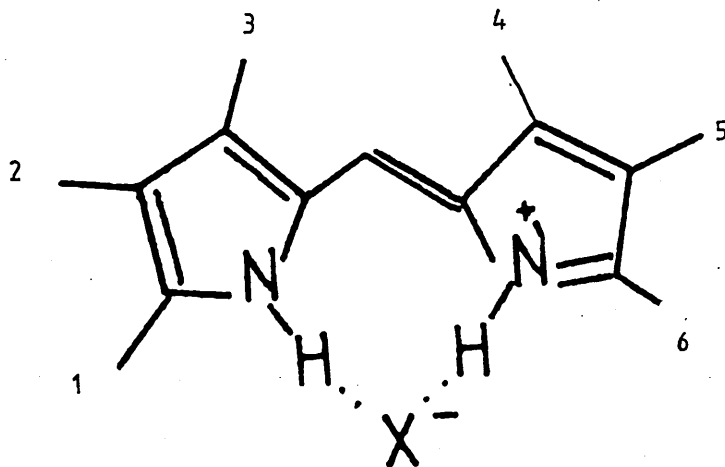


Figure: 3.2.15 The structure of the dipyrromethene donor molecule

The importance of the area around the anion for the formation of the charge-transfer complex was indicated by the failure of the hydroiodide dipyrromethenes to form complexes with TCNQ.

All the insulating complexes have methyl groups at both positions (1) and (6), which may prevent the complexes having favourable stacking properties.

The dipyrromethenes are essentially planar, but the steric crowding due to the additional methyl groups may produce a twisting about the central carbon-carbon bond to relieve this steric hindrance. This results in the dipyrromethene not being planar. The additional methyl groups may hinder the close intercolumnar contacts between the conjugated parts of the donor and acceptor systems and this may favour the formation of mixed stacks. However, the semiconducting pentamethyl TCNQ complex has no methyl group at position (6) which may facilitate favourable stacking within the crystals.

Similar steric effects, where the size of side groups affect the stacking characteristics, can be seen in the TCNQ complexes of TTF, tetramethyl-TTF and tetraethyl-TTF. Both the TTF and tetramethyl TTF-TCNQ complexes have segregated structures,⁵⁴⁻⁵⁶ but the tetraethyl-TTF has a less conductive mixed stack structure⁵⁷.

The degree of charge transfer of the pentamethyl dipyrromethene TCNQ complex derived from the infra-red spectrum was shown to be 0.4e on the TCNQ's. This satisfies the criteria established by Torrance^{58,59}, that a major condition for high conductivity is partial charge transfer.

The mean ionic charge in the hexamethyl dipyrromethene (3.2.2 Br) TCNQ complex was also shown to be 0.4e. This partial charge transfer may be offset by the structural characteristics which make the complex insulating.

3.3 Experimental

3.3.1 General Information

For the general experimental information (see appendix 1).

3.3.2 Experimental Methods

3-Methylpentan-2,4-dione (3.2.5)

The methylated acetylacetone (3.2.5) was prepared from pentan-2,4-dione (88.87g; 0.89 moles) and iodomethane (127g; 0.904 moles) using the method described by Johnson et al³⁴.
73g; 72%

I.R. (KBr): 3000; 2930; 1720; 840:

¹H NMR(CDCl₃): 4.0(q,1H); 2.2(s,6H); 2.1(s,3H); 2.0(s,1H);
1.45(d,3H):

Ethyl-2-oximinoacetoacetate (3.2.6)

The oxime (3.2.6) was prepared from ethyl acetoacetate (73ml; 0.58 moles) and sodium nitrite (45g; 0.65 moles) using the method described by Touster³⁵.

45g; 49%:

I.R.(KBr): 3300, 3000; ;2960; 1700; 1610; 970:

¹H NMR(CCl₄): 4.9(q,2H); 2.9(s,3H); 1.9(t,3H):

Methyl-2-oximinoacetoacetate (3.3.1)

The oxime (3.3.1) was prepared from methyl acetoacetate (66ml; 0.5 moles) and sodium nitrite (45g; 0.65 moles) using from the method described by Touster³⁵.

38g; 52%:

I.R. (KBr): 3300; 3010; 2980; 1700; 1620; 960:

¹H NMR (CCl₄): 10.3(s,1H); 4.1(s,3H); 2.9(s,3H):

2-Ethoxycarbonyl-3,4,5-trimethyl pyrrole (3.2.7)

The pyrrole ester (3.2.7) was prepared from ethyl 2-oximinoacetoacetate (3.2.6) (9.47g; 0.06 moles) and 3-methylpentan-2,4,-dione (3.2.5) (5.7g; 0.05 moles) using the method described by Kleinspehn³⁶.

7.9g; 87%; mp:115-117°C

I.R.(KBr): 3300; 2980; 2900; 1710; 1640; 1490:

¹H NMR (CCl₄): 9.1(s,1H); 4.5(q,2H); 2.5(s,6H); 2.1(s,3H); 1.8(t,3H).

2-Methoxycarbonyl-3,4,5-trimethyl pyrrole (3.2.10)

The pyrrole ester (3.2.10) was prepared from methyl 2-oximinoacetoacetate (3.3.1) (8.35g; 0.05 moles) and 3-methylpentan-2,4-dione (3.2.5) (5.3g; 0.046 moles) using the method described by Kleinspehn³⁶.

7.3g; 87%; mp:121-123°C

I.R.(KBr): 3200; 2990; 2910; 1700; 1650; 1480:

¹H NMR (CCl₄): 8.5(s,1H); 3.5(s,3H); 2.2(s,3H); 2.1(s,3H); 1.9(s,3H):

3,4,5,3'4',5'-Hexamethyl-dipyrrylmethene hydrobromide (3.2.2 Br)²⁹

To a hot solution of 90% formic acid (5ml) and concentrated hydrobromic acid (4ml) was added either 2-ethoxycarbonyl-3,4,5-trimethyl pyrrole (3.2.7) (3.62g; 0.02 moles) or 2-methoxycarbonyl-3,4,5-trimethyl pyrrole (3.2.10) (3.34g; 0.02 moles). The reaction mixture was heated. After three hours, the reaction vessel was cooled in ice. The dark red solid was filtered and washed with water, methanol and diethylether. The solid was recrystallised from a chloroform/petrol mixture.

1.45g; 25%: mp:291-293°C (lit mp:294-295°C)²⁹

I.R.(KBr): 3160; 3060; 1600; 1510; 1230:

¹H NMR (CDCl₃): 3.0(s,6H); 2.5(s,6H); 2.25(s,6H); 1.25(s,1H):

Microanalysis: Found C, 58.19%; H, 6.90%; N, 9.09%:

C₁₅H₂₁N₂Br requires C, 58.26%; H,6.84%; N,9.06%:

3,4,5,3',4',5'-Hexamethyl-dipyrrylmethene hydrochloride (3.2.2 Cl)²⁹

The dipyrrylmethene (3.2.2 Cl) was prepared from concentrated hydrochloric acid (2.3ml) using the method described for the dipyrrylmethene (3.2.2 Br)

1.58g; 30%:

I.R. (KBr): 3150; 3030; 1620; 1500; 1250:

¹H NMR (CDCl₃): 3.0(s,6H); 2.6(s,6H); 2.35(s,6H); 1.25(s,1H):

Microanalysis: Found C, 66.97%; H, 8.07%; N, 10.14%:

C₁₅H₂₁N₂Cl requires C, 68.04%; H, 7.99%; N, 10.58%:

3,4,5,3',4',5'-Hexamethyl-dipyrrylmethene hydroiodide (3.2.2I)²⁹

The dipyrrylmethene (3.2.2I) was prepared from concentrated hydroiodic acid (5.6ml) using the method described for the dipyrrylmethene (3.2.2 Br)

1.78g; 25%:

I.R.(KBr): 3300; 3100; 3000; 1630; 1510; 1230:

¹H NMR(CDCl₃): 2.9(s,6H); 2.6(s,6H); 2.3(s,6H); 1.2(s,1H):

Microanalysis: Found C, 49.67%; H,5.88%; N,7.72%:

C₁₅H₂₁N₂I requires C, 50.57%; H,5.94%; N,7.86%:

(3,4,5,3',4',5'-Hexamethyl-dipyrrylmethene hydrobromide)₂ TCNQ

(3.3.2)

To a cold solution of TCNQ (0.066g; 0.3.2 mmoles) in acetonitrile (150ml) was added a solution of the dipyrromethene (3.2.2 Br) (0.1g; 0.32 mmoles) in chloroform (25ml). The resulting solution was left to stand overnight. Dark brown elongated crystals were recovered from solution and washed with toluene and diethyl ether.

0.12g; 22%

I.R.(KBr): 3180; 3080; 2220; 1620; 1520; 1270:

Microanalysis: Found C, 61.12%; H,5.65%; N,13.51%:

C₄₂H₄₆N₈Br₂ requires C,61.32%; H,5.64%; N,13.62%:

UV/Visible Spectrum	Wavelength (nm)	Absorbance
---------------------	-----------------	------------

	470	2.91
--	-----	------

	393	2.35
--	-----	------

(3,4,5,3',4',5'-Hexamethyl dipyrromethene hydrochloride)₂ TCNQ

(3.3.3)

The TCNQ complex was prepared from the dipyrromethene (3.2.2 Br) (0.1g; 0.37 mmoles) and TCNQ (0.078g; 0.37 mmoles) from the method described for the charge transfer complex (3.3.2).

0.09g; 35%:

I.R.(KBr): 3160; 3060; 2210; 1630; 1540; 1440; 1280:

Microanalysis: Found C, 68.70%; H,6.25%; N,15.26%:

C₄₂H₄₆N₈Cl₂ requires: C,68.75%; H,6.32%; N,15.27%:

UV/Visible Spectrum	Wavelength (nm)	Absorbance
---------------------	-----------------	------------

	478	2.97
--	-----	------

	393	2.40
--	-----	------

Attempted preparation of:

(3,4,5,3',4',5'-Hexamethyl dipyrromethene hydroiodide)₂ TCNQ

(3.3.4)

To a cold solution of TCNQ (0.057g; 0.28 mmoles) in acetonitrile (150ml) was added a solution of the dipyrromethene (3.2.2 I) (0.1g; 0.28 mmoles) in chloroform (25ml). The resulting solution was allowed to stand for 72 hours. The reaction mixture was concentrated and a solid was filtered with suction and washed with toluene.

The product was identical with (3.2.2.I)

2,3,4-Trimethyl pyrrole (3.2.9)⁴²

To a solution of sodium hydroxide (22g; 0.55 moles) in water (50ml) was added the pyrrole ester (3.2.7)(10g; 0.06 moles) in ethanol (50 ml). The reaction mixture was heated under reflux for three hours and the ethanol then distilled off. The residue was allowed to cool to room temperature and carefully acidified with acetic acid.

The mixture was steam distilled and the distillate was collected over sodium hydrogen carbonate. The distillate was extracted with ether (2 x 100ml). The ether extracts were combined, dried (MgSO₄) and the ether removed under reduced pressure. The desired pyrrole (3.2.9) was obtained as an oil.

2.8g; 43%

I.R.(KBr): 3250; 3190; 2960; 2900; 1640:

¹H NMR(CDCl₃): 6.4(s,1H); 5.7(s,1H); 2.1(s,6H); 2.0(s,3H):

5-Formyl-2,3,4-trimethyl pyrrole (3.2.10)⁴³

To a solution of trimethylpyrrole (3.2.9) (5g; 0.05 moles) and N,N'-dimethylformamide (4.5g; 0.06 moles) in petroleum ether (100ml) at 0°C was added a few drops of ether and phosphorous oxychloride (8.0g; 0.052 moles) over 20 minutes. Stirring was continued for a further 15 minutes. The precipitated salt was then isolated and added to a 20% sodium hydroxide solution (160 ml), followed by the addition of chloroform (50ml) with stirring. After 30 minutes the organic layer was isolated and dried (potassium carbonate). The chloroform was removed in vacuo to yield the aldehyde.

4.3g; 62%; mp: 143-145°C (lit mp:146-147°C)⁴³

I.R.(KBr): 3300; 3200; 3010; 2950; 2890; 1710; 1640:

¹H NMR (CDCl₃): 8.8(s,1H); 2.20(s,6H); 1.9(s,3H):

3,5-Diethoxycarbonyl-2,4-dimethyl pyrrole (3.3.5)

The pyrrole diester was prepared from ethyl acetoacetate (279g; 2.15 moles), sodium nitrite (73g; 1.05 moles) and zinc granules (140.5g; 2.14 moles) using the method described by Fischer⁴⁵.

153g; 71%; mp: 133-134°C (lit mp:136-137°C)⁴⁵

I.R.(KBr): 3190; 2980; 2890; 1710; 1630; 1490:

¹H NMR (CCL₄): 4.2(m,4H); 2.5(s,6H); 2.0(s,3H); 1.9(s,3H):

2,4-Dimethyl pyrrole (3.2.13)

The dimethyl pyrrole (3.2.13) was prepared from the pyrrole diester (3.3.5) (71.62g; 0.3 moles) and potassium hydroxide (151.5g; 2.7 moles) using the method described by Fischer⁶⁰.

10.88g; 38%

I.R.(KBr): 3300, 3200; 2950; 2900; 1640:

¹H NMR (CDCl₃): 6.2(s,1H); 5.6(s,1H); 2.1(s,3H); 2.0 (s,3H):

5-Formyl-2,4-dimethyl pyrrole (3.2.11)

The pyrrole-5-carboxaldehyde (3.2.11) was prepared from the dimethyl pyrrole (3.2.13) (10g; 0.11 moles) and phosphorous oxychloride (18g; 0.12 moles) using the method described by De Groot et al⁴³

7.5g; 55%; mp:131-133°C

I.R.(KBr): 3350; 3190; 2950; 2890; 1700; 1640:

¹H NMR (CDCl₃): 9.00(s,1H); 5.4(s,1H); 2.3(s,3H); 2.2(s,3H):

1-Methoxycarbonyl pyrrole (3.3.6)

The 1-methoxycarbonyl pyrrole (3.3.6) was prepared from pyrrole (5g; 0.075 moles), potassium (2.9g; 0.076 moles) and methyl chloroformate (7.5g; 0.08 moles) using the method described by Gabel⁶¹.

5.6g; 60%

I.R. (KBr): 2990; 2890; 1730; 1640; 1310:

¹H NMR (CCl₄): 6.1(s,2H); 5.6(s,1H); 5.5(s,1H); 3.3(s,3H):

1,3,4-trimethoxycarbonyl Pyrrole (3.3.7)

The trimethoxycarbonyl pyrrole (3.3.7) was prepared from 1-methoxycarbonyl pyrrole (3.3.6) (4g; 0.032 moles) and dimethyl acetylene dicarboxylate (4.7g; 0.032 moles) using the method described by Gabel⁶¹.

2.9g; 38%; mp:66-68°C (lit mp:69°C)⁶¹

I.R.(KBr): 2980, 2880; 1720; 1620; 1340; 1275:

¹H NMR (CCl₄): 6.1(s,2H); 3.5(s,6H); 3.2(s,3H):

3,4-Dimethyl pyrrole (3.2.12)

The dimethyl pyrrole (3.2.12) was prepared from

1,3,4-trimethoxycarbonyl pyrrole (3.3.7) (5g; 0.021 moles) and LiAlH_4 (90 mls; 0.09 moles) using the method described by Hinman and Theodoropulos⁴⁴.

1.2gs; 60%

I.R.(KBr): 3310; 3220; 2990; 2820; 1620:

^1H NMR(CDCl_3): 6.1(s,2H); 2.0(s,6H):

3,5,3',5'-Tetramethyl dipyrromethene hydrobromide (3.2.3 Br)²⁸

To a solution of the pyrrole-2-aldehyde (3.2.11) (0.2095g; 1.7×10^{-3} moles) and dimethyl pyrrole (3.2.13) (0.209g; 2.2×10^{-3} moles) in methanol (10ml) and water (5ml) was added concentrated hydrobromic acid (0.2ml). The solution was kept at 0°C for two hours. After that time the dipyrromethene (3.2.3 Br) was isolated and washed with water, dried in vacuo and recrystallised from chloroform and petroleum spirit 40-60°. 0.275g; 57%:

I.R.(KBr): 3540; 3220; 3060; 2020; 2980; 2940; 1670; 1640; 1590; 1310:

^1H NMR (CDCl_3): 5.9(s,2H); 2.1(s,6H); 2.0(s,6H):

Microanalysis Found: C,55.60%; H,6.18%; N,9.70%:

$\text{C}_{13}\text{H}_{17}\text{N}_2\text{Br}$ requires: C,55.52%; H,6.09%; N,9.96%:

3,5,3',5'-Tetramethyl dipyrromethene hydrochloride (3.2.3 Cl)²⁸

The dipyrromethene (3.2.3 Cl) was prepared from the pyrrole-2-aldehyde (3.2.11) (0.2128g; 1.73×10^{-3} moles) and dimethyl pyrrole (3.2.13) (0.3608g; 3.8×10^{-3} moles) and concentrated hydrochloric acid (0.3ml) using the method described for the dipyrromethene (3.2.3 Br)

0.253g; 62%:

I.R. (KBr): 3450; 3190; 3080; 3010; 2980; 2900; 1620; 1590;
1550; 1290:

^1H NMR (CDCl_3): 6.1(s,2H); 2.3(s,6H); 2.2(s,6H):

Microanalysis: Found: C,66.02%; H,7.23%; N,11.90%:

$\text{C}_{13}\text{H}_{17}\text{N}_2\text{Cl}$ requires C,65.96%; H,7.19%; N,11.84%:

3,5,3',5'-Tetramethyl dipyrromethene hydroiodide (3.2.3I)²⁸

The dipyrromethene (3.2.3I) was prepared from the pyrrole-2-aldehyde (3.2.11) (0.2045g ; 1.66×10^{-3} moles) and dimethyl pyrrole (3.2.13) (0.2085g ; 2.19×10^{-3} moles) and concentrated hydroiodic acid (0.5ml) using the method described for the dipyrromethene (3.2.3 Br).

0.203g; 37%:

I.R.(KBr): 3400; 3180; 3050; 3000; 2990; 2900; 1650; 1580;
1550; 1280:

^1H NMR(CDCl_3): 6.0(s,2H); 2.1(s,6H); 2.0(s,6H):

Microanalysis Found: C,47.65%; H,5.23%; N,8.58%

$\text{C}_{13}\text{H}_{17}\text{N}_2\text{I}$ requires: C,47.58%; H,5.22%; N,8.54%:

3,4,5,3',5'-Pentamethyl dipyrromethene hydrobromide
(3.2.4 Br)²⁸

The dipyrromethene (3.2.4 Br) was prepared from the pyrrole-5-carbaldehyde (3.2.11) (0.1830g ; 1.3×10^{-3} moles), dimethyl pyrrole (3.2.13) (0.2341g ; 2.5×10^{-3} moles) and concentrated hydrobromic acid (0.2ml) using the method described for the dipyrromethene (3.2.3 Br).

0.21g; 53%:

I.R.(KBr): 3450; 3190; 3080; 3010; 2890; 1620; 1580; 1540;
1270:

^1H NMR (CDCl_3): 7.0(s,1H); 6.0(s,1H); 2.6(s,6H); 2.3(s,3H);

2.2(s,3H); 2.1(s,6H); 2.0(s,3H):

Microanalysis Found: C,56.87%; H,6.52%; N,9.32%:

$\text{C}_{14}\text{H}_{19}\text{N}_2\text{Br}$ requires: C,56.95%; H,6.48%; N,9.48%:

3,4,5,3',5'-Pentamethyl dipyrromethene hydrochloride

(3.2.4Cl)²⁸

The dipyrromethene (3.2.4Cl) was prepared from the pyrrole-5-carbaldehyde (3.2.11) (0.1945g ; 1.42×10^{-3} moles), dimethyl pyrrole (3.2.13) (0.2477g ; 2.6×10^{-3} moles) and concentrated hydrochloric acid (0.3ml) using the method described for the dipyrromethene (3.2.3 Br)

0.16g ; 45%

I.R.(KBr): 3420; 3170; 3010; 2900; 1610; 1550; 1530; 1260:

^1H NMR(CDCl_3): 6.9(s,1H); 6.0(s,1H); 2.8(s,6H); 2.4(s,3H);

2.3(s,3H); 2.2(s,6H); 2.0(s,3H):

Microanalysis Found: C,67.53%; H,7.61%; N,11.23%:

$\text{C}_{14}\text{H}_{19}\text{N}_2\text{Cl}$ requires: C,67.07%; H,7.58%; N,11.18%:

3,4,5,3',4'-Pentamethyl dipyrromethene hydrobromide (3.2.1

Br)²⁸

The dipyrromethene (3.2.1 Br) was prepared from the pyrrole-5-carbaldehyde (3.2.10) (0.2095g ; 1.5×10^{-3} moles), dimethyl pyrrole (3.2.12) (0.1652g ; 1.7×10^{-3} moles) and concentrated hydrobromic acid (0.2ml) using the method described for the dipyrromethene (3.2.3 Br).

0.18g ; 40%:

I.R.(KBr): 3460; 3180; 3010; 2910; 1620; 1560; 1530; 1260:

^1H NMR(CDCl_3): 7.0(s,1H); 6.5(s,1H); 2.6(s,6H); 2.2(s,6H);

2.1(s,6H); 1.9(s,3H); 1.8(s,3H):

Microanalysis Found: C,56.80%; H,6.51%; N,9.42%:

$C_{44}H_{19}N_2Br$ requires: C,56.95%; H,6.48%; N,9.48%:

(3,5,3',5'-Tetramethyl dipyrromethene hydrobromide)₂ TCNQ

(3.3.8)

The TCNQ complex (3.3.8) was prepared from the dipyrromethene (3.23 Br) (0.1g; 3.6×10^{-4} moles) and TCNQ (0.0816g; 4×10^{-4} moles) by the method described for the complex (3.3.2).

0.13g; 48%

I.R.(KBr): 3520; 3240; 3110; 2990; 2320; 1665; 1620; 1590; 1320:

Microanalysis Found: C,59.42%; H,4.93%; N,14.61%:

$C_{38}H_{38}N_8Br_2$ requires: C,59.53%; H,4.99%; N,14.61%:

UV/Visible Spectrum	Wavelength(nm)	Absorbance
	462	2.39
	393	1.86

(3,5,3',5'-Tetramethyl dipyrromethene hydrochloride)₂ TCNQ

(3.3.9)

The TCNQ complex (3.3.9) was prepared from the dipyrromethene (3.2.3 Cl) (0.1053g; 4.4×10^{-4} moles) and TCNQ (0.0917g; 4.5×10^{-3} moles) by the method described for the complex (3.3.2).

0.11g; 37%

I.R.(KBr): 3450; 3290; 3010; 2990; 2880; 2210; 1620; 1585; 1545; 1270:

Microanalysis Found: C,67.25%; H,5.59%; N,16.45%:

$C_{38}H_{38}N_8Cl_2$ requires: C,67.35%; H, 5.65%; N,16.53%:

UV/Visible Spectrum	Wavelength(nm)	Absorbance
	461	1.43
	392	0.89

(3,5,3',5'-Tetramethyl dipyrrylmethene hydroiodide)₂

TCNQ (3.3.10)

The TCNQ complex (3.3.10) was prepared from the dipyrrylmethene (3.2.3I) (0.1004g; 3.1×10^{-4} moles) and TCNQ (0.0673g; 3.3×10^{-4} moles) by the method described for the complex (3.3.2).

I.R. (KBr): 3400, 3190; 3050; 3010; 2990; 2980; 1650; 1550;

1280:

Microanalysis Found: C,47.70%; H,5.25%; N,8.62%:

$C_{38}H_{38}N_8I_2$ requires: C,53.02%; H,4.42%; N,13.02%:

(3,4,5,3',5'-Pentamethyl dipyrrylmethene hydrobromide)₂ TCNQ

(3.3.11)

The TCNQ complex (3.3.11) was prepared from the dipyrrylmethene (3.2.4 Br) (0.1010g; 3.4×10^{-4} moles) and TCNQ (0.0666g; 3.3×10^{-4} moles) by the method described for the complex (3.3.2).

0.09g; 33%:

I.R. (KBr): 3420; 3180; 3080; 3010; 2890; 2225; 1625; 1575;

1540; 1270:

Microanalysis Found: C,60.28%; H,5.31%; N,14.07%:

$C_{40}H_{42}N_8Br_2$ requires: C,60.46%; H,5.32%; N,14.10%:

UV/Visible Spectrum	Wavelength(nm)	Absorbance
	470	2.90
	389	2.89

(3,4,5,3',5'-Pentamethyl dipyrrylmethene hydrochloride)₂ TCNQ

(3.2.12)

The TCNQ complex (3.3.12) was prepared from the dipyrrylmethene (3.2.4Cl) (0.1051g; 4.2×10^{-4} moles) and TCNQ (0.0885g; 4.3×10^{-4} moles) by the method described for the complex (3.3.2).

0.10g; 33%

I.R. (KBr): 3420; 3170; 3020; 2890; 2230; 1610; 1550; 1520;
1240:

Microanalysis Found: C,67.93%; H,5.91%; N,15.83%:

$C_{40}H_{42}N_8Cl_2$ requires: C,68.18%; H,5.97%; N,15.91%:

UV/Visible Spectrum	Wavelength(nm)	Absorbance
	468	2.11
	390	2.08

(3,4,5,3'4'-Pentamethyl dipyrrylmethene hydrobromide)₂ TCNQ

(3.3.13)

The TCNQ complex (3.3.13) was prepared from the dipyrrylmethene (3.2.1 Br) (0.103g; 3.5×10^{-4} moles) and TCNQ (0.0755g; 3.7×10^{-4} moles) by the method described for the complex (3.3.2).

0.12g; 43%:

I.R. (KBr): 3460; 3180; 3020; 2900; 2200; 2185; 1630; 1550;
1520; 1250:

Microanalysis Found: C,60.98%; H,5.51%; N,13.98%:

$C_{40}H_{42}N_8Br_2$ requires: C,60.46%; H,5.32%; N,14.10%:

UV/Visible Spectrum	Wavelength(nm)	Absorbance
	476	1.97
	390	1.97

3.4 References

1. A. Cougrand, S. Flandrois, P. Delhaes, P. Dupuis, D. Chasseau, J. Gaultier and J. L. Miane, Mol Cryst. Liq. Cryst., 32,165 (1976).
2. M.A. Abkowitz, J.W. Brill, P.M. Chaikin, A.J. Epstein, M.F. Froix, C.H. Griffiths, W. Gunning, A.J. Heeger, W.A. Little, J.S. Miller, M. Novastry, D.B. Tanner and H.L. Slade, Anals. N.Y. Acad. of Sci. 313,459(1978)
3. M.A. Abkowitz, A.J. Epstein, C.H. Griffiths, J.S. Miller and H.L. Slade, J. Am. Chem. Soc., 99, 5304 (1977).
4. P. Delhaes, A. Cougrand, S. Flandrois, D. Chasseau, J. Gaultier, C. Hauw and P. Dupuis, Proceedings of Conference on organic conductors and semiconductors, Siofok, Hungary, 493 (1976).
5. P. Coppers, P. Leung, K.E. Murphy, R.V. Tilborg, A.J. Epstein and J.S. Miller, Mol. Cryst. Liq. Cryst. 61,1(1980).
6. M.A. Abkowitz, A.J. Epstein, C.H. Griffiths, J.S. Miller and H.L. Slade, J.Am.Chem.Soc., 99,355 (1977).
7. C. Coulon, S. Flandrois, P. Delhaes, C.Hauw and P. Dupuis; Phys.Rev.B, 23,2850(1981).
8. A. Filhol, B. Gallois, J. Laugier, P. Dupuis, C. Coulon; Mol. Cryst. Liq. Cryst, 84,17(1982).
9. C. Coulon, P. Delhaes, S. Flandrois, J. Amiell, E. Bonjour, and P. Dupuis; J.Physique, 46,783 (1985).
10. J.W. Brill, A.J. Epstein, J.S. Miller; Phys. Rev. B, 20,681(1979).
11. G.J. Ashwell, I.M. Sandy, A. Chyla and G.H. Cross; Synthetic Metals, 19,463(1987).

12. M. Lequan, R.M. Lequan and J. Padiou; Synthetic Metals, 9,489(1984).
13. M. Lequan; R.M. Lequan, G. Maceno, J. Amiell, P. Delhaes and C. Hauw; Nouveau J. De Chimie, 9,359(1985).
14. M. Lequan, R.M. Lequan, P. Delhaes and C. Hauw; Mol. Cryst. Liq. Cryst., 120,353(1985).
15. A. Barraud, M. Lequan, R.M. Lequan, P. Lesieur, J. Richard, A. Rudubel-Teixier and M. Vandevyuer; J.C.S. Chem. Comm., 797, (1987).
16. I.V. Melikhov, M.A. Prokofiev, Yu.N.Sychev and V.N. Sidorov; J. Cryst. Growth, 51,292(1981).
17. S. Flandrois, P. Libert and P. Dupuis, Prace Naukowe, Instytutu Chemii Organiznej Fizycznej Politechniki Wroclawskiej; 7,269(1974).
18. A. Lindegard-Andersen, M. Almeida, L. Alcacer and K. Mortensen; J.Phys, 44,C3-1325(1983).
19. H. Michel and E. Lippert; Organic Liquids; Structure, Dynamics and Chemical Properties, Wiley-Interscience(1978).
20. R.J. Jacobsen and Y. Mikawa; Applied Optics, 9,17(1970).
21. A.J. Epstein, S. Etemad, A.F. Garito and A.J. Heeger; Phys. Rev. B. 5,952(1972).
22. V. Walatka and J.H. Perlstein; Mol.Cryst.Liq.Cryst. 15,269,(1971).
23. R.C. Wheland and J.L. Gillson, J.Amer.Chem.Soc., 98,3916,(1976).
24. G.J. Ashwell, 'Private Communication'.
25. H. Fischer and H.Orth; Die Chemie des Pyrrols, Akad Verlag, Leipzig, II, 160, (1937).

26. H. Fischer, H. Friedrich, W. Lamatsch and K. Morgenroth;
Annchemie, 466, 147(1928).
27. H. Fischer and G. Stangler; Annalen, 459,53,(1927).
28. H. Fischer and A. Kirstahler; Annalen, 466,178(1928).
29. H. Fischer; Ann Chemie; 452, 268(1927).
30. H. Fischer and H.Orth; Die Chemie des Pyrrols, Akad Verlag
Leipzig II, 73, (1937).
31. H. Fischer and H.Orth; Die Chemie des Pyrrols, Akad Verlag,
Leipzig II, 1, (1937).
32. K.J. Brunings and A.H. Corwin; J.Am. Chem.Soc., 66,
337,(1944).
33. J.Chem.Soc.A, 3,440(1971)
34. A.W. Johnson; E. Markham and R. Price; Organic Syn.,
42,75,(1962).
35. O. Touster; Organic Reactions, 7,327(1953).
36. G.C. Kleinspehn; J.Am.Chem.Soc., 77,1546(1955)
37. P.G. Gassman and W.N. Schenk; J. Org.Chem; 42,918(1977).
38. J.Org.Chem. 41,586(1976).
39. T. Morita; Y. Okamoto and H. Sakurai; J.C.S. Chem.Comm.,874
(1978).
40. P.D.G. Dean; J.C.S., 6655,(1965).
41. H. Fischer and Walach; Ber, 58,2818(1925)
42. R.L.N. Harris, A.W. Johnson, I.T. Kay; J.Chem.Soc.(C)
22,(1966)
43. J.A. de Groot, G.M. Gorter-La Roy, J.A. Van Koveringe and
J. Lugtenburg; Organic Preparations and Procedures Int., 13,
97(1981).
44. R.L. Hinman and S. Theodoropulos; J.Org.Chem, 28, 3052(1963)

45. H. Fischer "Organic Synthesis" Coll Vol II, John Wiley & Sons Inc. New York N.Y. 202 (1943)
46. W. Becker and W.S. Sheldrick; Acta Cryst. (B), B34, 1021 (1978)
47. G. Struckmeier, J. Engel, U. Thewalt; Z. Naturforsch. B. Anorg Chem. Org. Chem., 33B, 753 (1978)
48. W.S. Sheldrick, A. Borkenstein, G. Struckmeier and J. Engel; Acta. Cryst. (B), B34, 329(1978)
49. M.J. Buerger; Crystal-Structure Analysis, Wiley, New York, 53(1960)
50. J.D. Dunitz; Acta. Cryst., 17,1299(1964)
51. F.H. Herbstein; Acta Cryst, 17,1094 (1964)
52. R.W. Tsien, C.M. Huggins and O.H. Leblanc; J.Chem.Phys., 45, 4370(1966)
53. J.S. Chappell, A.N. Bloch, W.A. Bryden, M. Maxfield, T.O. Poehler and D.O. Cowan, J.Am.Chem.Soc., 103, 2442(1981)
54. T.J. Kistenmacher, T.E. Philips and D.O. Cowan; Acta. Cryst., B30, 763(1974)
55. A.J. Schultz, G.D. Stuky, R.H. Blessing and P. Coppens, J.Amer.Chem. Soc. 98,3194(1976)
56. T.E. Philips, T.J. Kistenmacher, A.N. Bloch, J.P. Ferraris and D.O. Cowan; Acta. Cryst. B33,422(1977)
57. J.L. Galigne, J.M. Fabre and L. Giral Acta. Cryst, B33, 3827(1977)
58. J.B. Torrance; Acc. Chem. Res. 12,79(1979)
59. J.B. Torrance and B.D. Silverman; Phys. Rev., B15, 788 (1977)
60. H. Fischer; Organic Synthesis "Coll Vol II John Wiley & Sons, New York, N.Y. 217(1943).
61. N.W. Cabel; J.Org.Chem, 27, 301,(1962).

4.0 INTRODUCTION

The Langmuir-Blodgett(L-B) technique enables uniform ultra-thin organic films to be produced. These layers could find wide applications in electronic devices.

4.0.1 Historical Review

Scientific interest in monolayers spread on the surface of a liquid can be found in the writings of Benjamin Franklin¹ in the eighteenth century. Although, Lord Rayleigh² was the first to propose that such films were only one molecule thick, it was Irving Langmuir, while working at G.E.C. who developed the theory and experimental concepts that led to our present understanding of the behaviour of monolayers. Later with Katherine Blodgett, he devised a new method (the Langmuir-Blodgett technique) for transferring monolayers from a water surface onto solid substrates³.

Until the outbreak of the second World War, research into the properties of the monomolecular films flourished. However, few uses were found for monolayer and multilayer structures. Consequently, activity in the area declined.

Almost fifty years after their initial report, intense interest is again being shown in the science and technology of L-B films. Some of the initial interest arose when Kuhn and co-workers⁴ in the 1960's began a series of studies that showed how one could utilize monolayers to construct precise supermolecular structures. However, the resurgence of activity

in the academic and industrial fields can be mainly attributed to intriguing possibilities of these films in the fields of electronics and microelectronics^{5,6}.

4.0.2 Molecular Assembly Technique

Materials that form monomolecular layers typically possess both water-resistant (hydrophobic) and water-attracting (hydrophilic) chemical groups. These materials are termed amphiphiles (Figure: 4.0.1)

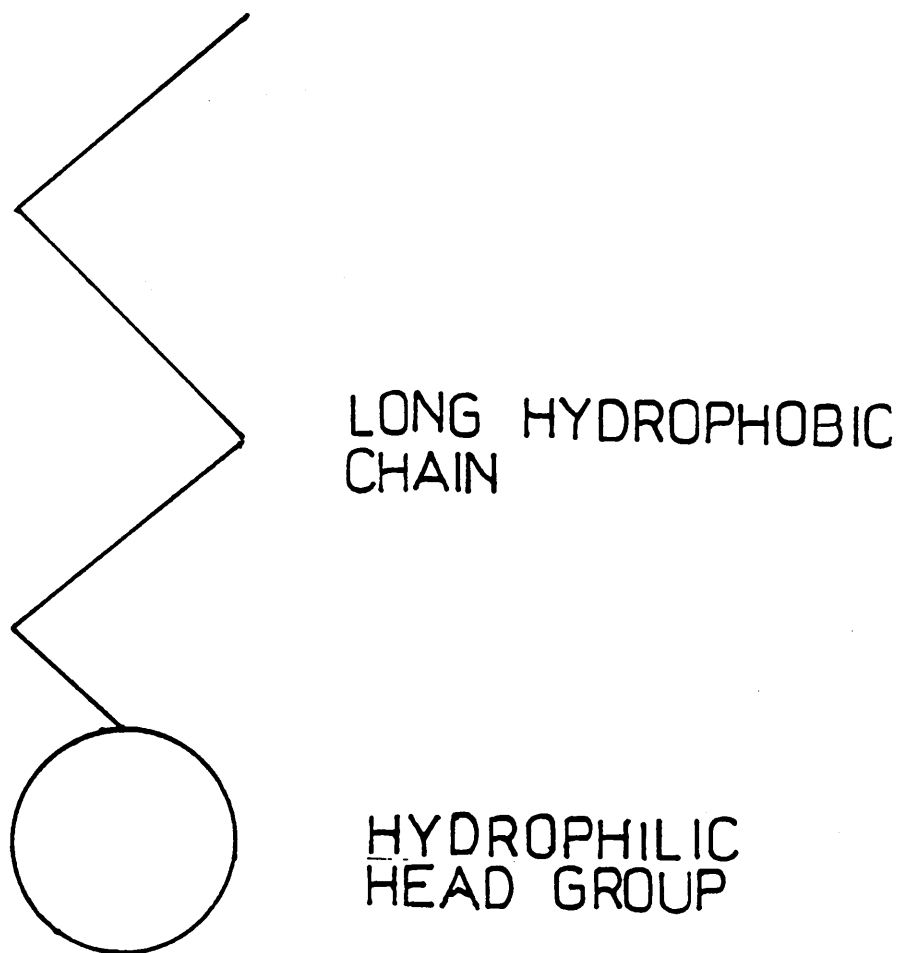


Figure: 4.0.1: An amphiphile

L-B films are prepared by first depositing a small quantity of the amphiphilic material dissolved in a volatile solvent on the water surface. When the solvent has evaporated the monolayer on the water surface is a two dimensional system (Figure: 4.0.2).

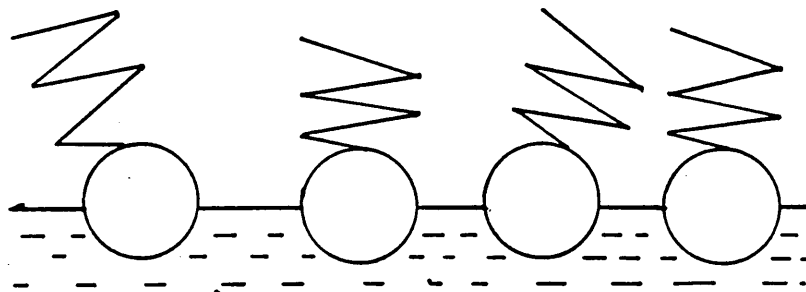


Figure: 4.0.2: Monolayer on a water surface, molecules are dispersed to form a 2-D gas.

If the surface pressure ($\bar{\pi}$) is small enough the monolayer is a two dimensional gas obeying the equation:

$$\bar{\pi}A = KT$$

Equation 4.0.1

A = the area per molecule

K = Boltzmann's Constant

T = Absolute temperature

On increasing $\bar{\pi}$, A decreases and the monolayer is transformed into the solid state (Figure: 4.0.3). The hydrophobic and hydrophilic terminations of the molecule ensure that during this process the individual molecules are all aligned in the same way.

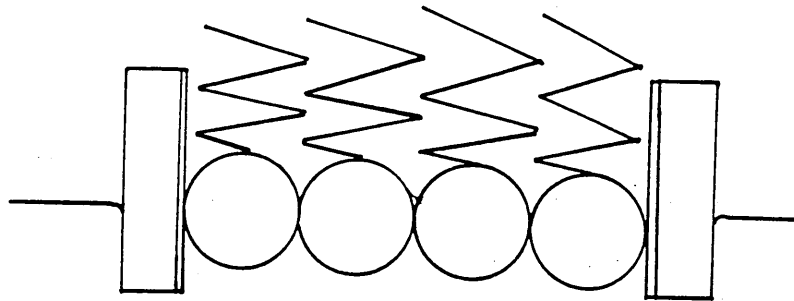


Figure: 4.0.3: Densely packed to form a two-dimensional solid

The monolayer undergoes a number of phase transformations during compression. Figure: 4.0.4 shows a typical plot of surface pressure (π) versus area occupied per molecule (\AA) for stearic acid. It should be noted that some materials do not show all these classic transitions.

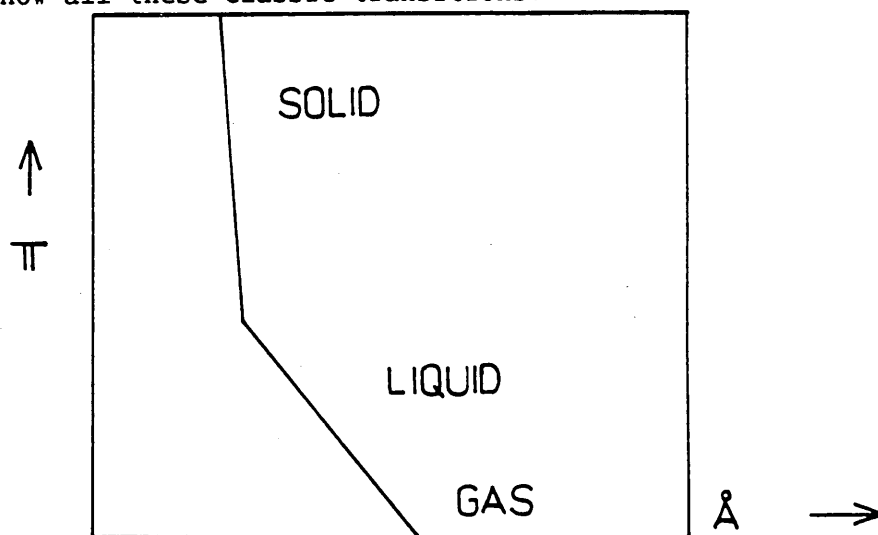


Figure: 4.0.4: Surface pressure versus area characteristic for stearic acid

When the film is in the condensed 'solid-form', the π -A plot is very steep indicating low compressibility in the monolayer. This reflects the presence of strong chain-chain interactions which hold the molecules in their closest-packed arrangement with little dependence on the surface pressure.

4.0.3 Deposition Techniques

In the 'solid' phase monolayers may be conveniently transferred from the water layer to a suitably prepared solid (substrate) by vertically dipping and raising it through the water surface. Careful control of the π of the monolayer is required during this process. Figure 4.0.5 shows a schematic diagram of one possible experimental arrangement for the deposition of L-B films.

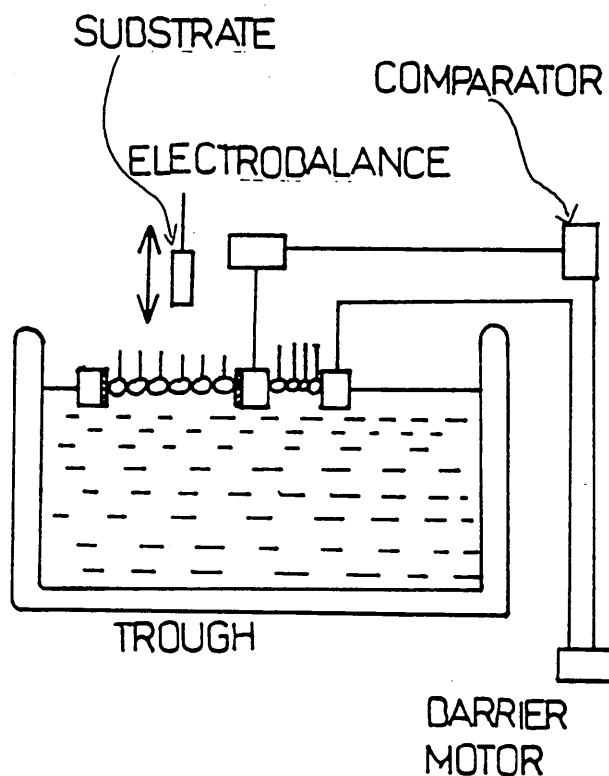


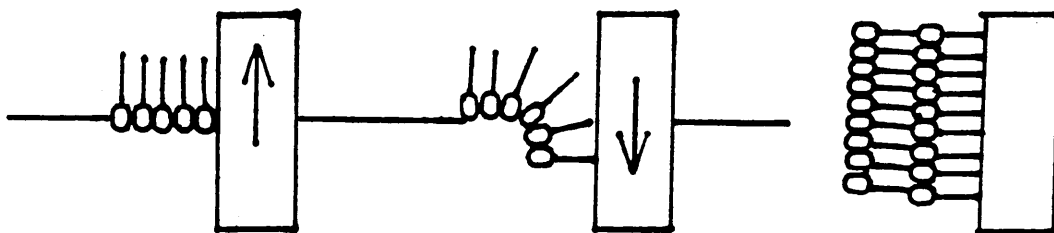
Figure: 4.0.5 A Langmuir trough

On each dipping and raising stroke the barrier is moved to the right if the monolayer is actually transferred. The decrease in the area of the water surface occupied by the monolayer divided by that of the substrate covered with the monolayer for each stroke is called the deposition ratio. The deposition ratios η for the upward (η_u) and downward (η_d) strokes respectively, should be either 0 or 1, otherwise rearrangements of molecules or incomplete pick up may occur during the transfer.

Three different types of deposition are recognised:

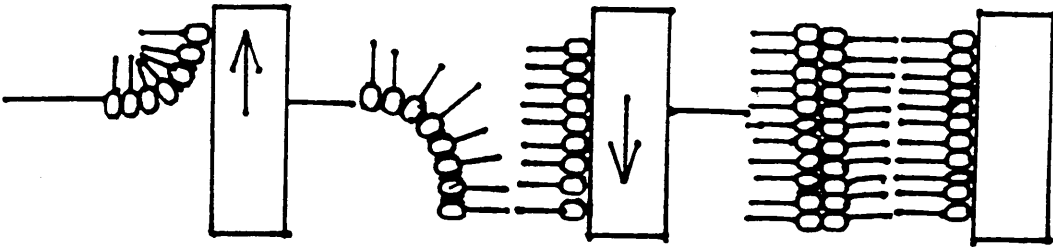
X-type

$$\eta_u = 0 \text{ and } \eta_d = 1$$



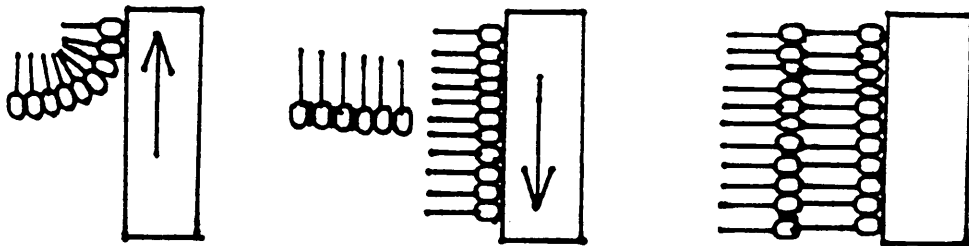
Y-type

$$\eta_u = 1 \text{ and } \eta_d = 1$$



Z-type

$$\eta_u = 1 \text{ and } \eta_d = 0$$



The X- and Z- types are associated with a single-layer unit cell along the direction normal to the film surface and the Y-type is characterised with a bilayer unit cell.

The type of deposition depends on:⁷

1. monolayer-forming materials;
2. the temperature, pH and composition of the aqueous subphase;
3. the surface pressure (π);
4. the speeds of dipping and raising;
5. the nature of the substrate surface⁸.

Recent developments in film deposition have resulted in a horizontal lifting technique as described by Nakahar and Fukuda^{9,10} who demonstrated the feasibility of obtaining X-type equivalent multilayer films even from gaseous and liquid monolayers at the air-water interface (Figure: 4.0.6).

4.0.4 Film Forming Materials

The classic L-B film forming materials are the alkanolic acids and their salts^{3,11,12} e.g. stearic acid which has sixteen CH_2 's that form a long hydrophobic chain with one end terminating in a hydrophilic carboxylic group. Unsaturated fatty acids, can also form monolayers^{13,14}, but disruption to the ordering of the chain is greatly reduced if the double bond is terminal. On exposure to suitable ultra-violet light polymerisation occurs. Diacetylenic acids have also been widely investigated¹⁵ because of their polymerizability. The polymerisation occurs within the L-B film, but results in an array of two dimensional domains whose size depends upon material purity.

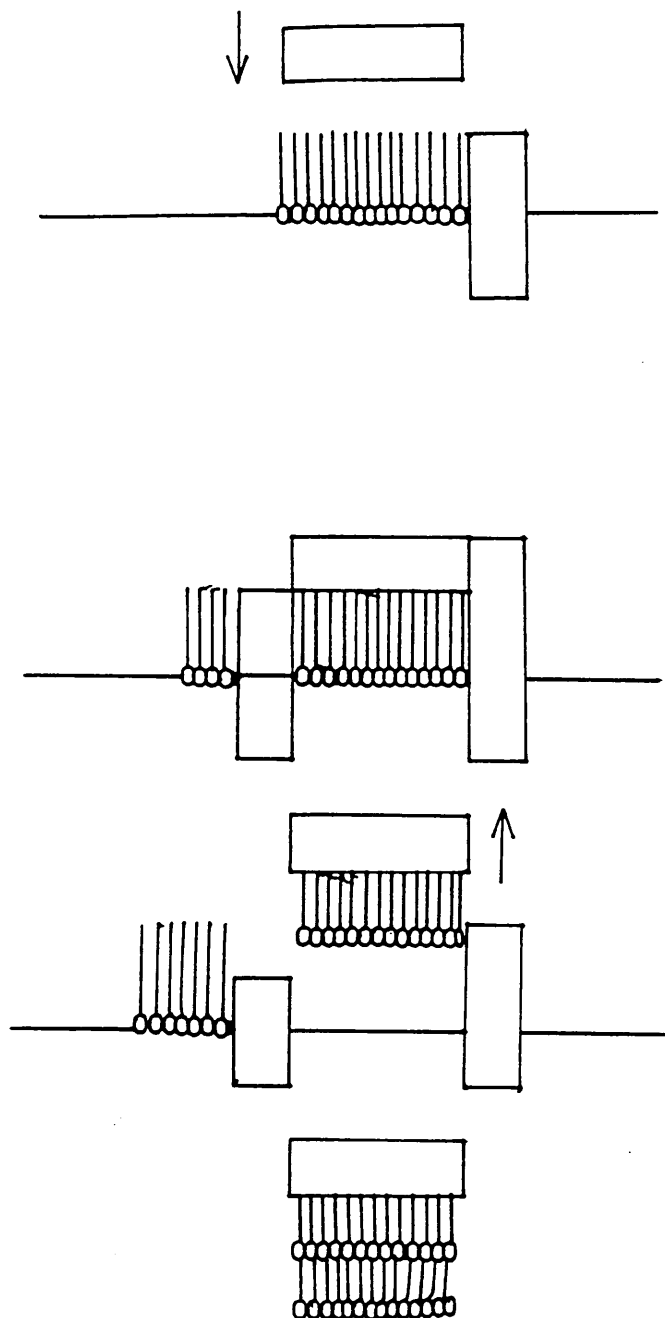


Figure: 4.0.6 Horizontal lifting technique

Recently the formation of L-B films from preformed polymers has been reported by Tredgold and his collaborators¹⁶. Good quality thin films were formed of one monolayer to 1 μ m thick which were stable at temperatures upto 300°C. A wide variety of pendant groups could be attached to produce a wide range of desired properties.

Other recent advances in L-B polymer thin films include the developments demonstrated by Japanese research groups of increasing the thermal stability of the thin films by removing the long alkyl chains at the air-water interface or after film deposition¹⁷⁻²¹.

The former possibility was demonstrated by spreading an amphiphilic Schiff base on the water containing phenylene diamine^{17,18}. The interface layer reacts with the phenylene diamine and is converted by transamination to a Schiff base polymer (Figure: 4.0.7). The polymer layer is then deposited onto a substrate via the horizontal lifting technique.

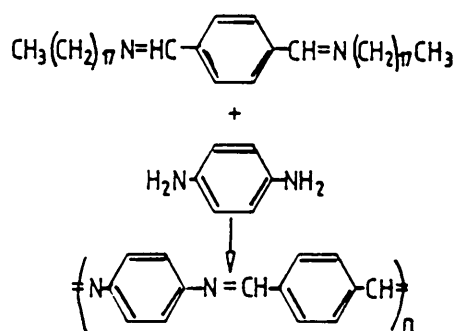


Figure: 4.0.7: Formation of wholly aromatic polymer layers at air-water interface

An example of the latter technique was developed by Hino and Imai et al^{19,20}. Polymer precursors, in the form of a long alkylamine salt, are used for a L-B film. The amine is extracted by a solution treatment after deposition and the film is converted to a polyimide (Figure 4.0.8).

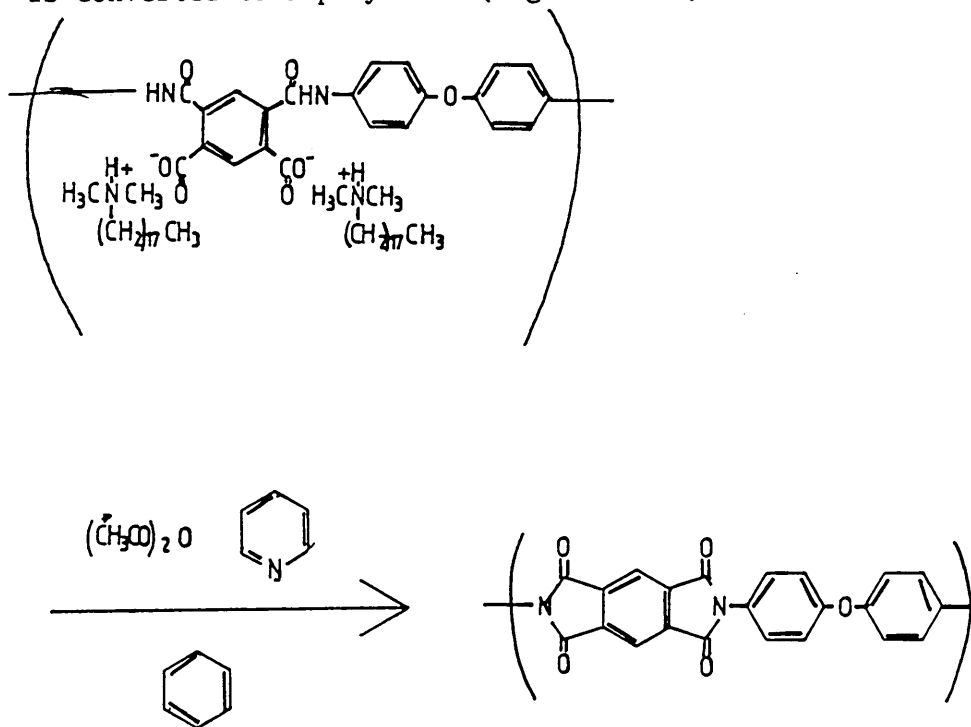


Figure: 4.0.8: formation of a polyimide layer by a solution treatment

In recent years, other materials that have received considerable attention have been the closely related porphyrins and phthalocyanines (Figure 4.0.9). They are known to exhibit properties of interest including thermal stability, rigidity, metal complex formation and gas adsorption which would be desirable to incorporate into L-B films.

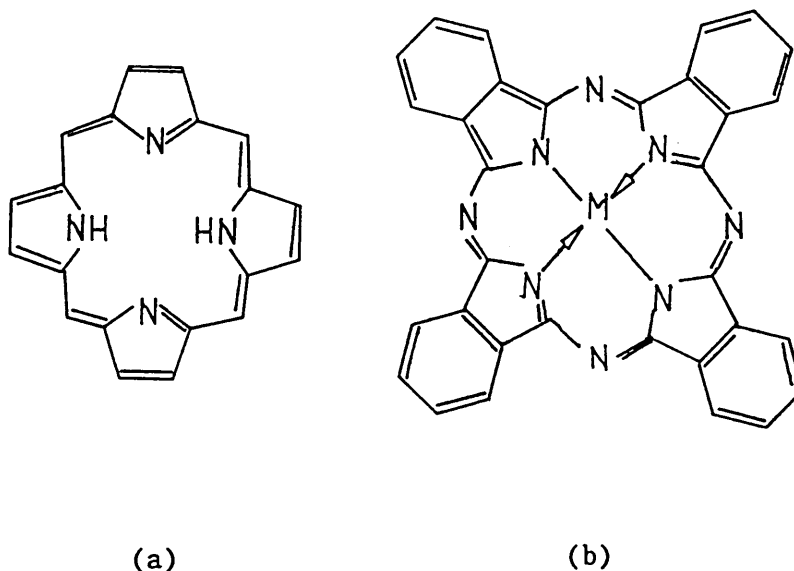


Figure 4.0.9: The basic a) porphyrin and b) phthalocyanine ring structures

Most of the published work on L-B films of porphyrins can be divided into two distinct categories:

1. The materials having hydrophilic groups at position 6,7 for example ester groups which are sufficiently polar to orient the film without causing solubility²²⁻²⁵.
2. The porphyrins which have either two or four long hydrocarbon chains attached to them²⁶⁻³¹.

The first group are of more interest for both their surface electronic properties and as gas sensors³². Recently it was reported that a group 1 porphyrin L-B film containing a metal-metal σ band had been synthesised and characterised³³.

The presence of the metal-metal bond offers possibilities for modifying the light adsorption emission characteristics of L-B films and further enhances their capabilities in catalysis.

The group 2 porphyrins are mainly used for characterisation of their structural environment and for study of their chemical reactivity in the solid state.

Roberts and co-workers at Durham University³⁴ were the first to demonstrate that phthalocyanines can be deposited as a thin film using the L-B technique. It was hoped to exploit its interesting optical and electronic properties such as variable electrical conductivity³⁵ and high thermal stability in sensors and electronic devices.

This led other research groups to look for phthalocyanine derivatives with desirable properties for the L-B method, particularly solubility in a suitable spreading solvent and preferential orientation and ordering of the molecules at the air-water interface^{36,37}.

The phthalocyanines that have attracted particular attention have been the tetra-*t*-butyl phthalocyanines^{34,38,39}. However, these materials are obtained as isomers which could lead to disruption in structural ordering in the film. The isomer problem is absent from octa substituted phthalocyanines obtained from symmetrically substituted precursors⁴⁰. Other recent developments include a series of metal free phthalocyanines having both hydrophobic and hydrophilic side chains⁴¹.

4.0.5 Conducting films

The first success in fabricating conducting L-B films was reported by Barraud and his collaborators⁴², who employed a charge-transfer complex N-docosylpyridinium-TCNQ (NDP-TCNQ) (Figure 4.0.10).

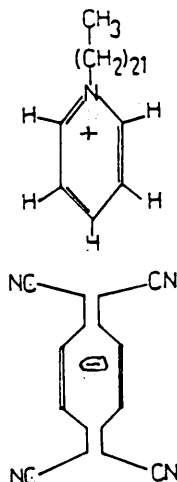


Figure: 4.0.10: The amphiphilic molecule N-docosyl pyridinium-TCNQ

In this charge-transfer complex, there are no aliphatic chains attached directly to the TCNQ molecule. The formation of the L-B film involves the positive amphiphile pyridinium molecule 'dragging' the negative TCNQ along the water surface and onto the solid substrate through coulombic interactions. The TCNQ keeps a sufficient degree of freedom to stack in its own crystalline form. The L-B film is blue and exhibits a low lateral conductivity (10^{-5} - 10^{-7} Scm^{-1}). Subsequent doping with iodine vapour raises the conductivity to 0.1 Scm^{-1} . Further studies have provided new information about the iodination process as well as the electrical properties^{43,44}. The π -A curve (Figure 4.0.11) is reproducible.

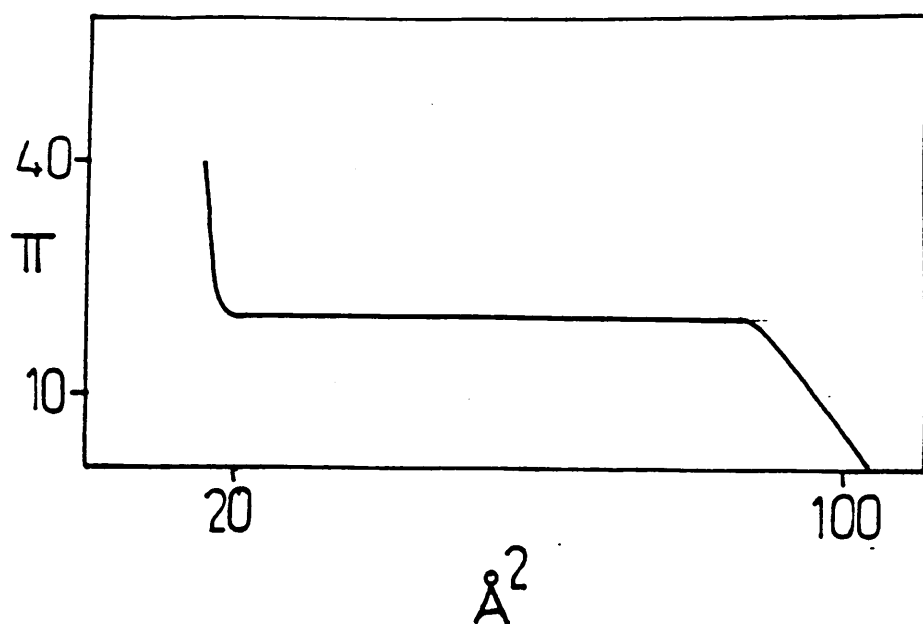


Figure: 4.0.11: Typical π vs \AA^2 for the compression of the charge-transfer complex N-docosyl pyridinium TCNQ

The surface pressure ranges from zero to about 35 mN/m at which \AA is found to be $20 \pm 4 \text{\AA}/\text{molecule}$. The most striking feature of the π - \AA curve is a plateau occurring at $\pi = 16 \text{ mN/m}$. At this constant pressure the area per molecule decreases from 60 to about 30\AA^2 . Furthermore, this plateau appears to be a transition between a region of smooth slope and region of high slope. Recently this transition has been studied by Vandevyver et al⁴⁵. A three dimensional (3D) crystallisation is observed as the film is compressed at the air-water interface. This crystallisation is clearly related to the plateau and can even arise at pressures as low as 10 mN/m if the time spent by the

film at the air-water interface is long enough. The higher the pressure the faster the area reduction and crystallisation phenomenon will be. The resulting 3D flat crystals are stable at the air-water interface, which is consistent with the irreversible character of the plateau.

Just before the crystallisation takes place the area per molecule is about 65\AA^2 /molecule and the film is a two dimensional monomolecular layer at the air-water interface. The ultraviolet-visible spectrum reveals the existence of a dimeric $(\text{TCNQ}^-)_2$ species. Taking into account these factors, it is proposed that the $(\text{TCNQ}^-)_2$ dimer molecular plane is parallel to the air-water interface with the cation standing near the outer parts of the dimer (Figure: 4.0.12).

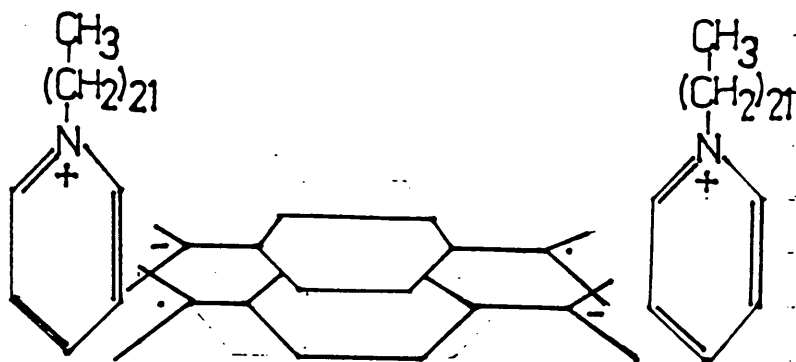


Figure: 4.0.12: The anion and cation species before the crystallisation phenomenon

Any other model would lead to a much smaller area per molecule. Within this model the hydrophilic polar head $(\text{Py}^+-\text{TCNQ}\cdot^-)_2$ occupies a much larger area than the hydrophobic chains. This implies that the plateau of the π -A isotherm should be considered as a 2D-3D transition. The properties of such 3D crystals may not be suitable for potential applications.

However, the films can be made conducting by iodine doping. Richard et al⁴⁴ have shown that the TCNQ molecules upon iodination undergo a 90° rotation.

They stand on edge with their molecular planes roughly perpendicular to the plane of the slide (Figure: 4.0.13).

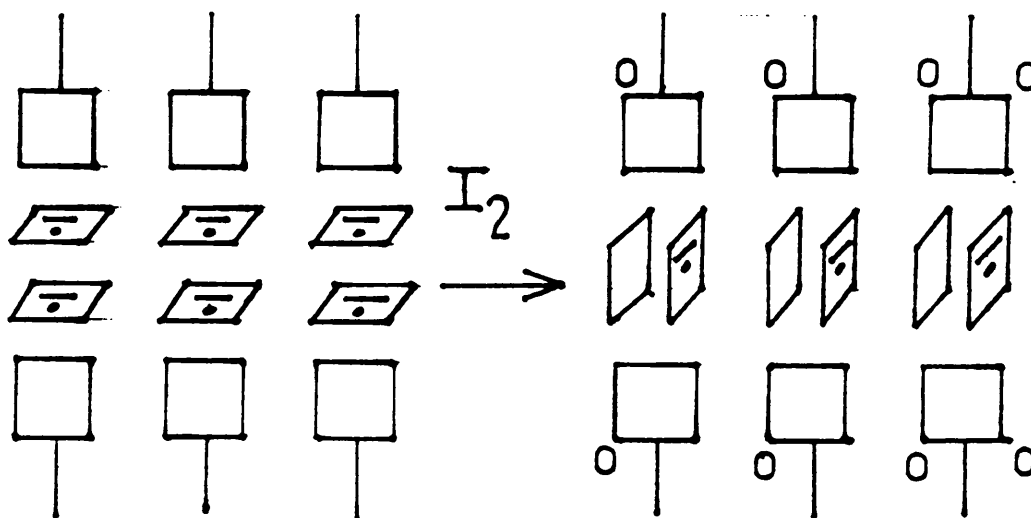


Figure: 4.0.13: The reorganisation of the semi-amphiphilic NDP-TCNQ salt upon solid state lattice controlled iodination

Conducting L-B films based upon NDP-TCNQ without the need for doping have recently been developed⁴⁶. Kawabata's group in the National Chemical Laboratory demonstrated that a 1:2 charge transfer complex of N-docosyl pyridinium-TCNQ⁴⁷ would realize the partially oxidised state of TCNQ. No plateau was reported on the π -A curve. A conductivity of 0.1 Scm^{-1} was obtained. The Durham research group of Dhindsa et al⁴⁸ have since reported a conductivity of 0.02 Scm^{-1} for a L-B film of the 1:1 complex N-octadecylpyridinium and TCNQ (NODP-TCNQ). The isotherms are similar to those obtained for (NDP-TCNQ), except the plateaus occur at a higher pressure. The ultra-violet visible spectrum of the L-B film reveals a strong absorption band at 320 nm which is consistent with the presence of neutral TCNQ⁴⁹.

Other advances in conducting L-B films involving different charge transfer complexes have included:

1. The preparation of the amphiphilic charge transfer complex TMTTF octadecyl TCNQ^{50,51,52}. The complex showed a conductivity of the order 1 Scm^{-1} , without any doping or further treatments.
2. A new family of semiamphiphilic TCNQ ionic salts of dimethyl octadecyl sulphonium⁵³, ethyl methyl octadecyl sulphonium and octadecyl trimethyl phosphonium cations⁵⁴. The conductivity of the films upon iodination is 10^{-1} Scm^{-1} .

However, the above charge transfer complex amphiphilic systems contain long insulating alkyl chains between the layers, which may result in diminished conductivities. Recently, Fujiki and Tabel⁵⁵ have reported that the films of $\text{TTF}_x(\text{TCNQ})_{1-x}$ alloys not having long alkyl chains, have been deposited onto a substrate by the horizontal lifting technique. The conductivity was 5.5 Scm^{-1} at $x=0.6$ which is the highest conductivity thus far attained for conducting L-B films. New possibilities in conducting thin films have been demonstrated by Japanese research groups; these include the electropolymerisation amphiphilic pyrrole derivatives (Figure: 4.0.14)⁵⁶.

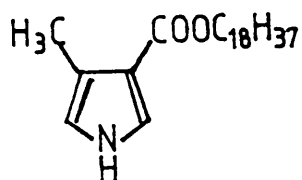


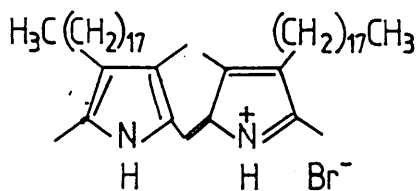
Figure: 4.0.14: Chemical structure of the surface amphiphilic pyrrole

Conducting L-B films are now one of the most important research fields in molecular engineering. The control of anisotropy and the increase in conductivity will be the targets for this decade.

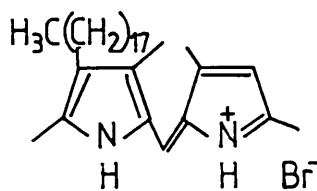
4.1 Aim

A number of mixed valence semi-amphiphilic TCNQ complexes give rise to Langmuir films at the surface of water or glycerol⁵⁷. Some of these films have been shown to be conducting and can be layered onto solid substrates by the L-B method. Applying the basic concept that the positive amphiphilic donor 'drags' the non-amphiphilic TCNQ from the subphase and onto a solid substrate, it was proposed to synthesise and investigate the film forming properties of a series of semi-amphiphilic TCNQ complexes.

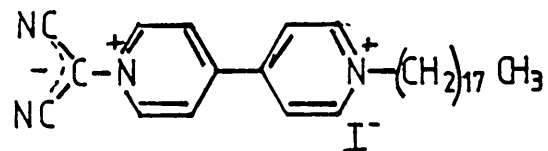
The amphiphilic donors (4.1.1, 4.1.2, 4.1.3) (Figure 4.1.1) were chosen because the chemistry of similar systems had previously been studied (Chapters 2 and 3). The target donor molecules were:



(4.1.1)



(4.1.2)



(4.1.3)

Figure 4.1.1: The proposed target amphiphilic donor molecules

The donor N-methyl-4-dioctadecylpicolinium (4.1.4) (Figure:4.1.2) was proposed to try to increase the area occupied by the hydrophobic aliphatic chains, which would hopefully lead to a more stable situation on the surface of the water and avoid the 3-D crystallisation as reported for the N-docosylpyridinium - TCNQ charge transfer salt^{42,45}.

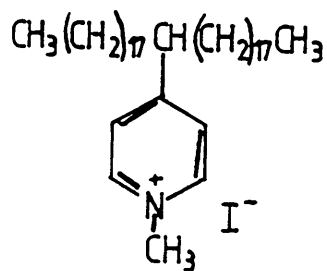


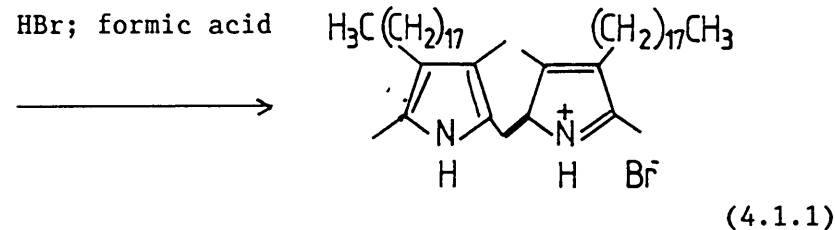
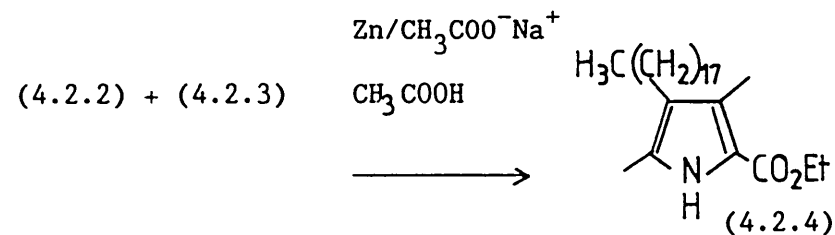
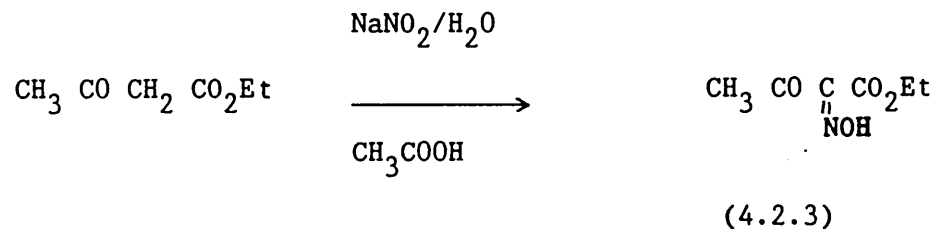
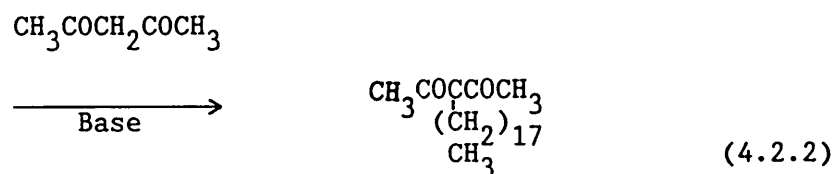
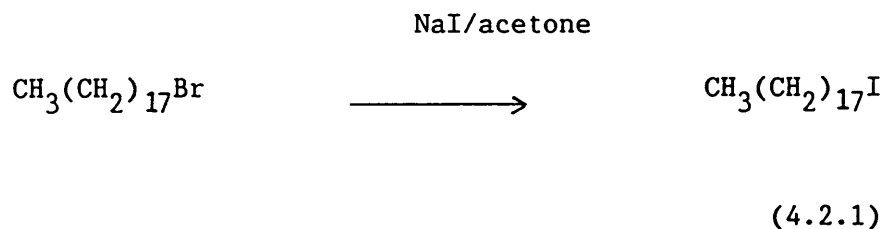
Figure: 4.1.2: The amphiphilic donor

N-methyl-4-dioctadecyl picolinium

4.2 Synthesis of the Amphiphilic Donors

4.2.1 Preparation of 3,5,3',5'-tetramethyl-4,4'-dioctadecyl-dipyrrylmethene hydrobromide (4.1.1)

The proposed reaction scheme was as follows:



The alkyl iodide (4.2.1) was prepared to reduce the reflux time and increase the yield in the alkylation of pentane-2,4-dione. The Knorrpyrrole synthesis for the preparation of the 5-ethoxycarbonyl-2,4-dimethyl-3-octadecyl pyrrole (4.2.4) was investigated on a small scale with the desired product being produced once, but only with a very poor yield. However, attempts to repeat this reaction failed with the diketone being recovered.

The normal solvent for the Knorrpyrrole synthesis is acetic acid, and this was initially used in the reaction of the oxime (4.2.3) and alkylated diketone (4.2.2). However, it was noticed that two layers were formed, presumably because the long alkyl chain caused the diketone (4.2.2) to be insoluble in the reaction mixture. Attempts to mix the two layers by vigorous stirring did not result in any improvement. The reaction was repeated using a mixed solvent of p-dioxane/acetic acid (p-dioxane was chosen because it had the desired boiling point and is frequently used to increase the solubility of organic compounds in aqueous media). At room temperature a homogenous mixture was produced but on refluxing two layers again formed. The product isolated was not the desired pyrrole, but was 2-nonadecanone, presumably formed from the diketone (4.2.2) by a retro-aldol reaction (Figure 4.2.1).

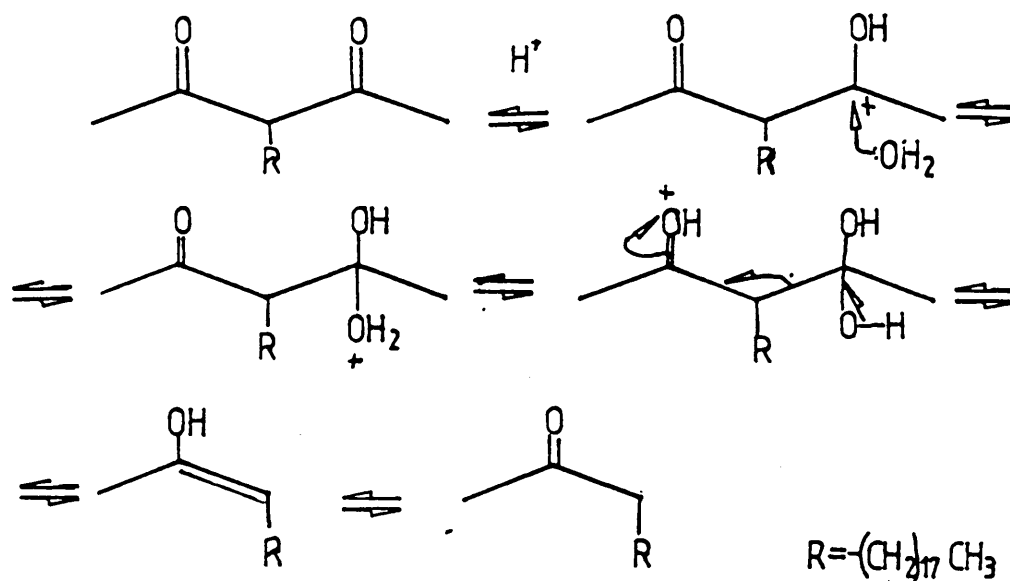
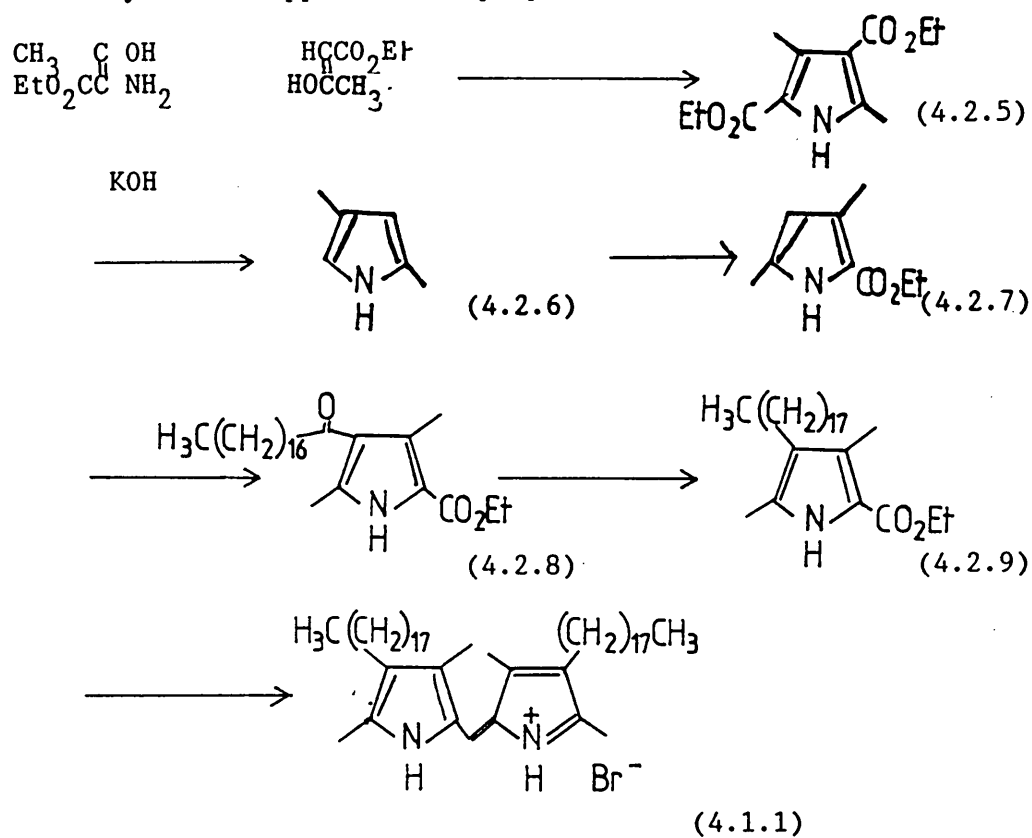


Figure: 4.2.1: Mechanism for retro-aldol condensation for the production of 2- onadecanone

A new synthetic approach was proposed as shown below:



The products (4.2.5, 4.2.6, 4.2.7) were prepared as described in the literature⁵⁸⁻⁶¹, with the yields comparable with the published work. The keto pyrrole ester (4.2.8) was prepared by a Friedel-Crafts acylation of the β -free pyrrole (4.2.7) with the acid chloride of stearic acid^{62,63} and this was followed by a reduction to the octadecyl pyrrole (4.2.9)⁶³. The conversion of the keto pyrrole ester (4.2.8) to the octadecyl pyrrole (4.2.9) was investigated on a small scale, with the reactions being followed by thin layer chromatography. High yields were eventually obtained using borane-methyl sulphide complex in a ten fold excess, which selectively reduced the ketone to a secondary alcohol.

The 'benzylic' alcohol is susceptible to further reduction to the alkane, since the -OH may act as a reasonable leaving group, assisted by the nitrogen lone pair (Figure 4.2.2).

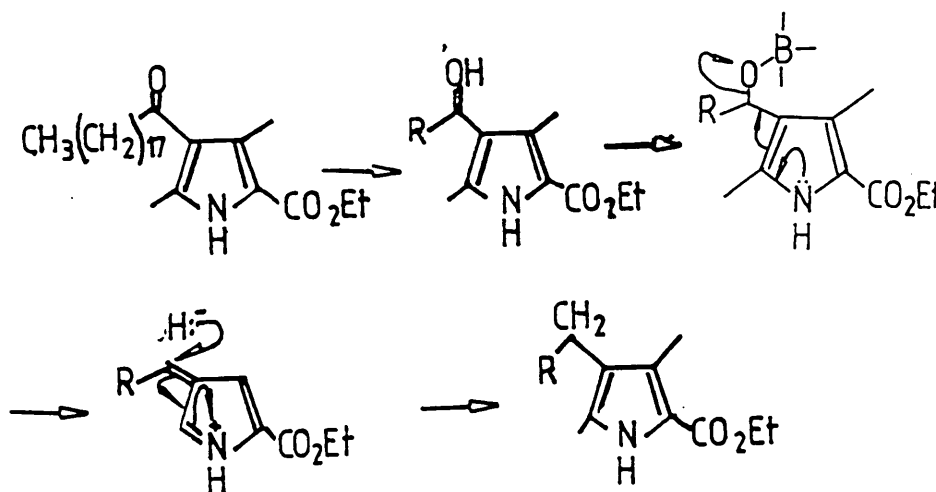


Figure: (4.2.2) Mechanism for the reduction of the keto pyrrole ester to the octadecyl pyrrole

The formation of the semi-amphiphilic dipyrromethene (4.1.1) is analogous to that for the dipyrromethenes previously discussed (see Chapter 3). The reaction between the dipyrromethene and TCNQ was studied. However, a short reflux in acetonitrile and attempts at increasing the reflux times failed to produce the desired charge transfer complex. Further attempts directed towards the modified method (see Chapter 3, Experimental) using a solvent mixture of acetonitrile and chloroform also failed.

Steric factors could be a possible explanation since the long alkyl chains on the dipyrromethene could encumber the close approach of the TCNQ making the formation of the complex unfavourable. This was supported by the low stability of the hexamethyl dipyrromethene-TCNQ complex (4.2.10) (Figure: 4.2.3) compared with the other dipyrromethene (see Chapter 3).

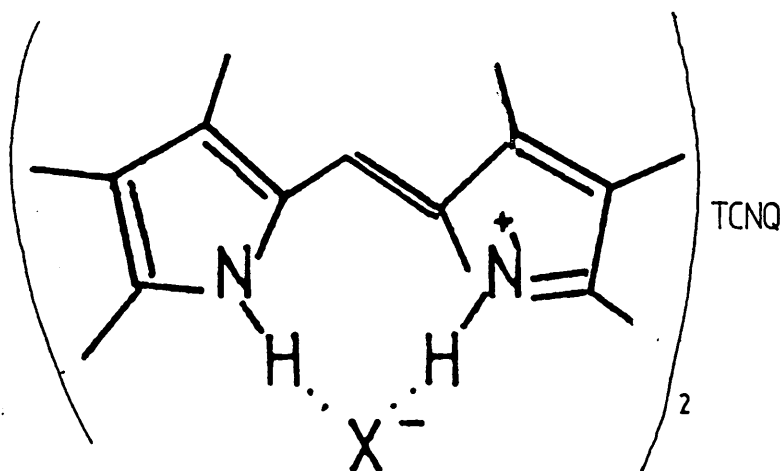
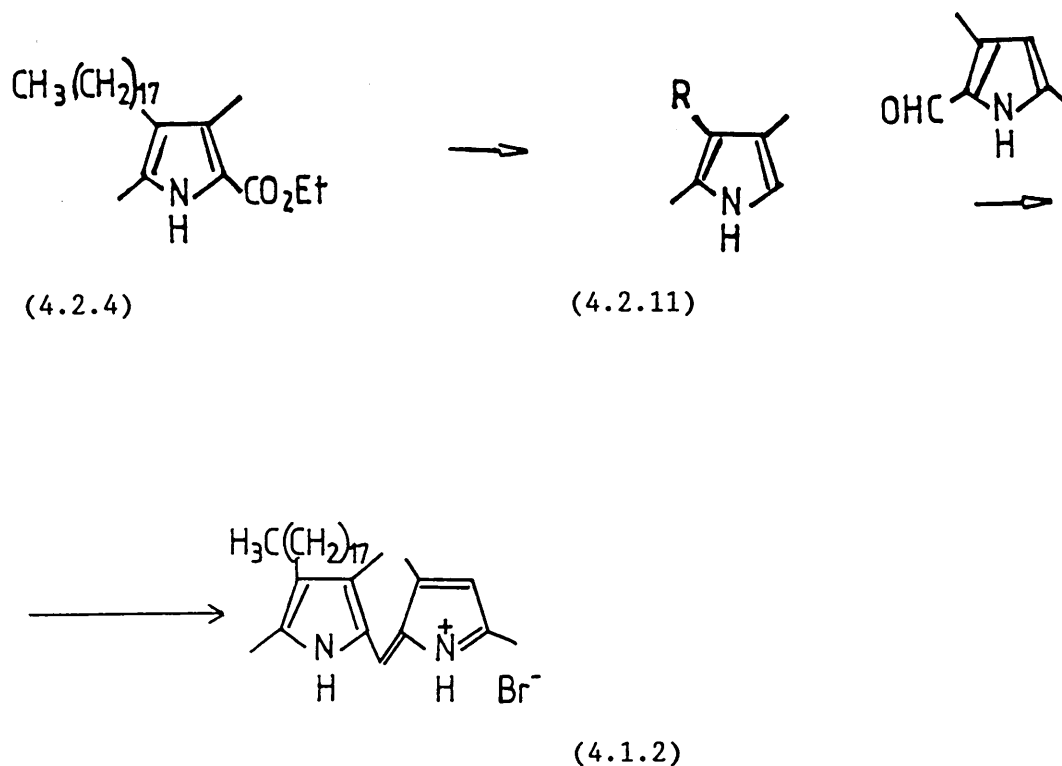


Figure: 4.2.3 The hexamethyl dipyrromethene complex (4.2.10)

To reduce the problem of the steric hindrance it was proposed to synthesise a semi-amphiphilic dipyrromethene with only one long alkyl chain i.e. 3,5,3',5'-tetramethyl-4-octadecyl dipyrromethene hydrobromide (4.1.2). The proposed synthetic pathway was:



Efforts were directed towards repeating and modifying the method used by Harris et al⁶⁴ for the production of the decarboxylated pyrrole (4.2.11), but all attempts proved to be unsuccessful. The method converts the pyrrole ester to its sodium salt which in turn is acidified to precipitate the acid. The precipitated acid is then decarboxylated in situ by steam distillation.

Thin layer chromatography confirmed the conversion to the salt, but acidification with acetic acid and an attempted steam distillation did not yield the desired product. The failure to steam distil the decarboxylated product was presumably because of the long alkyl chain on the pyrrole. The reaction was repeated using dilute hydrochloric acid (to aid the work up procedure), but on refluxing the reaction mixture turned purple. The product isolated was not the desired pyrrole, but a polymerisation product formed from the electrophilic attack by the protonated decarboxylated pyrrole towards a molecule of unprotonated pyrrole (Figure: 4.2.4).

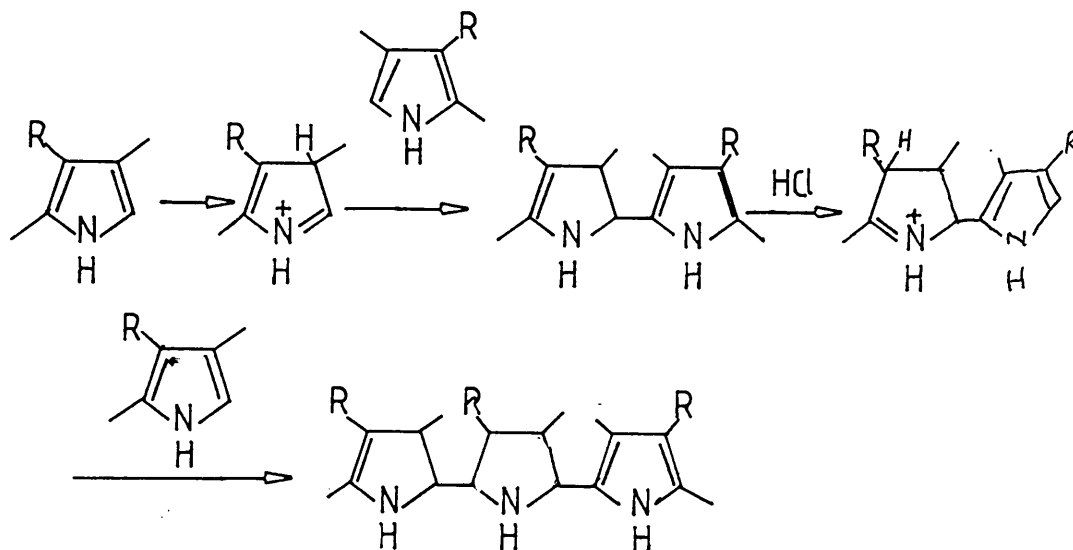


Figure: 4.2.4: The proposed mechanism for the formation of polymerisation product.

The sodium salt was found to be soluble in tetrahydrofuran

This would allow the acidification to be attempted at room temperature and hopefully avoid polymerisation. However, infra-red and nmr spectroscopy confirmed the formation of the dimer.

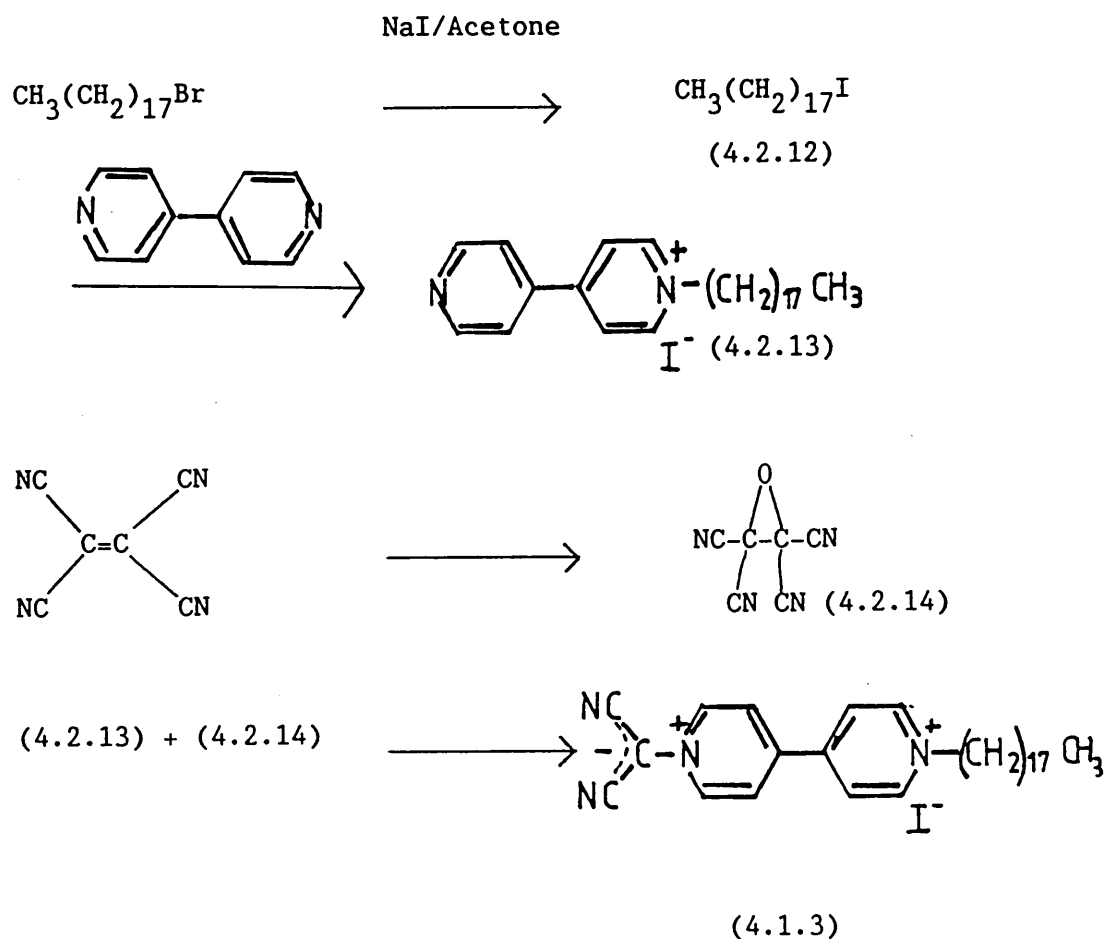
In view of the time restrictions the above reaction was abandoned. However, careful control of the pH may lead to the isolation of the decarboxylated product.

4.2.2 Synthesis of the semi-amphiphilic donor

N-dicyanomethylide-N'-octadecyl bipyridinium halide

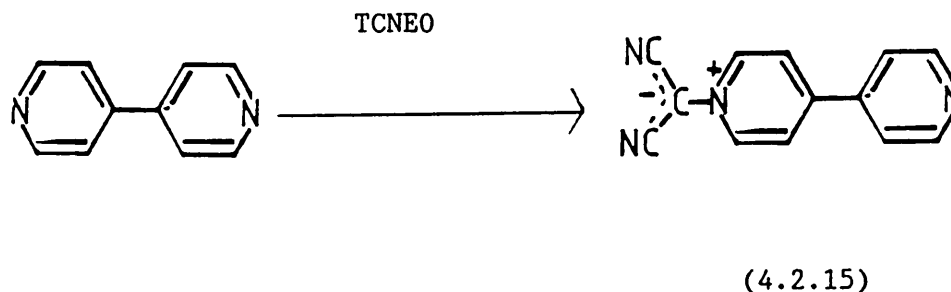
(4.1.3)

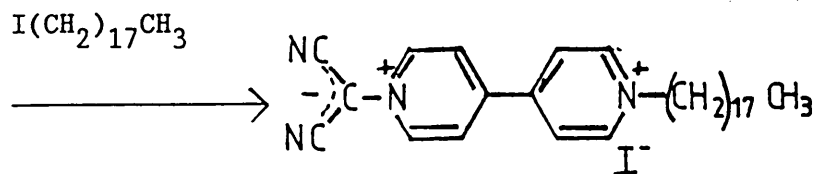
The proposed synthetic pathway for the production of the surface active charge transfer complex involved four steps:



The quaternisation of the dipyridyl was found to be easier using the alkyl iodide rather than the alkyl bromide. The colour change between the yellow monoquaternised iodide (4.2.13) and the red diquaternised diiodide enabled monitoring of the process and the isolation of monoquaternised product (4.2.12) in very good yields. The preparation of tetracyanoethylene oxide (TCNEO) (4.2.14) followed the procedure given by Linn et al⁶⁵, except the isolation of the epoxide was changed to avoid prolonged contact with water, and hydrolysis of the product. This improved the yield significantly. All efforts to prepare the desired target molecule (4.1.3) failed. The nucleophilic attack on the oxirane ring of TCNEO (4.2.14) was expected by the free nitrogen atom of bipyridinium but the TCNEO molecule can also react with the iodide counter ion⁶⁵, to form cyanogen and tricyanovinylalcoholate. The competition between the nitrogen and the iodide could be a possible explanation for the failure to isolate the desired product.

To remove the possibility of the halide ion reacting with the TCNEO a new reaction scheme was considered:



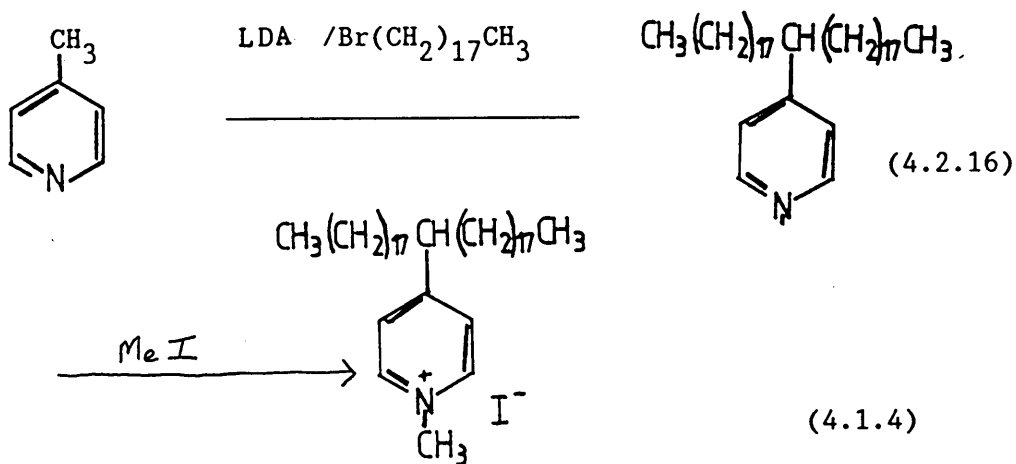


(4.1.3)

The N-dicyanomethylide-4,4'-bipyridinium (4.2.15) was produced in good yields, but unfortunately time restrictions prevented further investigations into the quaternisation of (4.2.15) using the long chain alkyl iodide.

4.2.3 Synthesis of the surface active donor N-methyl-4-dioctadecyl picolinium (4.1.4)

The proposed reaction scheme was as follows



After initial difficulties involving contamination with N-octadecyl-4-picoline (Figure: 4.2.5a) and 4-nonadecyl picoline (Figure: 4.25b), the dialkylated picoline (4.2.16) was isolated in good yields.

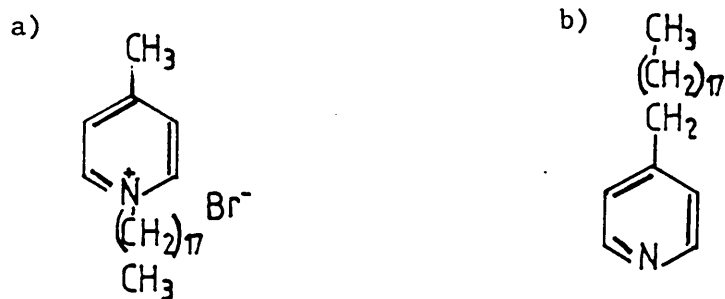


Figure: 4.2.5: The side products in the production of the dialkylated picoline (4.2.16)

The dialkylated picoline (4.2.16) was then N-methylated using methyl iodide (4.14) followed by refluxing with LiTCNQ in ethanol to produce the semi amphiphilic TCNQ complex.

4.3 Results and Discussion

4.3.1 Langmuir-Blodgett film of

4,4'-dioctadecyl-3,5,3',5'-tetramethyl dipyrromethene hydrobromide (4.1.1)

The dipyrromethene (4.1.1) has both a hydrophobic and a hydrophilic part which provide sufficient solubility and preferential orientation required for monolayer formation.

4.3.1.1 Formation of the Langmuir Film

A solution of the dipyrromethene (4.1.1) was made up in AnalaR chloroform at a concentration of 1mgml^{-1} . A $100\mu\text{l}$ sample was deposited onto the aqueous surface in the trough using an Agla syringe. A yellow tinge was observed at the surface of the water. The film was left for five minutes to allow complete evaporation of the chloroform before the isotherm was measured. A typical example of the isotherm measured after this time is shown in Figure 4.3.1.

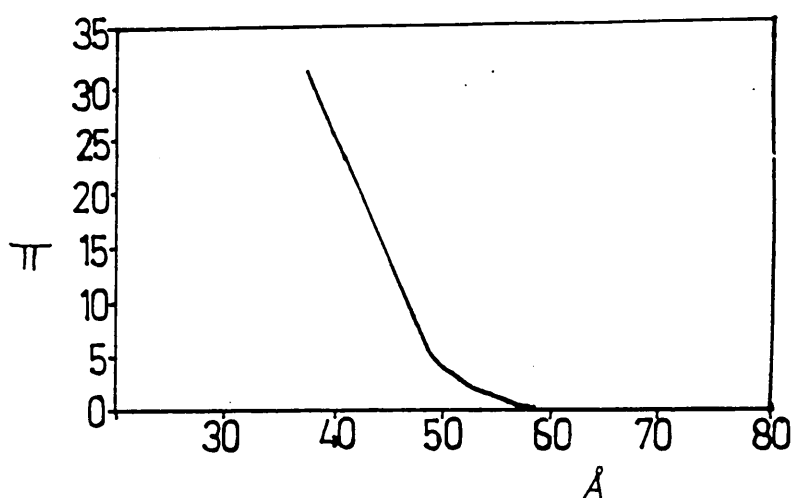


Figure: 4.3.1: Schematic diagram of the isotherm
for the dipyrromethene (4.1.1)
after 5 minutes.

Extrapolation through the x-axis of the solid portion of the curve from 5mNm^{-1} to 25mNm^{-1} yielded a surface area per molecule of 52\AA^2 . However, when the uncompressed film was left for two hours on the surface of the water, the surface pressure-area (π -A) curve yielded a molecular area of approximately 106\AA^2 (Figure 4.3.2).

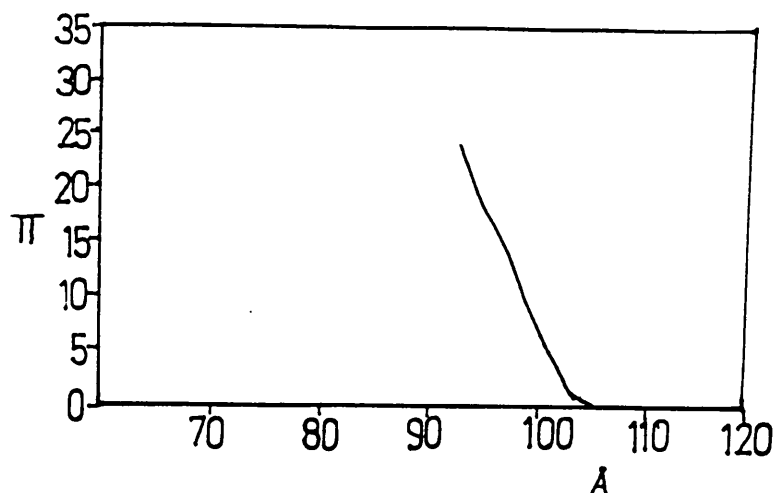


Figure: 4.3.2: Surface pressure v's area for
dipyrromethene (4.1.1) compressed
after two hours.

The surface pressure-area curves (Figures: 4.3.1, 4.3.2) show the classic transformations expected for the L-B technique during compression of gas to liquid to solid. The monolayers both collapsed between 35 to 40 mNm^{-1} , but below this pressure they were very stable and could sustain a surface pressure of 25mNm^{-1} for the transfer of the monolayers to the substrate.

The molecular area increased by a factor of 2.03 between the dipyrromethene (4.1.1) being compressed immediately and after two hours (Figures: 4.3.1, 4.3.2) indicating that a molecular re-orientation occurred.

Molecular rearrangement has also been shown to occur in the Langmuir films of protoporphyrin ester²². It was suggested that dimerization aggregation or polymerization via the vinyl groups of the protoporphyrin ester may be the cause, but these effects would produce a decrease in the film area.

Lower area per molecule values may also occur as a result of the amphiphilic molecules entering the subphase, either through solubility or the miscibility of the spreading solvent with the subphase⁴⁸.

The amphiphilic dipyrromethene (4.1.1) could possibly orientate itself between two extremes, one where the dipyrromethene rings are orientated parallel to the surface of the water (Figure: 4.3.3).

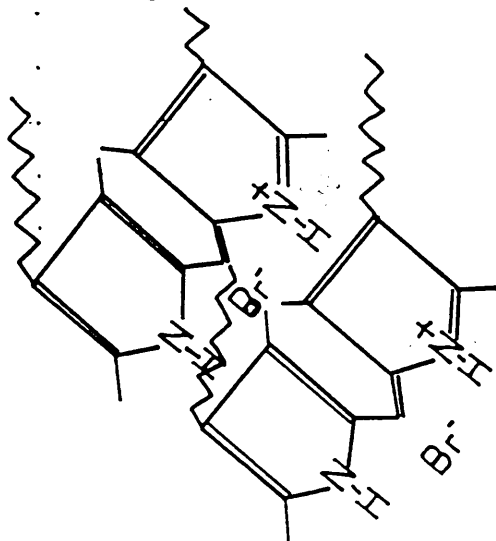


Figure: 4.3.3: The dipyrromethene (4.1.1) with its rings orientated parallel to the surface of the water.

and one where the rings are orientated perpendicular (Figure: 4.3.4)

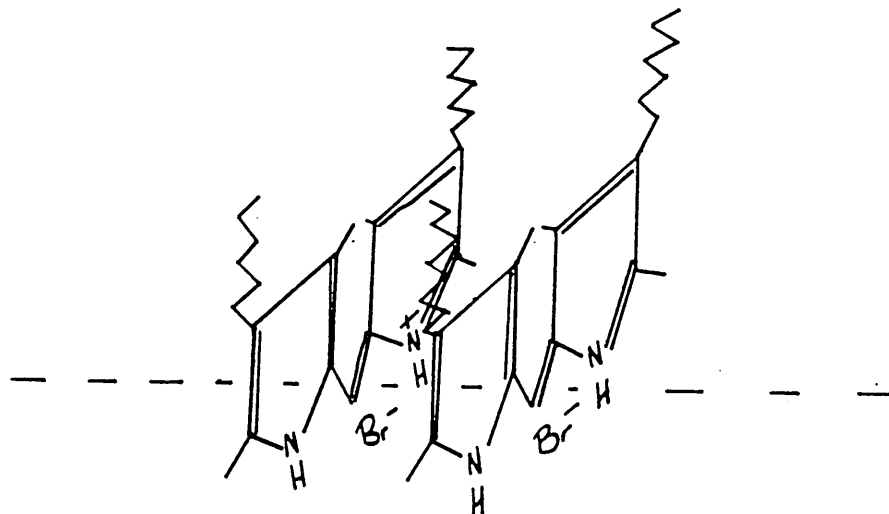


Figure: 4.3.4: The dipyrromethene (4.1.1) with its rings orientated perpendicular to the water.

Based on models, using average bond angles and lengths obtained from a number of dipyrromethene papers (Figure: 4.3.5)⁶⁶⁻⁶⁸, one would expect a molecular area of about 32.5\AA^2 if the dipyrromethene was orientated perpendicular and of about 110.5\AA^2 if it was orientated parallel to the surface of the subphase.

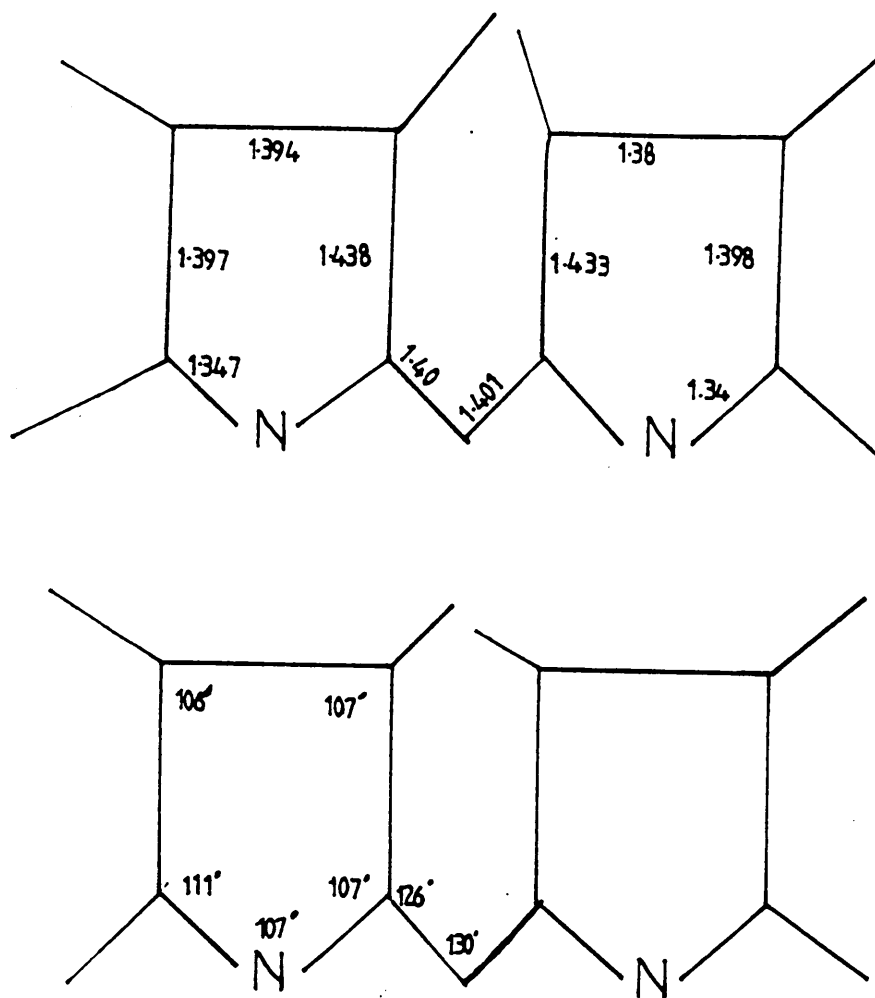


Figure: 4.3.5: The average bond angles and lengths of the dipyrromethenes.

The area per molecule obtained for the dipyrromethene from the compression after five minutes indicates that neither extreme is fulfilled. The area per molecule remains constant with subsequent cycles of expansion and compression up to

30mNm^{-1} . The molecular area of 52\AA^2 for the dipyrromethene suggests that the amphiphilic donor orientates itself with the faces in an 'upright' position to the air-water interface (Figure 4.3.4). The surface area per molecule of about 106\AA^2 for the dipyrromethene compressed after two hours is quite reasonable for the molecules oriented in a monolayer with the planar portion of the molecule parallel to the air-water interface and the octadecyl groups away from the water (Figure: 4.3.3).

4.3.1.2 Transfer of monolayers onto the substrate

The transfer of monolayers of the surface active dipyrromethene from the trough onto previously cleaned quartz slides was investigated. After the dipping conditions were optimized, multiple layers could be built up by the process of repeated insertion and withdrawals through the film-water interface. The deposition ratios (Figure 4.3.6, were monitored continuously and ranged from 10% to 100% for the downstrokes and 0% for the upstrokes, indicating transfer in an X-type fashion.

Ten layers of 4,4'-dioctadecyl-3,5,3',5'-tetramethyl dipyrromethene hydrobromide were built up on a quartz substrate, but the number of layers that could be transferred onto these slides seemed to be limited only by the amount of time one was willing to devote to dipping.

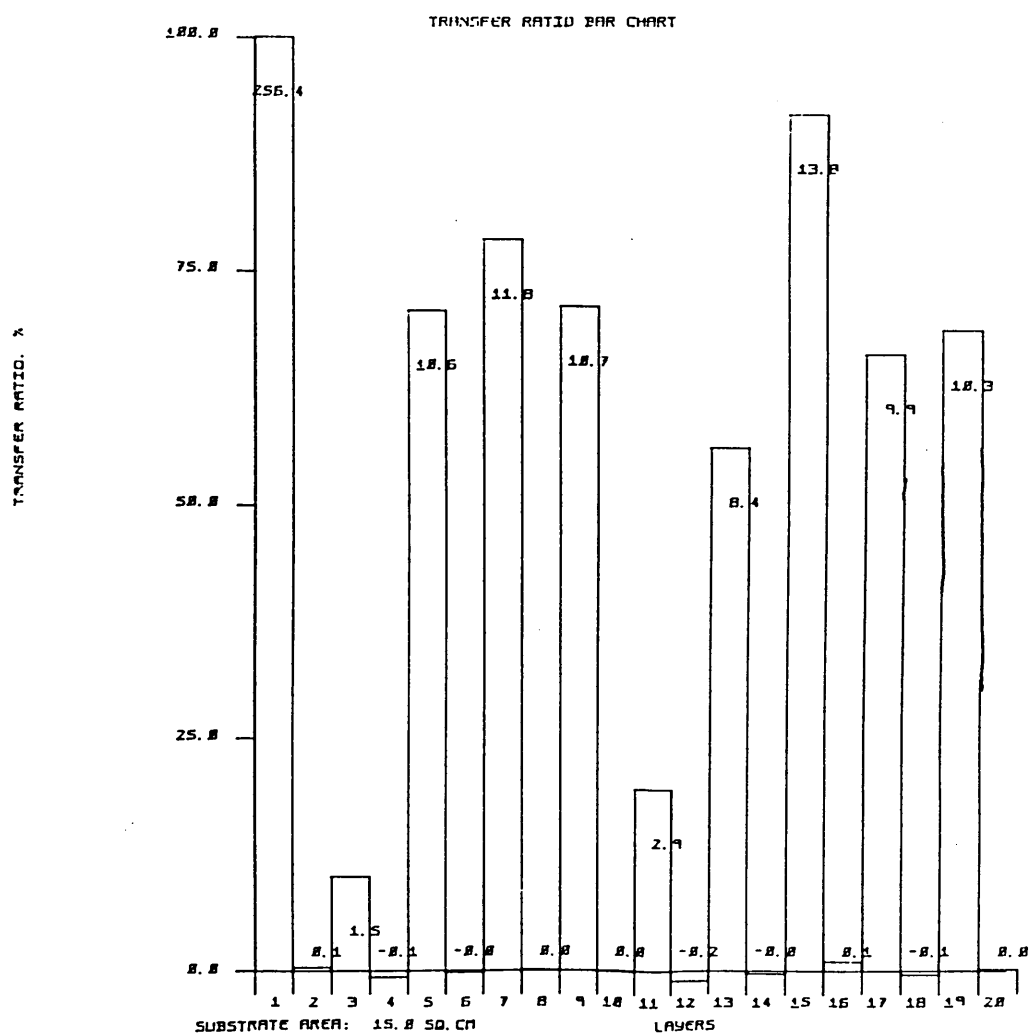


Figure 4.3.6: The deposition ratios for the
dipyrrylmethene (4.1.1)

4.3.1.3 Electronic Absorption Spectrum

The ten layer L-B films of the amphiphilic dipyrromethene on quartz slides were quite translucent and green/yellow in colour. The electronic absorption spectrum is shown in Figure: 4.3.7.

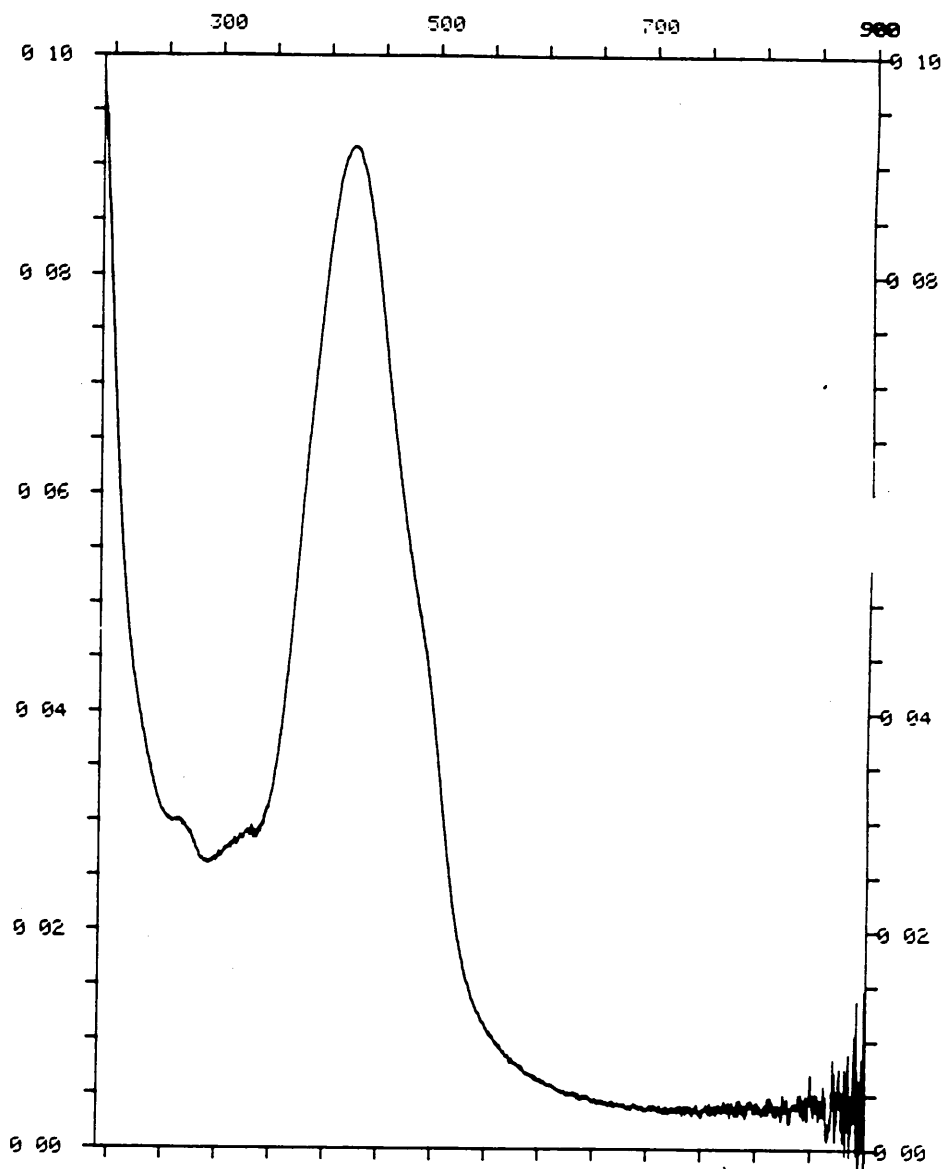


Figure: 4.3.7 The UV/visible spectrum of the
Langmuir-Blodgett film dipyrromethene (4.1.1)

The absorption due to the uncoated quartz slide has been subtracted out.

The spectrum of the L-B film shows a strong absorption band at 423.2 nm which is consistent with that obtained from the powdered complex.

4.3.2 Langmuir Film of N-methyl-4-dioctadecyl picolinium-TCNQ charge transfer salt

The surface active picolinium charge transfer salt was expected to form a Langmuir film with a well defined molecular order, avoiding the three dimensional crystallisation as reported by Barraud et al^{42,45} and Dhindsa et al⁴⁸ for NDP-TCNQ and N-octadecylpyridinium-TCNQ respectively.

4.3.2.1 Formation of the Langmuir film

A solution of the semi-amphiphilic charge transfer salt was made up in AnalaR chloroform at a concentration of 1mg ml^{-1} and 50 μl were deposited onto the water surface using an Agla syringe.

The film was left for five minutes to allow complete evaporation of the chloroform and a reproducible isotherm (Figure: 4.3.8) was measured after this time with a compression rate of $40\text{ cm}^2\text{ min}^{-1}$.

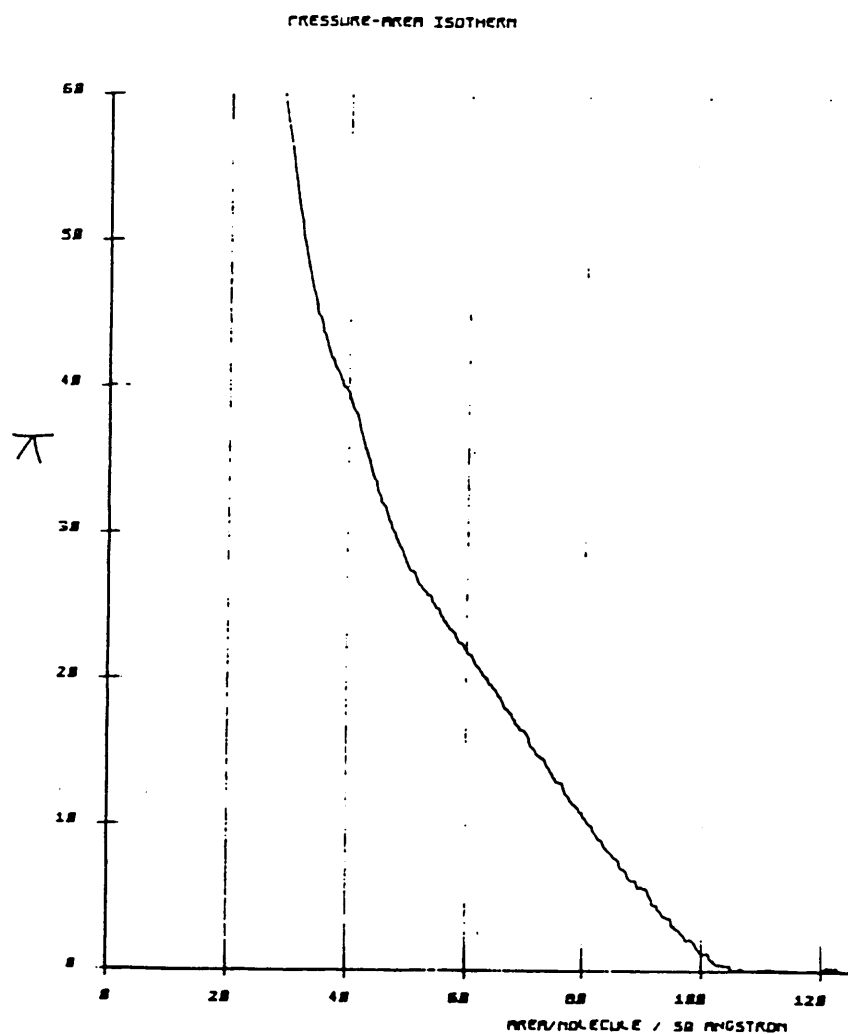


Figure: 4.3.8: Surface pressure v's area for the charge-transfer complex of TCNQ and the dialkylated picolinium (4.1.4)

4.3.2.2 Pressure area isotherm

The phase transition of a two dimensional gas to liquid to solid can clearly be seen from the isotherm with no existence of a plateau as described by Barraud et al^{42,45}.

Extrapolation through the x-axis of the solid portion of the curve from 30 mNm^{-1} to 40 mNm^{-1} yielded a surface area per molecule of 64 \AA^2 , which is comparable with the area per molecule of 65 \AA^2 ⁴⁵ observed for the NDP-TCNQ monolayer before the onset of the three-dimensional crystallisation. Therefore their molecular orientations would be expected to be similar with the TCNQ existing as a dimeric species $(\text{TCNQ}^-)_2$ parallel to the air-water interface and the cation standing near the region of the CN groups of the dimer (Figure: 4.3.9)

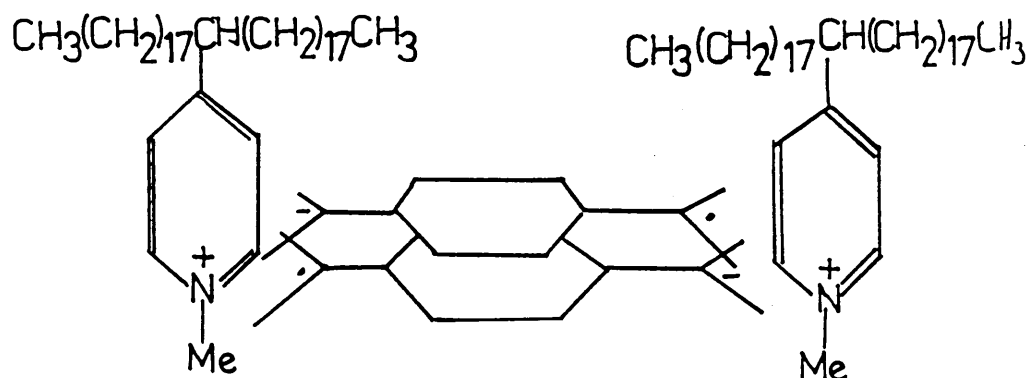


Figure: 4.3.9: The outline of the anion and cation species before the crystallisation phenomenon.

The hydrophilic polar head for the NDP-TCNQ monolayer occupies a much larger area (72\AA^2) than that of the hydrophobic aliphatic chain (40\AA^2) which induces some instability and leads to crystallisation⁴⁵.

The increase in the area of the hydrophobic aliphatic chains in 4.1.4 to approximately 80\AA^2 afforded by the extra chains would lead to the amphiphilic molecule having the hydrophilic part (72\AA^2) occupying about the same area as the hydrophobic parts. This is believed to cause a stable situation which prevents three-dimensional crystallisation.

4.4 Experimental

4.4.1 The Langmuir Trough

The Langmuir trough in which the experiments were performed was a commercial trough (Nima Alternate Layer trough (Fig. 4.4.1)) made of non-porous polytetrafluoroethylene (P.T.F.E). It was equipped with two compartments each with an independently movable barrier, whose position was monitored by the surface pressure of the film. The surface pressure was monitored by a Wilhelmy plate: the probe was made of a single strip of filter paper which was lowered onto the surface of the subphase. The subphase was water which was purified using a Millipore Milli-Q system.

The substrates were microscope slides which were wiped with methylene chloride and then cleaned by ultrasound with methylene chloride, water, and isopropanol.

NIMA Alternate Layer
Langmuir-Blodgett Trough.

- * All PTFE construction
- * No cross contamination between compartments
- * Built-in anti-vibration mount and thermostating channels.
- * Run with IBM (compatible) PC

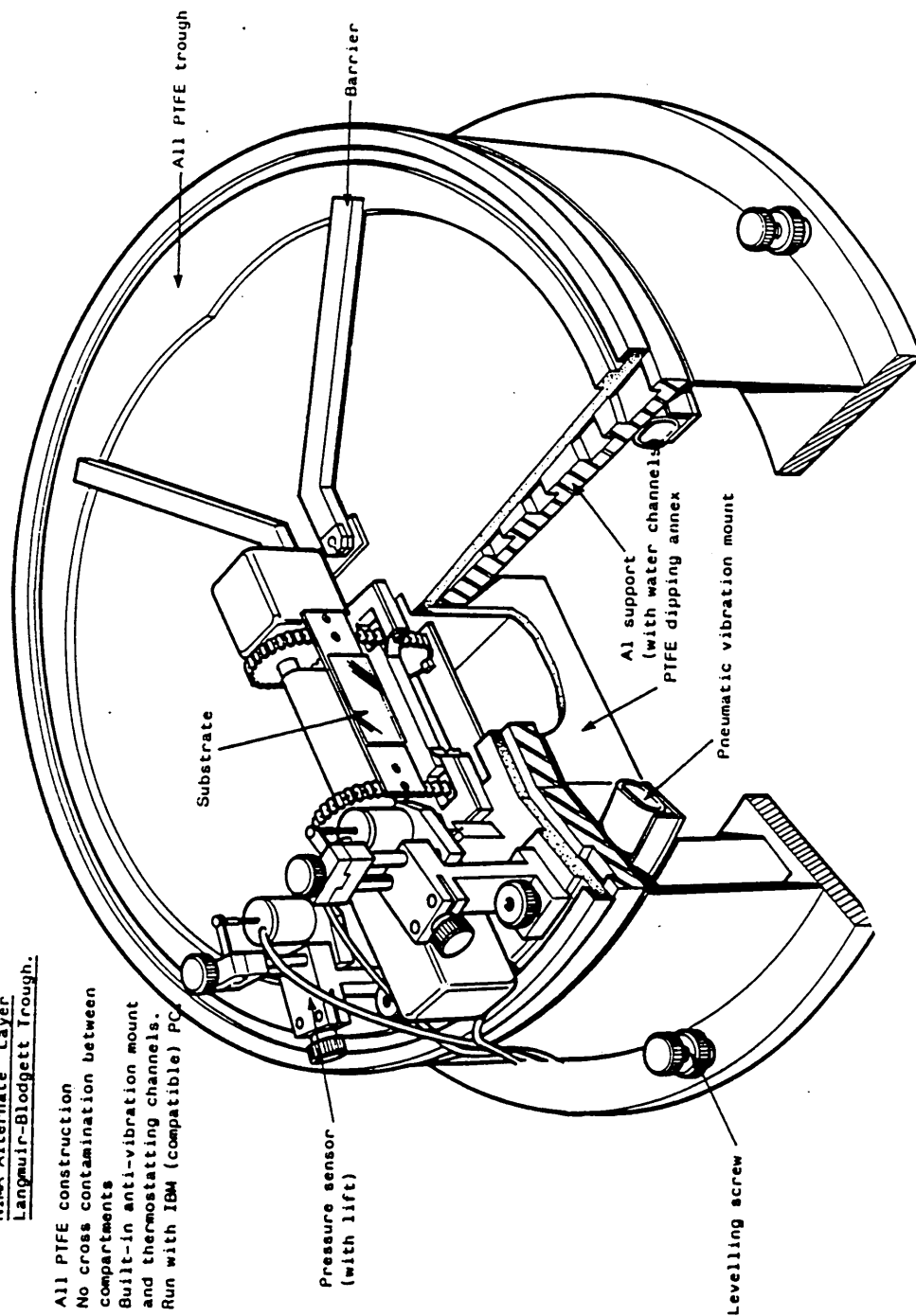


Figure 4.4.1: The Nima Alternate Layer Trough

The substrate was carried around the dividing barrier by means of a pulley mechanism which ensures vertical movement of the substrate through the subphase surface.

4.4.2 Experimental procedure for a L-B film

1. The trough was filled with ultra pure water (1000 cm^3)
2. The barriers were closed to their minimum area and the surface of the subphase was cleaned by suction.
3. A π -A isotherm was recorded, to check the subphase surface was free from dust.
4. A freshly made up solution was prepared by dissolving the amphiphilic salt in a suitable solvent at an approximate concentration of 1mgml^{-1} .
5. The solution was spread onto the water surface via a syringe.
6. The solvent was allowed to evaporate.
7. The film was slowly compressed and the π -A isotherm recorded.
8. A suitable pressure for dipping was chosen.
9. Points 1-6 were repeated for both compartments.
10. The substrate was passed through the water surfaces at the predetermined dipping speed.

4.4.2 General Information

For the general experimental information (see appendix 1).

4.4.3 Experimental methods:

1-Iodooctadecane

A solution of 1-bromooctadecane (20g; 0.066 moles) and sodium iodide (12.1g; 0.081 moles) in dry acetone (100ml) was refluxed for 48 hours. The reaction mixture was cooled, and filtered to remove solid sodium bromide. The organic filtrate was evaporated to an oil which solidified on standing yielding 1-iodooctadecane.

18.7g; 81%:

I.R.(KBr): 2930; 2840; 1480; 1390; 720:

^1H NMR(CDCl_3): 3.1(t, 2H); 1.5(s, 28H); 1.0(t, 3H):

3-octadecyl-pentane-2,4-dione⁶⁹ (4.2.2)

A mixture of pentan-2,4-dione (22.60g; 0.23 moles), 1-iodooctadecane (79.22g; 0.23 moles) and anhydrous potassium carbonate (40g) in dry acetone (100ml) was refluxed for 24 hours. The reaction mixture was cooled. The potassium carbonate was removed by suction filtration and washed with 1:1 mixture of acetone/petrol (200ml). The combined washings and filtrates were concentrated to give a brown oil which solidified on standing. The crude product was purified by vacuum distillation (170°C; 0.05mmHg). The resulting oil residue, solidified on standing yielding

3-octadecane-pentane-2,4-dione.

22.52g; 30%:

I.R.(KBr): 2920; 2860; 1700; 1580; 800; 720:

^1H NMR (CDCl_3): 2.1(s, 6H); 1.2(s, 30H); 1.0(t, 3H):

Ethyl 2-oximinoacetoacetate (4.2.3)

The oxime was prepared from ethyl acetoacetate (73ml; 0.58 moles) and sodium nitrite (45g; 0.65 moles) using the method described by Touster⁷⁰.

45g; 49%:

I.R.(KBr): 3300; 3000; 2960; 1700; 1610; 970:

¹H NMR(CCl₄): 4.9(q,2H); 2.9(s,3H); 1.9(t,3H):

2-Ethoxy carbonyl-3,5-dimethyl-4-octadecyl Pyrrole (4.2.4)

The pyrrole ester was prepared from ethyl 2-oximinoacetoacetate (2.28g; 0.014 moles) and 3-octadecyl -pentan-2,4-dione (4.1g; 0.013 moles) using the method described by Kleinspehn⁷¹.

0.2g; 40%

I.R.(KBr): 3310; 2920; 2860; 1670; 1470; 1270; 770; 720:

¹H NMR (CDCl₃): 4.1(q,2H); 2.1(m,9H); 1.3(s,30H); 0.9(t,3H):

Note: Attempts to repeat this reaction failed, with 3-octadecyl pentan-2,4-dione being recovered:

I.R.(KBr): 2920; 2860; 1700; 1580; 800; 720:

¹H NMR (CDCl₃): 2.1(s,6H); 1.3(s,30H); 0.9(t,3H):

The Knorr-pyrrole synthesis as described by Kleinspehn was repeated again using a solvent mixture of p-dioxane (45ml) and acetic acid (10ml).

0.2g; 23%:

I.R.(KBr): 2920; 2860; 1690; 1460; 720:

¹H NMR (CDCl₃): 2.0(s,3H); 1.3(s,30H); 0.9(t,3H):

3,5-Diethoxycarbonyl-2,4-dimethyl pyrrole (4.2.5)

The pyrrole diester was prepared from ethyl acetoacetate (279g; 2.15 moles), sodium nitrite (73g; 1.05 moles) and zinc granules (140.5g; 2.14 moles) using the method described by Fischer⁵⁸.

153g; 71%; mp: 132°-134° (lit mp 136-137°C)⁵⁸

I.R.(KBr): 3190; 2980; 2890; 1710; 1630; 1490:

¹H NMR (CCl₄): 4.2(m,4H); 2.5(s,6H):

2,4-Dimethyl pyrrole (4.2.6)

The dimethyl pyrrole was prepared from

3,5-diethoxycarbonyl-2,4-dimethyl pyrrole (4.25) (71.62g; 0.3 moles) and KOH (151.5g; 2.7 moles) from the method described by Fischer⁵⁹.

10.88 g; 38%

I.R.(KBr) 3200; 2950; 2900; 1640:

¹H NMR (CDCl₃): 6.2(s,1H); 5.6(s,1H); 2.1(s,3H); 2.0(s,3H)

2,4-Dimethyl-5-ethoxycarbonyl pyrrole (4.2.7)

The pyrrole ester was prepared from 2,4-dimethyl pyrrole (4.2.6) (29.9g; 0.31 moles) magnesium (11.4g; 0.45 moles), ethyl bromide (49.9g; 0.46 moles) and ethyl chloroformate (45.5g; 0.42 moles) using the method described by Fischer^{60,61}

16.72g; 32%; mp:120-123°C (lit mp:123-124°C)^{60,61}

I.R.(KBr): 3170; 2940; 2900; 1710; 1650; 1450:

¹H NMR (CDCl₃): 5.8(s,1H); 4.3(q,2H); 2.3(s,3H); 2.26(s,3H);
1.4(t,3H):

(4.2.8)

To a stirred solution of stearic acid (4.25g; 0.015 moles) under nitrogen in dichloromethane (70ml) was added DMF (0.5ml) and oxalyl chloride (2mls; 0.023 moles) in one portion. The reaction mixture was allowed to warm to room temperature with stirring. After 1.5 hours the mixture was cooled in an ice bath and 2,4-dimethyl-5-ethoxycarbonyl pyrrole (2.0g; 0.012 moles) was added, followed by stannic chloride (2ml; 0.17 moles) over a period of 35 minutes and the reaction mixture was stirred for a further 1.5 hours. The solution was poured into 2M hydrochloric acid (50ml) and the dichloromethane layer separated. This was washed with sodium bicarbonate solution, dried (anhydrous sodium sulphate) and evaporated. The resultant oil was dissolved in ethanol (50ml). Water was added which precipitated a solid which was filtered by yield: 2,4-dimethyl-5-ethoxycarbonyl-3-octadecanyl pyrrole (4.2.8) 3.2g; 55%; mp: 74-76°C

I.R.(KBr): 3300; 2920; 2860; 1680; 1655; 1280; 780; 750; 720:

¹H NMR (CDCl₃): 4.3(q, 2H); 2.6(s, 3H); 2.5(s, 3H); 1.3(s, 32H); 0.9(t, 3H):

Microanalysis: Found: C, 74.68%, H, 10.84%; N, 3.31%:

C₂₇H₄₇NO₃: requires: C, 74.78%; H, 10.92%; N, 3.23%:

2,4-Dimethyl-5-ethoxycarbonyl-3-octadecyl pyrrole⁶³ (4.2.9)

To a stirred solution of (4.2.8) (5.04g; 0.0116 moles) under nitrogen in dry tetrahydrofuran (25ml) was added borane-methyl sulphide complex (5.4 mls; 0.0675 moles) in one portion. The

reaction mixture was allowed to stir for a further 3 hours. The reaction was then quenched by the slow careful addition of glacial acetic acid (25ml). Water was added (50 mls) and the resulting white solid was filtered. The solid was re-crystallised from petrol yielding pure

2,4-dimethyl-5-ethoxycarbonyl-3-octadecyl pyrrole. (4.2.9)

3.33g; 68%; mp:56-58°C

I.R.(KBr): 3300; 2920; 2860; 1670; 1280; 770; 760; 740; 720:

^1H NMR(CDCl_3): 4.2(q,2H); 2.2(s,6H); 1.3(s,34H); 1.0(t,3H)

Microanalysis Found: C,77.30%; H,11.82%; N,3.29%:

$\text{C}_{27}\text{H}_{49}\text{NO}_2$ requires: C,77.27%; H,11.77%; N,3.34%:

4,4'-Di-octadecyl-3,5,3',5'-tetramethyl dipyrromethene

hydrobromide (4.1.1)

The dipyrromethene (4.1.1) was prepared from 2,4 dimethyl-5-ethoxycarbonyl-3-octadecyl pyrrole (1.0g; 0.02 moles), hydrobromic acid (4ml) and formic acid (5ml) using method described by Fischer et al⁷²

0.7g; 37%; mp:108- 110°C

I.R.(KBr): 3160; 3080; 2920; 2860; 1610; 1255; 740; 730; 690; 660:

^1H NMR (CDCl_3): 2.5(s,3H); 2.1(s,3H); 2.0(s,6H); 1.3(s,68H); 0.9(t,6H)

Microanalysis Found: C,74.84%; H,11.39%; N,3.50%:

$\text{C}_{49}\text{H}_{89}\text{N}_2\text{Br}$: requires: C,74.86%; H,11.41%; N,3.56%:

N-octadecyl-4,4'-bipyridinium iodide (4.2.13)

To a stirred solution of 4,4'-bipyridyl (5.35g; 0.03 moles) in acetone (50 ml) was added a solution of iodoctadecane (6.32g; 0.016 moles) in acetone (50ml). The reaction was refluxed for 24 hours. The precipitate was filtered and re-crystallised from ethyl acetate to yield a yellow solid of N-octadecyl-4,4'-bipyridinium iodide.

3.25g: 38% mp:117-118°C

I.R.(KBr): 3400; 3010; 2910; 2860; 1640; 1470; 820; 720:

Microanalysis Found: C,62.43%; H,8.40% N,5.12%:

$C_{28}H_{45}N_2I$: requires: C,62.68%; H,8.45%; N,5.22%:

Tetracyanoethylene oxide⁶⁵ (4.2.14)

To a stirred solution of tetracyanoethylene (10g; 0.078 moles) in acetonitrile (100ml) in an ice bath was added 30% hydrogen peroxide (8.85ml). The temperature of the reaction mixture was maintained between 4-10°C during the addition and was then allowed to rise to 20°C. The lemon-yellow solution was poured into an ice and water mixture (400 ml).

The resulting precipitate was extracted with dichloroethane (3x150 ml), dried (sodium sulphate), and concentrated to 150ml. The concentrate was boiled with charcoal, filtered and cooled to yield TCNEO.

10.17g; 90% mp: 182-184°C (lit mp 177-178°C)⁶⁵

I.R.(KBr): 2280; 2260; 1600; 1500; 1360; 970; 960; 890; 720;

Microanalysis Found: C,49.91%; N,38.69%:

C_6N_4O : requires: C,50.01%; N,38.89%:

The attempted synthesis of:

N-Dicyanomethylide-N'-octadecyl-4,4'-bipyridinium iodide

(4.1.3)

To stirred refluxing solution of N-octadecyl bipyridinium iodide (1.0g; 1.80 mmoles) in acetonitrile (50ml) was added a solution of tetracyanoethylene oxide (0.63g; 4.4 mmoles) in acetonitrile (50ml). The resulting solution was refluxed for 24 hours. The acetonitrile was removed under reduced pressure to yield a solid. This was dissolved in acetone and precipitated with ether.

0.43g; 39%:

It was identical with the starting material (4.2.13)

N-Dicyanomethylide-4,4'-bipyridinium (4.2.15)

To a stirred solution bipyridyl (2.0g; 0.012 moles) in dry tetrahydrofuran (25ml) was added a solution of TCNEO (0.70g; 0.0049 moles) in dry tetrahydrofuran (10 ml) dropwise over hour. The mixture was stirred overnight and filtered to y N-dicyanomethylide-4,4'-bipyridyl (4.2.15).

0.97g; 90%: mp: 328-330°C (lit mp: 337-338°C)⁷³

I.R.(KBr): 3100, 3070; 3030; 2170; 2140; 1655; 1620; 1590; 1505; 1475; 1455; 1400; 1270; 800:

Microanalysis Found: C,70.63%; H,3.74%; N,25.71%:

C₁₃H₈N₄: requires C,70.90%; H,3.66%; N,25.44%:

4-Dioctadecyl picoline (4.2.16)

To a stirred solution of diisopropylamine (14.99mls; 0.107 moles) in dry tetrahydrofuran (50ml) under nitrogen was added 1.5M butyllithium (71.33ml, 0.110 moles). After half an hour freshly distilled 4-picoline (10g; 0.107 moles) in dry

tetrahydrofuran (25ml) was added. After one hour 1-bromo-octadecane (35.99g; 0.108 moles) in dry tetrahydrofuran (50ml) was added dropwise over a period of 30 minutes. The reaction mixture was stirred for a further three hours. The tetrahydrofuran was removed under reduced pressure and ether (100ml) was added to the resultant liquor. This was acidified with dilute HCl(100ml) which precipitated a white solid. This solid was filtered off and added to dilute NaOH (100ml). The solution was re-extracted with ether (2x100ml) and evaporated. The resultant oil solidified. The solid was recrystallised with ethanol to yield 4-dioctadecyl picoline as a white solid. 7.07g; 11%: mp: 59-61°C

I.R.(KBr): 3020; 3000; 2980; 2910; 1650; 1610; 1200; 710:

^1H NMR (CDCl_3): 9.4(d,2H); 7.8(d,2H); 2.2(s,1H); 1.3(s,68H), 0.9(t,6H):

N-Methyl-4-dioctadecyl picolinium iodide (4.1.4)

To a stirred refluxing solution of 4-dioctadecyl picoline (2.13g; 0.0036 moles) in chloroform (50ml) was added methyl iodide (0.6g; 0.0042 moles) dropwise over a period of 30 minutes. The reaction mixture was refluxed for a further 24 hours. The chloroform was removed under reduced pressure and the resulting solid was recrystallised from petroleum spirit 40-60° to yield a yellow solid N-methyl-4-dioctadecyl picolinium iodide:

2.2g: 83%

I.R.(KBr): 3030; 2900; 2910; 1650; 1600; 1210; 1170; 730:

^1H NMR(CDCl_3): 9.3(d,2H); 7.8(d,2H); 4.7(s,3H); 2.2(s,1H); 1.3(s,68H); 0.9(t,6H):

Microanalysis Found: C,69.65%; H,11.09%; N,1.80%:

$\text{C}_{43}\text{H}_{82}\text{NI}$: requires C,69.79%; H,11.17%; N,1.89%:

N-methyl-4-dioctadecyl picolinium TCNQ

To a stirred refluxing solution of N-methyl-4-dioctadecyl picolinium iodide (0.2g; 0.27 mmoles) in ethanol (25ml) was added LiTCNQ (0.06g; 0.28 mmoles) in ethanol (25ml). The reaction mixture was refluxed for a further two hours. The ethanol was reduced to yield a solid which was filtered and washed with warm water to produce a blue solid

N-methyl-4-dioctadecyl picolinium TCNQ.

I.R.(KBr): 3030; 3010; 2980; 2910; 2220; 2190; 1660; 1620; 1210; 1150; 730:

Microanalysis Found: C,80.80%; H,10.69%; N,8.53%:

$C_{55}H_{86}N_5$: requires C,80.83%; H,10.61%; N,8.57%:

4.5 References

1. B. Franklin; Phil Trans R. Soc., 64,445, (1774)
2. Lord Rayleigh; Phil Mag, 48,337 (1889)
3. K.B. Blodgett; J. Am Chem Soc, 57,1007, (1938)
4. H. Kuhn, D., Mobius and H. Bücher; Physical methods of chemistry 1,577, (1972)
5. G.G. Roberts and C.W. Pitt (editors). Proceedings Durham Conference on Langmuir Blodgett films; Thin solid films, Volume 99 (1983)
6. G.G. Roberts, Advances in Physics, 34, 475 (1985)
7. G.S. Galletti and A. Gurseppi-Elie; Thin solid films, 132, 163, (1985)
8. D.M. Mattox; Thin solid films, 124, 3 (1985)
9. K. Fukuda, H. Nakahara, T.Kato; J. Colloid Interface Sci, 54,430 (1976)
10. H. Nakahara, K. Fukuda; J. Colloid Interface Sci, 69,24 (1979)
11. I. Langmuir; J. Am Chem Soc, 39, 1848 (1917)
12. K. Blodgett; J. Am Chem Soc, 56, 495 (1934)
13. G. Veale, I.R. Girling, I.R. Peterson; Thin solid films, 127, 293 (1985)
14. I.R. Peterson and G.J. Russell; Thin solid films, 134, 143 (1985)
15. H. Bäessler; Adv Poly Sci, 63, 1 (1984)
16. R.H. Tredgold; Thin solid films, 152, 223 (1987)
17. A.K. Engel; T. Yoolen; K. Sanui and N. Ogata; J. Am Chem Soc 107, 8308, (1985)

18. A.K. Engel, N.Ogata, H, Fowler and M. Suzuki; Proc 3rd Int Symp. on molecular electronic devices Arlington VA 1986 North Holland Amsterdam
19. M. Suzuki, M. Katimoto, T. Konishi, Y. Imai, M. Iwamoto and T. Hino, Chem Letts, 395 (1986)
20. M. Kakimoto, M. Suzuki, T. Konishi, Y. Imai, M. Iwamoto and T. Hino, Chem Letts, 823 (1986)
21. M. Uekita; H. Awaji and M. Murata; Proc 3rd Int Symp on molecular electronic devices Arlington VA 1986 North Holland, Amsterdam
22. R. Jones, R.H. Tredgold and P. Hodge; Thin solid films, 99,25 (1983)
23. R.H. Tredgold; A.J. Vickers; A. Hootfar, P. Hodge and E. Khoshdel; J. Phys D; App Phys 18, 1139 (1985)
24. R. Jones, R.H. Tredgold, A. Hootfar, and P. Hodge; Thin films 113, 115 (1984)
25. R. Jones, R.H. Tredgold and A. Hootfar; Thin solid films, 123, 307 (1985)
26. M. Vandevyver, A. Barraud, A. Ruau~~del~~ - Teixier, P. Maillard and C. Gianotti, J. Colloid and Interface Science, 88, 571 (1982)
27. A. Ruau~~del~~-Teixier, A. Barraud, B. Belbeoch and M. Roulliay, Thin solid films, 99, 33 (1983)
28. M. Vandevyver, A. Ruau~~del~~-Teixier, L. Brehamet and Latz Thin solid films, 99,41 (1983).
29. A. Miller, W. Knoll, H. Mohwald and A. Ruau~~del~~-Teixier, Thin solid films 133, 83 (1985)

30. C. Lecomte, C. Baudin, F. Berleur, A. Ruaudel-Teixer, A. Barraud and M. Momenteau, Thin solid films, 133, 103 (1985)
31. C.B. McArdle and A. Ruaudel-Teixier, thin solid films, 133, 93 (1985)
32. R.H. Tredgold, M.C.J. Young, P. Hodge and A. Hootfar, IEE Proc I 132, 151 (1985)
33. S.Y. Luk, F.R. Mayers and J. O. Williams, J. Chem Comm 215, (1987)
34. S. Baker; M.C. Petty, G.G. Roberts and M.V. Twigg; Thin solid films, 99,53 (1983)
35. T.J. Marks, D.W. Kalina in J.S. Miller (ed) Extended Linear chain compounds vol. 1 Plenum N.Y. 197 (1982)
36. R.A. Hann, S.K. Gupta, J.R. Fryer, B.L. Eyres, Thin solid films 134, 35 (1985)
37. M.J. Cook, A.J. Dunn, A.A. Gold and A.J. Thomson, M.F. Daniel, J. Chem Soc Dalton Trans 6, 158 (1988)
38. J.B. Fryer, R.A. Hann and B.L. Eyres, Nature, 313, 382 (1981)
39. M.J. Cook, M.F. Daniel, A.J. Dunn, A.A. Gold and A.J. Thomson, J. Chem Soc Chem Commun, 863, (1986)
40. D.W. Kalina, S.W. Crane, Thin solid films 134, 109 (1985)
41. M.J. Cook, M.F. Daniel, K.J. Harrison, N.B. McKeown, A.J. Thomson, J. Chem Soc Chem Commun, 1149 (1987)
42. A. Ruaudel-Teixier, M. Vandevyver and A. Barraud, Mol Cryst. Liq Cryst 120, 319 (1985)
43. J. Richard, M. Vandevyver, P. Lesieur, A. Barraud, Holczerk J. Phys D. Appl Phys 19, 2421 (1986)
44. J. Richard, M. Vandevyver, P. Lesieur, A. Ruaudel-Teixier and A. Barraud, J. Chem Phys 86(4), 2428 (1987)

45. A Barraud M. Florsheimer, H. Möhwald, J. Richard, A. Ruau~~del~~-Teixier and M. Vandevyver, J. of Colloid and Interface Sci, 121, 491 (1988)
46. T. Nakmura, M. Matsumoto, F. Takei, M. Tanaka, T. Sekiguchi, E. Manda and Y. Kawabata, Chemistry letters 709 (1986)
47. M. Matsumoto, T. Nakamura, F. Takei, M. Tanaka, T. Sekiguchi, M. Mizuno, E. Manda and Y. Kawabata, Synthetic metals, 19, 675 (1987)
48. A.S. Dhindsa, M.R. Bryce, J.P. Lloyd, M.C. Petty, Synthetic metals, 22, 185 (1987)
49. L.R. Melby, R.J. Harder, W.R. Hertler, W.Mahler, R.E. Benson and W.E. Mochel, J. Am Chem Soc, 84 3374, (1962)
50. J. Tanaka, M. Tanaka, T. Kawai, T. Takabe, O. Maki, Bull Chem Soc Jpn; 49, 2358 (1976)
51. T. Nakamura, F. Takai, M. Tanaka, M. Matsumoto, T. Seki, E. Manada, Y. Kawabata, G. Saito, Chemistry Letter, 323, (1986)
52. Y. Kawabata, T. Kakamura, M. Matsumoto, M. Tanaka, T. Sekiguchi, H. Konizu, E. Manda and G. Saito, Synthetic Metals, 19, 663 (1987)
53. A Barraud, M. Lequan, R.M. Lequan, P. Lesieur, J. Richard, A. Ruau~~del~~-Teixier and M. Vandevyver, J.C.S. Chem Comm II 797, (1987)
54. M. Vandevyver, J. Richard, A. Barraud, A. Ruau~~del~~-Teixier, M. Lequan and R.M. Lequan, J. Chem Phys, 87, 6754 (1987)
55. M. Fujiki and H. Tabei, Synthetic metals, 18, 815 (1987)

56. T. Iyoda, M. Ando, T. Kaneko, A. Ohtani, T. Shimidzu and K. Honda, Tetrahedron letters, 27, 5633 (1986)
57. A. Barraud, J. Leloup, P. Lesieur, Thin solid films, 133, 113 (1986)
58. H. Fischer, Organic Synthesis Collective Vol II John Wiley and sons Inc. New York N.Y. 1943 p202
59. H. Fischer, Organic Synthesis collective Vol II John Wiley and Sons Inc. New York N.Y. 1943 p 217.
60. H. Fischer, Organic Synthesis collective Vol II John Wiley and Sons Inc. New York N.Y. 1943 p198
61. H. Fischer, Weiss and Schubert, Ber, 56,1199 (1923)
62. Buckley and Rapopa, J. Am Chem Soc, 103, 6162 (1981)
63. B. Morgan and D. Dolphin, J. Org Chem, 52, 5364 (1987)
64. R.L.N. Harris, A.W. Johnson and I.T. Kay, J. Chem. Soc (C), 22 (1966)
65. W.J. Linn, O.W. Webster and R.E. Benson, J. Am Chem Soc. 3652 (1965)
66. W. Becker, W.S. Sheldrick and J. Engle, Acta Cryst, B34, 102 (1978)
67. G. Struckmeier, J. Engel and U. Thewalt, Z. Naturforsch B. Anorg. Chem. Org. Chem, 33B, 753 (1978)
68. W.S. Sheldrick, A. Borkenstein, G. Struckmeier and J. Engel Acta Cryst B34, 329 (1978)
69. A.W. Johnson, E. Markham and R. Price, Org. Syn, 42,75 (1962)
70. O. Touster, Organic Reactions, 7, 327 (1953)
71. G.C. Kleinspehn, J. Am Chem Soc, 77, 1546 (1955)
72. H. Fischer and A. Kirstahler, Ann, 466, 178 (1928)
73. Private Communication G. J. Ashwell

Appendix 1

GENERAL INFORMATION

Proton magnetic spectra were obtained from a Jeol PMX 60MHz N.m.r. spectrometer. Chemical shifts are quoted on the delta scale, using tetramethyl silane as an internal standard, its resonance being assigned a value of zero on that scale.

Abbreviations: s = singlet, d = doublet, t = triplet, q = quartet,
m = multiplet

All infrared spectral data were obtained from either a Pye Unicam SP1000, SP3-100 or a Perkin Elmer 783 Infrared spectrophotometer. Data are given in cm^{-1} . The samples were prepared either as a potassium bromide dispersions or as thin liquid films.

The ultra-violet/visible spectroscopic studies were obtained upon Perkin Elmer 550S or a Perkin Elmer Lambda 7 spectrophotometer.

The micro-analytical data were performed by the City University, Chemistry Department, London.

Thin layer chromatograms were obtained using Merck 5554.

Alufolien Kieselgel 60F₂₅₄ plates with fluorescent indicator incorporated. Compounds were visualised by quenching the fluorescence upon irradiation with ultra-violet light (254 nm).

Dry tetrahydrofuran (THF) was obtained by distillation from potassium metal. Petrol refers to that fraction of petroleum spirit boiling between 40 and 60°C.

All reactions requiring an inert atmosphere were performed under white spot nitrogen.

Melting points are uncorrected.

Magnetic Measurements

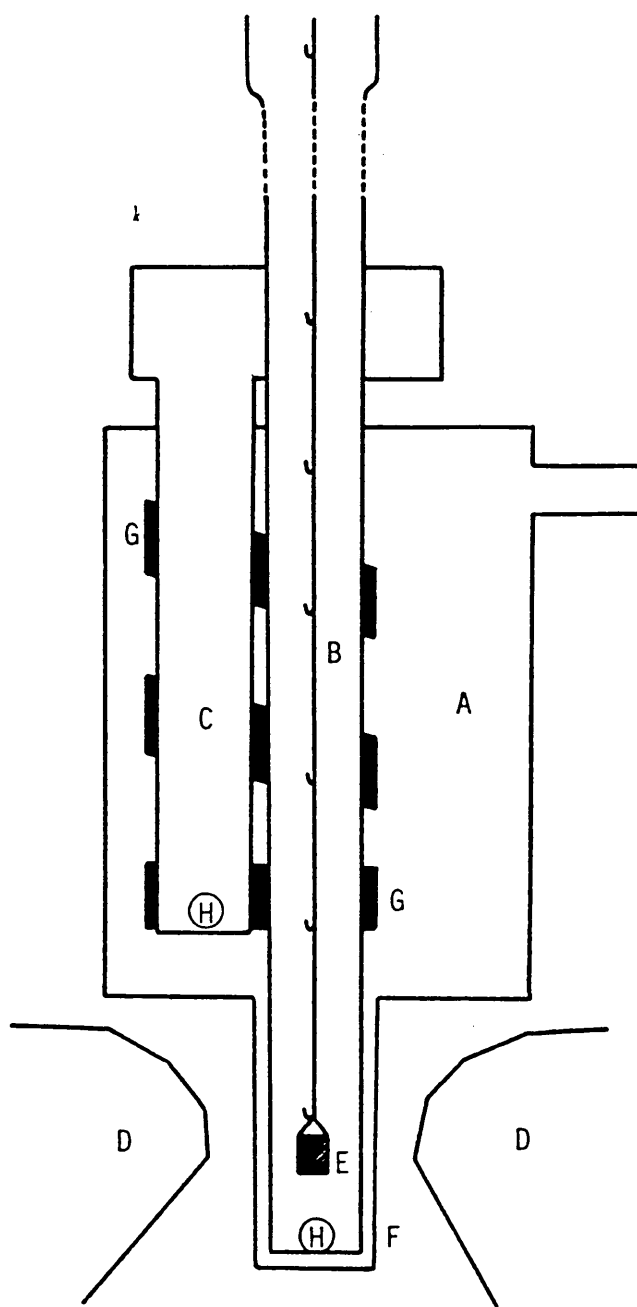
The Faraday method was employed for the determination of the magnetic susceptibility.

The Faraday magnetic balance consists of:

- i. Refrigerator unit with temperature controller: the temperature control was provided by an Air Products 'Displex' closed cycle helium refrigerator equipped with a vacuum shroud (Figure: 1). The cooling cycle was controlled by an Oxford Instruments temperature controller and sweep generator to a rate of 0.5k/min.
- ii. Microbalance: A. C.I. Robel microbalance was used with a rated sensitivity of 1 μ g.
- iii. Magnetic field: A magnetic supply of 10A was supplied by a K.S.M. type S.C.T. stabilised power supply.

Measurement Procedure

1. The P.T.F.E. bucket was washed with acetone, dried and its weight change observed in the magnetic field.
2. A sample of between 20 and 100mg was placed in the bucket and lowered into position.
3. The balance and sample were pumped to 10^{-5} mbar overnight to remove residual oxygen and water vapour.
4. The system was then backfilled with helium exchange gas to 0.1 bar (at room temperature). The helium supply was maintained throughout the experiment and the pumping and backfilling rates were controlled by an in-line leak valve.



KEY : A ... Vacuum shroud (pumped to 10^{-5} mbar)
 B ... Sample tube (dry He gas at 0.1 bar)
 C ... Cold head
 D ... Magnet pole piece
 E ... Sample bucket (PTFE)
 F ... Diamagnetic casing (copper)
 G ... Thermal tape
 H ... Platinum sensor

Figure 1: Faraday magnetic balance; cold head and sample position

5. The weight change of the sample was recorded when the field was applied. The effects of thermomolecular pressure and adsorption of gas were controlled by sweeping the field up and down at each temperature.
6. Part 5 was repeated at intervals of 5K within the temperature range 25-300K.

Magnetic Susceptibility

The magnetic susceptibility is related to the force exerted on a sample by a magnetic field of constant field x field gradient by:

$$g\Delta m = m\chi_g[H(dH/dZ)] \dots\dots\dots \text{Equation 1}$$

g = acceleration due to gravity (981 cms^{-2})

H = field strength

Z = axis perpendicular to the field

χ_g = gramme susceptibility

m = mass of sample

Δm = apparent mass of sample when field is applied

The total molar susceptibilities were then calculated from:

$$\chi_m = \frac{\Delta m}{m} \cdot M \cdot C \dots\dots\dots \text{Equation 2}$$

M = Molecular Mass

$C = \frac{g}{[H(dH/dZ)]}$

However the molar spin susceptibility is derived from the total susceptibility by

$$\chi_s = \chi_m + \chi_{DIA} \dots\dots\dots \text{Equation 3}$$

χ_s = spin susceptibility

χ_{DIA} = Diamagnetic Susceptibility

Therefore:

$$\chi_s = \left[\frac{\Delta m \cdot M \cdot C}{m} \right] + \chi_{DIA} \dots\dots\dots \text{Equation 4}$$

The Δm values were calculated by subtracting the observed value of the empty bucket from the weight change of the sample and the bucket. A study of the empty bucket showed a temperature independent weight change throughout the range 25-2300K of $-1.20 \pm 0.03\text{mg}$.

The susceptibility values were converted to acceptable c.g.s. units using the conversion factor²;

$$\chi_s(\text{c.g.s.}) = \chi_s(\text{S.I.}) / 4\pi \dots\dots\dots \text{Equation 5}$$

The position of the sample was adjusted to maximise $H(dH/dZ)$. The product of field and field gradient was calibrated using a sample of pure, dry $\text{HgCo}(\text{CNS})_4$ for which, $\chi_g = 206.67 \times 10^{-6} \text{cm}^3 \text{g}^{-1}$.

The reliability of the technique was determined by measuring the susceptibility of a sample of ferric acetyl acetonate, by the Gouy method. The experimental value determined by this technique ($\chi_{TOT} = 0.181 \text{cm}^3 \text{mol}^{-1}$) is in close agreement with the result obtained by the Faraday method ($\chi_{TOT} = 0.208 \text{cm}^3 \text{mol}^{-1}$). The absolute accuracy of the susceptibility is limited by paramagnetic impurities.

Electrical Measurements

The D.C. conductivity measurements were made on compactions of the salts.

The compacted samples were prepared from microcrystals or powders previously dried for 24 hours at room temperature in an evacuated drying chamber. Samples were ground and compressed at 75MPa in a 3 mm evacuated die for 2 minutes.

The measurement of the high resistivity samples was by a 2-point probe method using a solatron 7150 multimeter accurate to 5 decimal places.

The two needles were applied to either side of a thin disc (Figure 2).

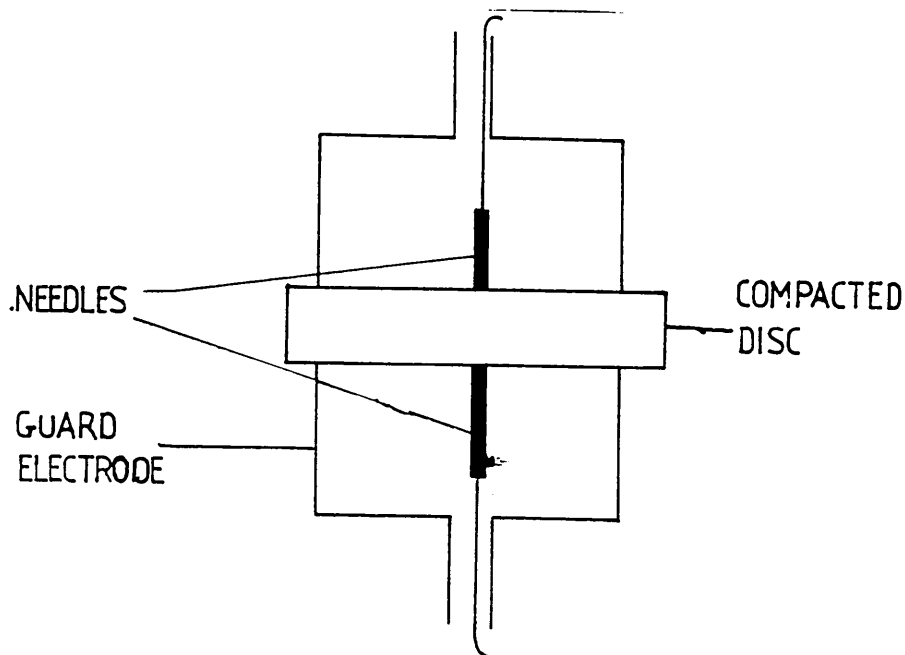


Figure 2 Sample contact geometry. The 2 point probe technique.

The volume resistivity is related to the measured resistance R between the probes by

$$\rho = \frac{RA}{L} \dots\dots\dots \text{Equation 6}$$

where A and L are the cross-sectional area and the length of the disc between the probes respectively.

The room temperature conductivities and the temperature dependence results of the semi-conducting samples were obtained using a 4-point probe method (Figure 3).

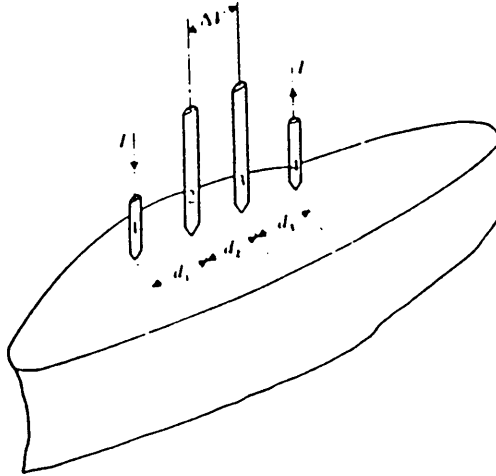


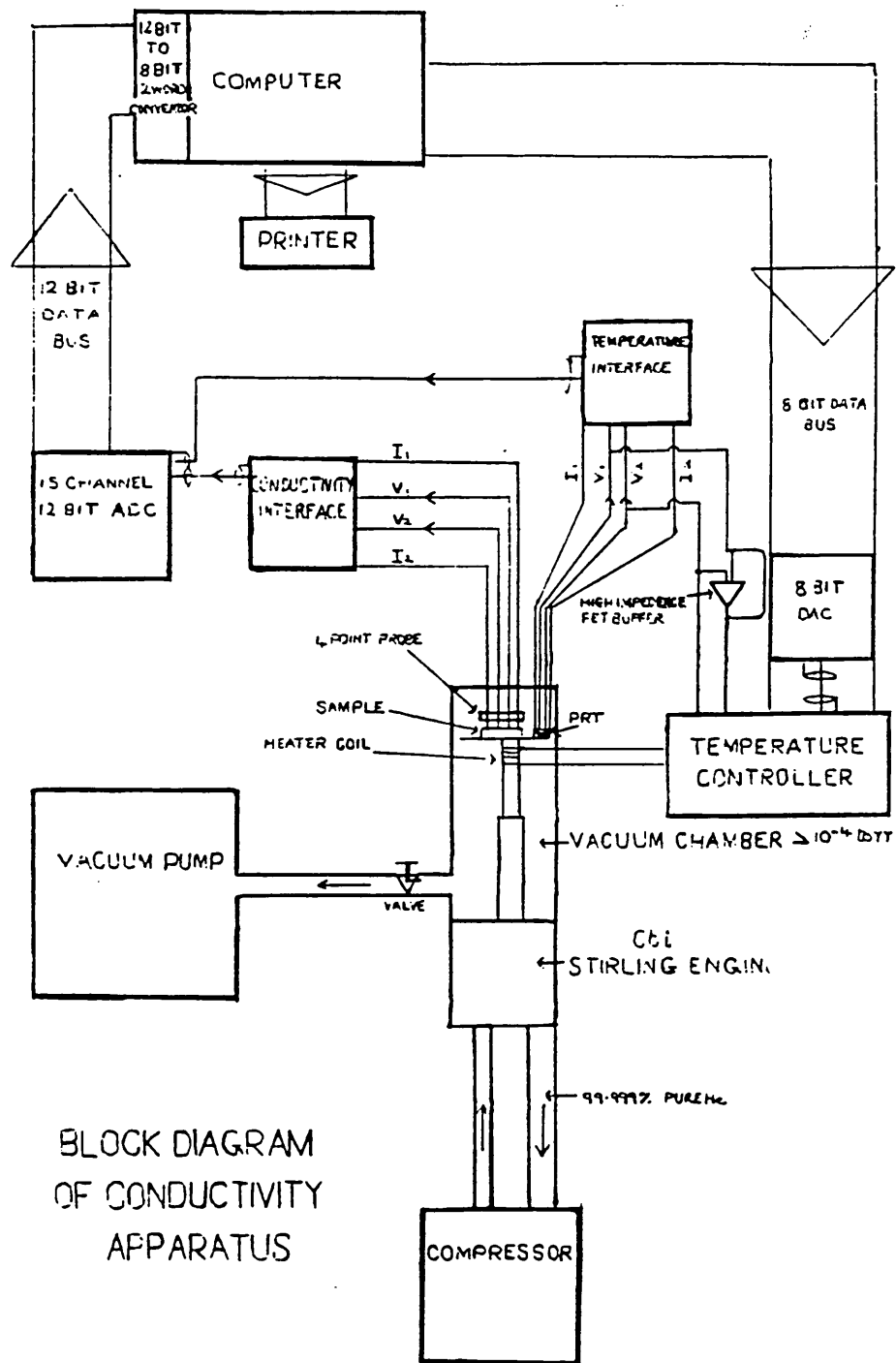
Figure 3: Sample Contact Geometry. The 4 contact technique.

A block diagram of the conductivity apparatus is shown in figure 4.

The compactions were mounted at the 4k station of the expander module in an air products 'Displex' closed cycle helium refrigerator system. The sample contact wires were wound tightly around the length of the 'cold finger' to ensure good thermal contact for the sample.

Temperature control was made with an Oxford Instruments sweep generator and temperature controller. Temperature sensing was made using an Oxford Instruments platinum sensor linear in response in the range 15-400K. The temperature was swept at a rate of approximately 0.5K/min.

The analogue voltage signals from the sensor and the sample were received and converted to digital output by a Solartron 7150 microprocessor voltmeter coupled to a 15 channel solatron 'Minite' scanner. The voltmeter was interfaced to and controlled from a teletype model 43 printer.



BLOCK DIAGRAM
OF CONDUCTIVITY
APPARATUS

Figure 4: Block Diagram of Conductivity Apparatus

References

1. See for example The Magnetic Properties of Matter, J. Crangle
(Edward Arnold, 1977).
2. T. Cvitas and N. Kalley; J.Chem.Ed, 54,530(1977).

Appendix 2

Reading List

1. Organic Conductors and Semiconductors (ed. L. Pal, G. Gruner, A. Janossy and J. Solyom). Lecture Notes in Physics, Springer Verlag, 65 (1977).
2. Synthesis and properties of Low-dimensional Materials, Annals N.Y. Acad. Sci., 313 (1978).
3. The Physics and Chemistry of Low-dimensional Solids (ed. L. Alcacer), NATO Advanced Study Institute Series C: Mathematical and Physical Sciences, D. Reidel Publishing Company, 56 (1980).
4. Proceedings of The International Conference of Low-dimensional Synthetic Metals (Helsinki), Chemica Scripta 17 (1981).
5. Proceedings of The International Conference on Low-dimensional Conductors (Boulder), Mol. Cryst. Liq. Cryst., 86 (1982).
6. Colloque International du CNRS sur la Physique et al Chimie des Metaux Synthetiques et Organiques (Les Arcs), J. de Physique, C3 (1983).
7. Conference Internationale sur la Physique et al Chimie des Polymeres Conducteurs (Les Arcs), J. de Physique, C3 (1983).
8. Electrical and Related Properties of Organic Solids (ERPOS 4 - Zamek Ksiaz), Materials Science, X (1984).
9. Proceedings of The International Conference on The Physics and Chemistry of Low-dimensional Synthetic Metals (ICSM 84 - Abano Terme), Mol. Cryst. Liq. Cryst. 118 (1985).

10. The Bipyridium Pesticides, L.A. Summers, Academic Press, London (1980).
11. X-ray Structure Determination, A Practical Guide, G.H. Stout and L.H. Jensen, Macmillan, (1968).
12. Direct Methods in Crystallography, C. Giacovazzo, Academic Press, London (1980).

Appendix 3

As part of my postgraduate studies I attended:

- | | | |
|------------------------------|---|--|
| The Fourth Firth Symposium | - | University of Sheffield
(3rd February 1988) |
| Molecular Electronics Course | - | University of Durham,
Industrial Research
Laboratories
(29th & 30th September 1987) |
| Numerous Internal Symposia | - | Sheffield City Polytechnic
(1985-1988) |